Distribution Agreement

In presenting this thesis or dissertation as a partial fulfillment of the requirements for an advanced degree from Emory University, I hereby grant to Emory University and its agents the non-exclusive license to archive, make accessible, and display my thesis or dissertation in whole or in part in all forms of media, now or hereafter known, including display on the world wide web. I understand that I may select some access restrictions as part of the online submission of the thesis or dissertation. I retain all ownership rights to the copyright of the thesis or dissertation. I also retain the right to use in future works (such as articles or books) all or part of this thesis or dissertation.

Signature:

_____ _____

Michael P East Date

ELMO Domain Containing (ELMOD) Proteins: Phylogenetic, Structural, and Functional Characterization

By

Michael Patrick East
Doctor of Philosophy

Graduate Division of Biological and Biomedical Science
Biochemistry, Cell, and Developmental Biology

_____
Richard A. Kahn, Ph.D.
Advisor

_____
Victor Faundez, M.D., Ph.D.
Committee Member

_____
John R. Hepler, Ph.D.
Committee Member

_____
Eric A. Ortlund, Ph.D.
Committee Member

_____
James Q. Zheng, Ph.D.
Committee Member

Accepted:

_____
Lisa A. Tedesco, Ph.D.
Dean of the James T. Laney School of Graduate Studies

_____
Date

ELMO Domain Containing (ELMOD) Proteins: Phylogenetic, Structural, and Functional Characterization

By

Michael Patrick East
B.S., Kennesaw State University

Advisor: Richard A. Kahn, Ph.D.

An abstract of
A dissertation submitted to the Faculty of the
James T. Laney School of Graduate Studies of Emory University
in partial fulfillment of the requirements for the degree of
Doctor of Philosophy
In
Graduate Division of Biological and Biomedical Sciences
Biochemistry, Cell, and Developmental Biology

Abstract

ELMO Domain Containing (ELMOD) Proteins: Phylogenetic, Structural, and Functional Characterization

By Michael Patrick East

The ELMO domain containing proteins (ELMODs) are a novel group of GTPase activating proteins (GAPs) that act on members of the Arf family of regulatory GTPases, though they lack the previously characterized, conserved Arf GAP domain. Very little is known about the functions of the ELMODs but the human family members have been implicated in non-syndromic familial deafness or idiopathic pulmonary fibrosis. The ELMODs belong to the ELMO family of proteins which includes three ELMODs and three ELMOs in humans and is defined by the presence of the ELMO domain in each of its members. The ELMOs function as key regulators of cell migration and actin dynamics as unconventional guanine nucleotide exchange factors for the Rho family GTPase Rac1. Unlike the ELMODs, the ELMOs lack any detectable GAP activity for Arf family GTPases. In this dissertation, I show that ELMODs and ELMOs are two phylogenetically distinct groups of proteins despite being members of the same gene family. The ELMODs represent the more ancient form of the protein and were likely present in the last eukaryotic common ancestor, suggesting some ancient function(s) of the ELMODs important or even essential for eukaryotic life. I mapped the GAP motif of the ELMODs to a region within the ELMO domain and provided initial characterization of this motif by identifying an arginine residue essential for efficient GAP activity. I also provide the first functional information for the ELMODs and present models for the cellular roles of ELMOD1 and ELMOD3 as a regulator of Arf signaling at the Golgi and as an activator of RhoA signaling at the trailing edge of migrating cells, respectively. However, additional cellular localizations of each of the ELMODs and putative binding partners identified in this dissertation are suggestive of other, novel roles for the ELMODs in cells. Together these data represent the majority of the available information on the ELMODs and provide the foundation for our later studies to provide a better understanding of the biology of the ELMODs and their roles in cell biology and human diseases.

ELMO Domain Containing (ELMOD) Proteins: Phylogenetic, Structural, and Functional Characterization

By

Michael Patrick East
B.S., Kennesaw State University

Advisor: Richard A. Kahn, Ph.D.

A dissertation submitted to the Faculty of the
James T. Laney School of Graduate Studies of Emory University
in partial fulfillment of the requirements for the degree of
Doctor of Philosophy
in
Graduate Division of Biological and Biomedical Sciences
Biochemistry, Cell, and Developmental Biology
2014

Table of Contents

Chapter I

General Introduction

Michael Patrick East

Department of Biochemistry and Program in Biochemistry, Cell, and Developmental Biology, Emory University, Atlanta GA 30322

The ELMO domain containing proteins (ELMODs) are a novel group of GTPase activating proteins (GAP) for Arf family GTPases. The Arf family is a family of proteins within the Ras superfamily of ~20 kDa regulatory GTPases and consists of 30 members in mammals [1, 2]. Like all members of the Ras superfamily of GTPases, Arf family GTPases cycle between GTP and GDP bound states and function in cells as molecular switches (Fig 1). Binding to GTP causes a conformational change in the GTPase that increases affinity for effector proteins responsible for downstream signaling. When GTP is hydrolyzed, affinity for effector proteins in lost, resulting in termination of GTPase signaling. The GTPase cycle is mediated by two groups of proteins. Guanine nucleotide exchange factors (GEFs) facilitate the exchange of bound GDP for GTP to activate GTPase signaling and GTPase activating proteins (GAPs) catalyze the hydrolysis of bound GTP to GDP to terminate GTPase signaling. This model for the role of GAPs in the GTPase cycle is limiting because many GAPs have also been shown to function as effectors of their substrate GTPases [3-5] . Thus, GAPs have complex roles both as terminators of GTPase signaling and as effectors (Fig 1).

The ELMODs belong to the ELMO family of proteins consisting of six members in humans characterized by the presence of the ELMO domain (Fig 2). The ELMO family is evenly divided into two groups based on protein size and domain architecture [6]. The three ELMODs range from 32 to 43 kDa and are single domain proteins consisting of little more than the ELMO domain itself. The ELMOs are approximately twice the size of the ELMODs and have multiple domains including the ELMO domain, a PH domain, ERM and Ras binding domains, and autoinhibitory domains [7, 8]. The Conserved Domain Database identified another domain within the ELMOs named domain of unknown function (DUF) 3361 [9]. This domain is only found in ELMOs and overlaps with the ELMO inhibitory domain (EID). Thus, DUF 3361 and EID are likely the same functional domain. Each of the ELMOs share <20% sequence identity with each of the three ELMODs and ELMOD3 shares ≤20% sequence identity with any of the

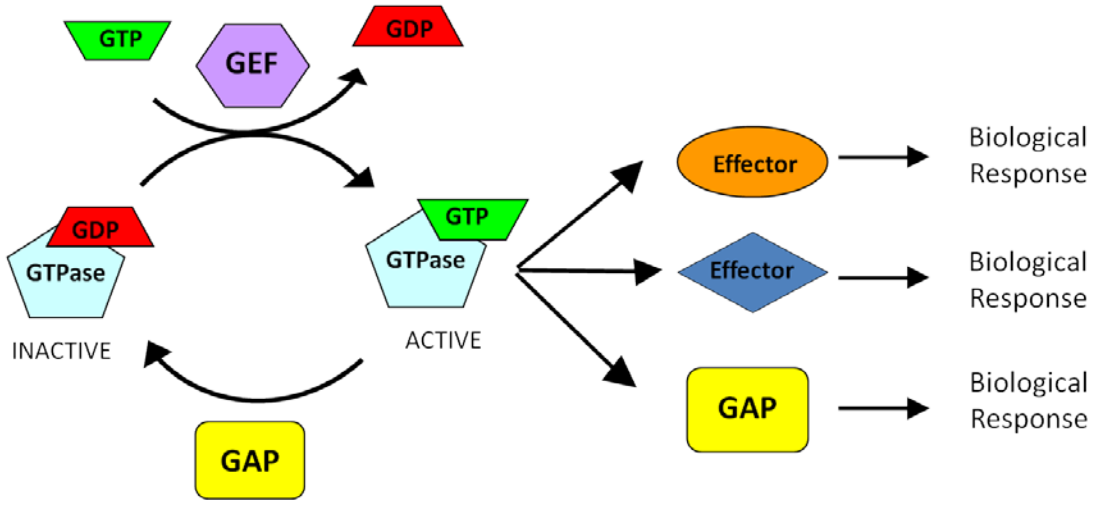

Figure 1: The GTPase cycle. GTPases behave in cells as molecular switches. They cycle between an active and inactive state depending on the nucleotide bound. Binding GTP induces a conformational change that increases affinity of the GTPase for effector molecules to stimulate a downstream biological response. When GTP is hydrolyzed to GDP, this affinity for effector molecules is lost and the GTPase is rendered inactive. Guanine nucleotide exchange factors (GEF) facilitate the exchange of bound GDP for GTP and GTPase activating proteins (GAP) catalyze the hydrolysis of bound GTP to GDP. GAPs also commonly function as effectors of their substrate GTPases to mediate a downstream biological response.

other ELMOs or ELMODs. The only region of homology among all six proteins lies within the ELMO domain [6]. Despite being the defining characteristic of the protein family and the only region of homology between all six members, the ELMO domain was a domain of unknown function prior to my studies. I mapped the GAP domain of the ELMODs to the ELMO domain providing the first functional information associated with this domain [9]. The function of the ELMO domain within the ELMOs, which lack GAP activity, is still unknown.

There are three ELMODs in humans and mice (ELMOD1-3) and the first functional information reported for any of these proteins was the biochemical purification of ELMOD2 from bovine testis based on its GAP activity for the Arf-like protein Arl2 [6]. This activity is conserved in each of the three human ELMODs [6, 10]. The ELMODs were the first GAPs ever identified for any of the 22 mammalian Arf-like (Arl) GTPases and represent the founding members of the Arl GAP family of proteins. Further characterization of the GAP activity of ELMODs revealed broad specificity for Arf family GTPases including both Arfs and Arls [6, 10]. The Arfs and Arls are both members of the Arf family of GTPases based on structural homology but are functionally very different [11-13]. There is very little precedence in the literature for cross-talk between the Arfs and the Arls and the ELMODs are among a small handful of proteins linking the two groups of GTPases [14, 15]. Over 30 GAPs for the six mammalian Arfs have been identified [16] but none have ever been reported to exhibit GAP activity against any Arl. All of the known Arf GAPs use the canonical Arf GAP domain consisting of a four cysteine zinc finger positioning in a catalytic arginine residue to confer GAP activity [17, 18]. The ELMODs lack this canonical Arf GAP domain. At the time I began my studies, the GAP domain in the ELMODs was not known. I defined the Arl GAP domain and putative catalytic arginine residue for the first time [9]. Because the ELMODs also use Arfs as substrates in the GAP reaction, this work also defined a novel Arf GAP domain, the first that does not use the zinc finger motif.

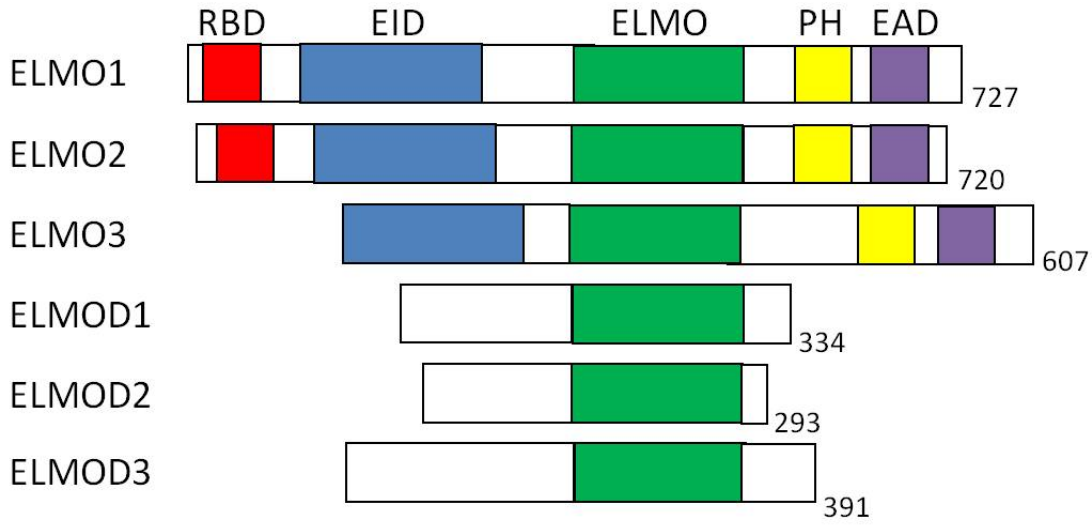

Figure 2: Domain architecture of the ELMO family of proteins. The ELMO family of proteins is equally divided into three ELMOs and three ELMODs all containing the ELMO domain (green). The ELMOs also have a Ras binding domain (RBD; red), a pleckstrin-homology domain (PH; yellow), and two autoregulatory domains (EID, ELMO inhibitory domain; blue and EAD, ELMO autoregulatory domain; purple). ELMOs also have an ezrin/radixin/moesin (ERM) binding domain that has been mapped to within the first 280 amino acids that is not shown in the schematic.

Since the identification of ELMODs as the first Arl GAPs, only two other Arl GAP proteins have been identified; Retinitis pigmentosa 2 (RP2) and cofactor C are GAPs for Arl3 [19]. The crystal structure of RP2 has been solved and the GAP domain has been mapped [19]. RP2 and cofactor C share some structural homology within their GAP domains but share little to no structural homology with the ELMODs. RP2 and cofactor C also lack any detectable GAP activity for the Arfs. Thus, the GAP domain of RP2 and cofactor C are not conserved in the ELMODs. The ELMODs remain the only GAPs that have activity for both Arfs and Arls and are uniquely poised to facilitate cross-talk between these two functionally distinct groups of GTPases.

ELMOD2 is the best characterized of the ELMODs in the literature and has been linked to mitochondrial dynamics, the antiviral response, and idiopathic pulmonary fibrosis [20](Newman *et. al.* in press). ELMOD2 has the highest specific activity for each of the GTPases tested to date [10]. Despite the high specific activity, the only direct functional information available for ELMOD2 revealed a role as an effector of Arl2 in mitochondria (Newman *et. al.* in press). ELMOD2 localized to the mitochondrial matrix and knockdown of ELMOD2 resulted in mitochondrial fragmentation and clustering around the nucleus, phenocopying depletion of Arl2 or expression of a dominant negative mutant of Arl2 (Newman *et. al.* in press). The mechanism of Arl2 or ELMOD2 in the regulation of mitochondrial morphology and motility is unknown. A genetic linkage analysis in six families identified ELMOD2 as a candidate gene for idiopathic pulmonary fibrosis and ELMOD2 mRNA expression levels were reduced in patients with the disease [20]. Thus, ELMOD2 is one of a very short list of proteins linked to idiopathic pulmonary fibrosis. ELMOD2 expression was also required for activation of the Toll-like receptor 3 antiviral response and expression of target genes [21]. The specific mechanism of ELMOD2 in this process is unknown.

Considerably less is known about the cellular functions of ELMOD1 and ELMOD3 but each of these proteins has been linked to deafness in mice and humans, respectively. The only available literature for ELMOD1 comes from the characterization of laboratory mice with randomly occurring exon duplications or deletions in the ELMOD1 gene. The only reported phenotypes of these mice were deafness and balance defects associated with deafness [22]. Scanning electron microscopy of inner ear hair cells revealed morphological defects and loss of stereocilia in inner ear hair cells within weeks after birth. Development of stereocilia was not disrupted suggesting that ELMOD1 is only required for the maintenance of stereocilia [22]. In a human family, a mutation (L265S) in ELMOD3 was also linked to deafness [23]. The same study showed that endogenous ELMOD3 predominantly localized to stereocilia in hair cells of mouse inner ear explants and that ectopically expressed ELMOD3 localized to actin structures at the cell surface in cultured cells. Pharmacological disruption of the actin cytoskeleton also disrupted the localization of ectopically expressed ELMOD3 suggesting some association between ELMOD3 and the actin cytoskeleton. Thus, ELMOD1 and ELMOD3 are essential for hearing and presumably have some important but unidentified role in stereocilia. Stereocilia are the highly specialized sensory organelles of inner ear hair cells essential for mechanoelectrical transduction of sound waves [24]. Unlike motile or primary cilia which have a microtubule based support structure, stereocilia are actin based structures and rely heavily on actin associated proteins, including several different myosin motor proteins, for proper function [25, 26]. Many of the mutations identified with links to deafness and stereocilia defects are in genes with physical links to actin and myosin [24-26].

The ELMOs have a defined role as important activators of Rac1, a member of the Rho family of GTPases. The ELMOs were first described in *C. elegans* where the single ortholog CED-12 was essential for **e**ngu**l**fment of apoptotic cells and cell **mo**tility [27, 28]. Worm CED-12 and mammalian ELMO1 or ELMO2 primarily exist in the cell bound to an obligate binding

partner, CED-5/DOCK180 and functions as an unconventional GEF for Rac1 [27, 29-32]. DOCK180 binds to Rac1 and has some low intrinsic Rac1 GEF activity *in vitro* but binding to ELMO1 was required for Rac1 GTP loading in cells, the relief of DOCK180 auto-inhibition, and helped DOCK180 stabilize nucleotide free Rac1 [29, 30, 33]. DOCK180 lacks the Dbl homology (DH) domain found in every other known Rac GEF and instead binds to nucleotide free Rac1 to facilitate GTP loading [29, 30]. The ELMOs lack any detectable GAP activity for Arf family GTPases [6, 10]. Thus, the ELMOs and ELMODs appear to have fundamentally different functions with respect to the GTPase cycle and presumably regulate two different families of GTPases. This difference makes the function of the ELMO domain far more intriguing as it is the only region of homology between these two functionally distinct groups of proteins.

Rac1 is a member of the Rho family GTPases which, like the Arf family, falls within the Ras superfamily of regulatory GTPases. Rho family GTPases are key regulators of actin dynamics and cell migration [34]. Rac1 functions primarily at the leading edge of migrating cells where it stimulates actin polymerization through activation of the Arp2/3 complex [35, 36]. Localized polymerization of actin provides the protrusive force required for membrane ruffling and lamellipodia formation. The ELMO/DOCK180 complex is an important regulator of this process as it is one of the primary GEFs for Rac1 at the leading edge [37]. Interestingly, key regulators of ELMO/DOCK180 include the Arf family GTPase Arf6 and its GEF, ARNO. Arf6 activation via ARNO induces activation of Rac1 and lamellipodia formation in an ELMO/DOCK180 dependent manner [38, 39]. Thus, Arf6 is upstream of ELMO/DOCK180. The prevailing model in the field suggests that Arf6 helps recruit ELMO/DOCK180 to the plasma membrane at the leading edge of the cell [40]. There is no indication in the literature as to the mechanism of this recruitment or whether there is a direct interaction between Arf6 and

ELMO/DOCK180. It is also unclear whether Arf6 functions only to recruit ELMO/DOCK180 to the leading edge or whether it also activates ELMO/DOCK180 GEF activity.

Rac1 has an antagonistic relationship with another Rho family GTPase, RhoA [41]. Activation of the two proteins is largely compartmentalized in the cell and facilitates very different functions during cell migration [34, 42]. Whereas Rac1 functions primarily at the leading edge of a migrating cell, RhoA functions primarily at the cell tail and within the cell body. RhoA is a key regulator of actomyosin contraction at the trailing edge of migrating cells to generate the force required to pull the cell rear along during migration [43, 44]. This process is mediated by activation of myosin motor activity along actin stress fibers. Myosin motors cross-link actin filaments in stress fibers and motor activity causes shortening of the stress fibers generating the pulling force. Activation of myosin motor activity via RhoA is primarily a product of the RhoA/Rho kinase (ROCK)/myosin light chain (MLC) signaling cascade [45]. In the cell body, RhoA activation also stimulates the formation of actin stress fibers. Stress fiber formation is mediated by ROCK but also requires another effector of RhoA, mDia1 [45].

In this study, I provide some of the first functional and biochemical characterization for any of the ELMODs and offer some explanation for the differences between ELMODs and ELMOs. I mapped the Arf family GAP domain of the ELMODs to the ELMO domain and provided initial characterization of the GAP domain by identifying a putative catalytic arginine residue important for GAP activity. I performed the most thorough phylogenetic analysis of the ELMO family of proteins to date indicating that ELMOs evolved from the much more ancient ELMODs but lost key residues within the GAP domain, consistent with the biochemical differences between ELMODs and ELMOs. This work also supports a diverse array of functions for ELMODs throughout the cell and includes models for ELMOD1 as an Arf GAP at the Golgi and for ELMOD3 as a novel regulator of the actin cytoskeleton through a RhoA dependent

mechanism. These models provide the framework for our understanding of the roles of ELMOD1 and ELMOD3 in hair cells and in the deafness phenotype.

References

1. Kahn, R.A., et al., *Nomenclature for the human Arf family of GTP-binding proteins: ARF, ARL, and SAR proteins.* J Cell Biol, 2006. **172**(5): p. 645-50.
2. Wennerberg, K., K.L. Rossman, and C.J. Der, *The Ras superfamily at a glance.* J Cell Sci, 2005. **118**(Pt 5): p. 843-6.
3. East, M.P. and R.A. Kahn, *Models for the functions of Arf GAPs.* Semin Cell Dev Biol, 2011. **22**(1): p. 3-9.
4. Zhang, C.J., M.M. Cavenagh, and R.A. Kahn, *A family of Arf effectors defined as suppressors of the loss of Arf function in the yeast Saccharomyces cerevisiae.* J Biol Chem, 1998. **273**(31): p. 19792-6.
5. Veltel, S., et al., *Specificity of Arl2/Arl3 signaling is mediated by a ternary Arl3-effector-GAP complex.* FEBS Lett, 2008. **582**(17): p. 2501-7.
6. Bowzard, J.B., et al., *ELMOD2 is an Arl2 GTPase-activating protein that also acts on Arfs.* J Biol Chem, 2007. **282**(24): p. 17568-80.
7. Patel, M., et al., *An evolutionarily conserved autoinhibitory molecular switch in ELMO proteins regulates Rac signaling.* Curr Biol, 2010. **20**(22): p. 2021-7.
8. Grimsley, C.M., et al., *Characterization of a novel interaction between ELMO1 and ERM proteins.* J Biol Chem, 2006. **281**(9): p. 5928-37.
9. East, M.P., et al., *ELMO domains, evolutionary and functional characterization of a novel GTPase-activating protein (GAP) domain for Arf protein family GTPases.* J Biol Chem, 2012. **287**(47): p. 39538-53.

10. Ivanova, A.A., et al., *Characterization of Recombinant ELMOD (Cell Engulfment and Motility Domain) Proteins as GTPase-activating Proteins (GAPs) for ARF Family GTPases.* J Biol Chem, 2014. **289**(16): p. 11111-21.

11. Burd, C.G., T.I. Strochlic, and S.R. Gangi Setty, *Arf-like GTPases: not so Arf-like after all.* Trends Cell Biol, 2004. **14**(12): p. 687-94.

12. Kahn, R.A., et al., *Arf family GTPases: roles in membrane traffic and microtubule dynamics.* Biochem Soc Trans, 2005. **33**(Pt 6): p. 1269-72.

13. Gillingham, A.K. and S. Munro, *The small G proteins of the Arf family and their regulators.* Annu Rev Cell Dev Biol, 2007. **23**: p. 579-611.

14. Liu, Y.W., et al., *Role for Gcs1p in regulation of Arl1p at trans-Golgi compartments.* Mol Biol Cell, 2005. **16**(9): p. 4024-33.

15. Van Valkenburgh, H., et al., *ADP-ribosylation factors (ARFs) and ARF-like 1 (ARL1) have both specific and shared effectors: characterizing ARL1-binding proteins.* J Biol Chem, 2001. **276**(25): p. 22826-37.

16. Kahn, R.A., et al., *Consensus nomenclature for the human ArfGAP domain-containing proteins.* J Cell Biol, 2008. **182**(6): p. 1039-44.

17. Schlacht, A., et al., *Ancient complexity, opisthokont plasticity, and discovery of the 11th subfamily of Arf GAP proteins.* Traffic, 2013. **14**(6): p. 636-49.

18. Cukierman, E., et al., *The ARF1 GTPase-activating protein: zinc finger motif and Golgi complex localization.* Science, 1995. **270**(5244): p. 1999-2002.

19. Veltel, S., et al., *The retinitis pigmentosa 2 gene product is a GTPase-activating protein for Arf-like 3.* Nat Struct Mol Biol, 2008. **15**(4): p. 373-80.

20. Hodgson, U., et al., *ELMOD2 is a candidate gene for familial idiopathic pulmonary fibrosis.* Am J Hum Genet, 2006. **79**(1): p. 149-54.

21. Pulkkinen, V., et al., *ELMOD2, a candidate gene for idiopathic pulmonary fibrosis, regulates antiviral responses.* Faseb J, 2010. **24**(4): p. 1167-77.

22. Johnson, K.R., C.M. Longo-Guess, and L.H. Gagnon, *Mutations of the mouse ELMO domain containing 1 gene (Elmod1) link small GTPase signaling to actin cytoskeleton dynamics in hair cell stereocilia*. PLoS One, 2012. **7**(4): p. e36074.

23. Jaworek, T.J., et al., *An alteration in ELMOD3, an Arl2 GTPase-activating protein, is associated with hearing impairment in humans.* PLoS Genet, 2013. **9**(9): p. e1003774.

24. Ciuman, R.R., *Auditory and vestibular hair cell stereocilia: relationship between functionality and inner ear disease.* J Laryngol Otol, 2011. **125**(10): p. 991-1003.

25. Angeli, S., X. Lin, and X.Z. Liu, *Genetics of hearing and deafness.* Anat Rec (Hoboken), 2012. **295**(11): p. 1812-29.

26. Drummond, M.C., et al., *Actin in hair cells and hearing loss.* Hear Res, 2012. **288**(1-2): p. 89-99.

27. Gumienny, T.L., et al., *CED-12/ELMO, a novel member of the CrkII/Dock180/Rac pathway, is required for phagocytosis and cell migration.* Cell, 2001. **107**(1): p. 27-41.

28. Chung, S., et al., *A common set of engulfment genes mediates removal of both apoptotic and necrotic cell corpses in C. elegans.* Nat Cell Biol, 2000. **2**(12): p. 931-7.

29. Brugnera, E., et al., *Unconventional Rac-GEF activity is mediated through the Dock180-ELMO complex.* Nat Cell Biol, 2002. **4**(8): p. 574-82.

30. Lu, M., et al., *PH domain of ELMO functions in trans to regulate Rac activation via Dock180.* Nat Struct Mol Biol, 2004. **11**(8): p. 756-62.

31. Wu, Y.C., et al., *C. elegans CED-12 acts in the conserved crkII/DOCK180/Rac pathway to control cell migration and cell corpse engulfment.* Dev Cell, 2001. **1**(4): p. 491-502.

32. Zhou, Z., et al., *The C. elegans PH domain protein CED-12 regulates cytoskeletal reorganization via a Rho/Rac GTPase signaling pathway.* Dev Cell, 2001. **1**(4): p. 477-89.

33. Lu, M., et al., *A Steric-inhibition model for regulation of nucleotide exchange via the Dock180 family of GEFs.* Curr Biol, 2005. **15**(4): p. 371-7.

34. Hall, A., *Rho family GTPases.* Biochem Soc Trans, 2012. **40**(6): p. 1378-82.

35. Eden, S., et al., *Mechanism of regulation of WAVE1-induced actin nucleation by Rac1 and Nck.* Nature, 2002. **418**(6899): p. 790-3.

36. Chen, Z., et al., *Structure and control of the actin regulatory WAVE complex.* Nature, 2010. **468**(7323): p. 533-8.

37. Grimsley, C.M., et al., *Dock180 and ELMO1 proteins cooperate to promote evolutionarily conserved Rac-dependent cell migration.* J Biol Chem, 2004. **279**(7): p. 6087-97.

38. Santy, L.C., K.S. Ravichandran, and J.E. Casanova, *The DOCK180/Elmo complex couples ARNO-mediated Arf6 activation to the downstream activation of Rac1*. Curr Biol, 2005. **15**(19): p. 1749-54.

39. Santy, L.C. and J.E. Casanova, *Activation of ARF6 by ARNO stimulates epithelial cell migration through downstream activation of both Rac1 and phospholipase D.* J Cell Biol, 2001. **154**(3): p. 599-610.

40. Myers, K.R. and J.E. Casanova, *Regulation of actin cytoskeleton dynamics by Arf-family GTPases.* Trends Cell Biol, 2008. **18**(4): p. 184-92.

41. Sander, E.E., et al., *Rac downregulates Rho activity: reciprocal balance between both GTPases determines cellular morphology and migratory behavior.* J Cell Biol, 1999. **147**(5): p. 1009-22.

42. Raftopoulou, M. and A. Hall, *Cell migration: Rho GTPases lead the way.* Dev Biol, 2004. **265**(1): p. 23-32.

43. Ridley, A.J., et al., *Cell migration: integrating signals from front to back.* Science, 2003. **302**(5651): p. 1704-9.

44. Small, J.V., et al., *Assembling an actin cytoskeleton for cell attachment and movement.* Biochim Biophys Acta, 1998. **1404**(3): p. 271-81.

45. Pellegrin, S. and H. Mellor, *Actin stress fibres.* J Cell Sci, 2007. **120**(Pt 20): p. 3491-9.

Chapter II

ELMO domains: evolutionary and functional characterization of a novel GTPase activating protein (GAP) domain for Arf family GTPases

Michael P. East[1], J. Bradford Bowzard[1], Joel B. Dacks[2], and Richard A. Kahn[1,3]

[1]From the Department of Biochemistry
Emory University School of Medicine, Atlanta, GA 30322

[2]Department of Cell Biology, Faculty of Medicine and Dentistry, University of Alberta, Edmonton, Alberta, Canada

This chapter was originally published in its entirety in J Biol Chem, 2012. **287**(47): p. 39538-53

ELMO domains: evolutionary and functional characterization of a novel GTPase activating protein (GAP) domain for Arf family GTPases*

Michael P. East[1], J. Bradford Bowzard[1], Joel B. Dacks[2], and Richard A. Kahn[1,3]

[1]From the Department of Biochemistry

Emory University School of Medicine, Atlanta, GA 30322

[2]Department of Cell Biology, Faculty of Medicine and Dentistry, University of Alberta, Edmonton, Alberta, Canada

*Running Title: Evolutionary and functional analyses of ELMO domains

To whom all correspondence should be addressed: Richard A. Kahn, Department of Biochemistry, Emory University School of Medicine, 1510 Clifton Road, Atlanta, GA, USA, Tel.: (404) 727-3561; E-mail: rkahn@emory.edu

Running title: Evolutionary and functional analyses of ELMO domains

Keywords: Arl2, phylogenetics, GTPase, Arf, Arl3, ELMO, GTPase activating protein (GAP)

Background: ELMOD family proteins function either as Rac guanine nucleotide exchange factors or Arf GTPase activating proteins.

Results: The ELMOD family spans eukaryotic diversity and contains a putative catalytic arginine, essential for Arf GAP function.

Conclusion: The ELMOD family is ancient and GAP activity lies within the ELMO domain.

Significance: This study establishes a function of the ELMO domain as a GTPase activating domain.

SUMMARY

The human family of ELMO domain-containing proteins (ELMODs) consists of six members and is defined by the presence of the ELMO domain. Within this family are two sub-classifications of proteins, based on primary sequence conservation, protein size and domain architecture, deemed ELMOD and ELMO. In this study, we used homology searching and phylogenetics to identify ELMOD family homologs in genomes from across eukaryotic diversity. This demonstrated not only that the protein family is ancient but also that ELMOs are potentially restricted to the supergroup Opisthokonta (Metazoa and Fungi), while proteins with the ELMOD organization are found in diverse eukaryotes and thus were likely the form present in the Last Eukaryotic Common Ancestor. The segregation of the ELMO clade from the larger ELMOD group is consistent with their contrasting functions as unconventional Rac1 guanine nucleotide exchange factors and Arf family GTPase activating proteins, respectively. We used this unbiased, phylogenetic sorting and sequence alignments to identify the most highly conserved residues within the ELMO domain to identify a putative GAP domain within the ELMODs. Three independent but complementary assays were used to provide an initial characterization of this domain. We identified a highly conserved arginine residue critical for both the biochemical and cellular GAP activity of ELMODs. We also provide initial evidence of the function of human ELMOD1 as an Arf family GAP at the Golgi. These findings provide the basis for future study of the ELMOD family of proteins and a new avenue for the study of Arf family GTPases.

The human family of ELMO proteins consists of six members defined by the presence of the ELMO domain. These six proteins have been further divided into two subgroups, ELMOs and ELMODs, based on protein size and domain architecture (Fig 1). ELMOs are approximately twice as large as ELMODs and contain multiple domains including a domain of unknown function (DUF) 3361, predicted to contain Armadillo repeats, and a PH domain (1,2). The ELMODs consist of little more than the ELMO domain itself, which are typically ~300 residues in length. The only sequence homology between the ELMOs and ELMODs lies within the ELMO domain and, thus, this domain is the only common feature linking these two groups of proteins (3). However, no biochemical or cellular function or activity has been linked to the ELMO domain and it remains a domain of unknown function.

ELMO1 regulates actin rearrangement and is essential for phagocytosis and cell migration in *Caenorhabditis elegans (4-7)*. ELMO1 is also essential for the clearance of apoptotic germ cells and spermatogenesis (8,9) and has been implicated in the regulation of fibronectin expression levels (10,11). When bound to Dock180, the heterodimer functions as an unconventional guanine nucleotide exchange factor (GEF) for Rac1, a key regulator of actin dynamics, despite the absence of the Dbl homology domain (that is a characteristic of other Rac GEFs) on either ELMO or Dock180 (1). Instead, the ELMO1/Dock180 complex binds nucleotide-free Rac1 through the Docker domain of Dock180 to facilitate GTP loading (1,2). The Rac GEF activity is found within the Dock180 protein, though is stabilized or increased by its binding to ELMO (1,5,12,13). ELMO2 has also been shown to bind Dock180 and regulate the same pathways as ELMO1, but no functional information is currently available for ELMO3 (5). The regions of ELMO1 required to mediate both Rac1 GEF activity and changes to the actin cytoskeleton have been mapped to areas outside of the ELMO domain (5,7,12,14). Thus, the function of the ELMO domain in these or other processes remains unknown.

ELMOD2 was purified based on its GTPase activating protein (GAP) activity for Arl2, a member of the Arf family of regulatory GTPases (3). The Arf family consists of at least 30

members in mammals including 6 Arf, 22 Arl, and 2 Sar proteins (15). Arf and Sar regulate membrane traffic at virtually every step of the endocytic and secretory pathways to initiate carrier formation by coordinate recruitment of soluble adapters and coat machinery to the surface of the membrane as well as localized changes to phospholipid metabolism (16,17). Arls are largely functionally distinct from Arf and Sar and are involved in a diverse array of cellular functions including energy metabolism, cytoskeleton dynamics (18), cytokinesis, lipid droplet formation, cilia functions (19,20), recruitment of Golgins to the Golgi (21,22), and other aspects of membrane traffic (23). ELMOD2 represents the first GAP identified for any of the 22 mammalian Arl proteins and tests of the other ELMO family members revealed that only ELMOD1 shared this Arl2 GAP activity (3). To date, only one other GAP for any mammalian Arl protein has been identified, retinitis pigmentosa protein 2 (RP2), which has GAP activity for Arl3 (24), though it shares no sequence homology with ELMOD1 or ELMOD2.

Tests of the specificity of ELMOD2 for a limited number of other Arf family members revealed that ELMOD2 also had GAP activity for each of the Arf family members tested; including Arl3, Arf1, and Arf6 (3). Such specificity for both Arfs and Arls is unprecedented, as none of the 31 known human Arf GAPs have been shown to exhibit GAP activity for any Arl proteins. The Arf GAP Gcs1 in *Saccharomyces cerevisiae* was shown to possess GAP activity for both Arfs and Arl1, a key regulator of membrane traffic at the Golgi, but this was not completely unexpected given their close sequence conservation and functional relatedness (25). ELMOD2 lacks the canonical Arf GAP domain found in every other known Arf GAP, consisting of a zinc finger motif of four cysteine residues with specific spacing culminating in a highly conserved arginine residue that functions as a "catalytic arginine" residue ($CX_2CX_{16-18}CX_2CX_4R$) (26,27). The catalytic arginine is the only residue that the GAP contributes to the site of GTP hydrolysis and even subtle mutations of this arginine are usually sufficient to reduce GAP activity by several orders of magnitude (28). Thus, the catalytic arginine is critical for the biochemical GAP activity of the Arf GAPs. This catalytic arginine mechanism extends well beyond the Arf family and is a

very common, but not universal, feature of GAPs acting on other small regulatory GTPases including Rho and Ras family members, despite the highly divergent sequences and structures of the different GAPs (28).

Considering that ELMODs consist of little more than the ELMO domain itself, it is likely that the GAP activity of these proteins resides within the ELMO domain but Arl2 GAP activity was not detected for any of the ELMOs. Thus, the defining domain of the family may have distinct cellular and biochemical functions between ELMOs and ELMODs and potentially even within the subgroups.

ELMO family members have only been described in metazoans (primarily mammals and *C. elegans*) and in two studies with the amoeba, *Dictyostelium discoideum* (29,30) suggesting some evolutionary conservation. One study examined the phylogenetics of the ELMO family but only examined five species sampling fungi, metazoa, and *D. discoideum (31)*. The diversity of eukaryotes extends well beyond this range, encompassing parasites, algae and plants in six large taxonomic divisions or 'super-groups' of eukaryotes (32). Molecular evolutionary studies of proteins involved in membrane traffic have demonstrated that, with some important exceptions (33), much of the protein machinery implicated in vesicular transport is conserved across this span implying generality of cell biological models and a surprisingly complex endomembrane system in the LECA (34,35).

In this study, we used homology searching and phylogenetic analysis of ELMO domains to discover that ELMODs are an ancient family and that the ELMOs emerged as a distinct clade only in the Opisthokonta and are thus predicted to have acquired a distinct set of cellular functions. We also identify the GAP domain of the ELMODs and perform initial characterization of the most highly conserved arginine in ELMODs throughout eukaryotic evolution and test it for potential function as a catalytic arginine. Results of this study also offer initial evidence for the function of ELMOD1 as an Arf GAP in cells.

EXPERIMENTAL PROCEDURES

Identification of ELMO Family Members – Candidate ELMO family members were identified by protein Basic Local Alignment Search Tool (BLASTp) of each of the six full length human ELMO family members against predicted proteomes spanning as much eukaryotic diversity as possible. Based on the present understanding of eukaryotic relationships (36,37), our sampling represents the full span of eukaryotic diversity. Candidate protein sequences were identified by initial BLASTp expect value ≤ 0.05 for any single human ELMO family member. Candidate protein sequences were verified by reciprocal BLASTp expect values of ≤ 0.05. The full list of species searched, along with all putative ELMO and ELMOD candidate homologs and their relevant accession number is found in Table S1.

Phylogenetic Analysis – The ELMO domain from each protein sequence was identified and isolated by BLAST against the Conserved Domain Database. Protein sequences without ELMO domains recognized by the Conserved Domain Database were excluded from the analysis (e.g. four of 75 proteins). Isolated ELMO domains were aligned using MUSCLE v3.6 (38) and manually adjusted to only include regions of unambiguous homology. An initial set of 71 sequences from 24 species spanning eukaryotic diversity consisting of 123 homologous positions was used to analyze the distribution of ELMOs and ELMODs among eukaryotes. A second analysis was then performed using a set of 20 genes identified as ELMOs from 11 species of metazoa consisting of 709 homologous positions was used to resolve the emergence order of metazoan ELMOs. For each analysis, ProtTest (v. 2.4; http://darwin.uvigo.es/software/prottest.html; (39)) was used to determine the optimal model for sequence evolution. Three phylogenetic algorithms were used to analyze each dataset: PhyML (v. 2.44; http://www.atgc-montpellier.fr/phyml/; (40)), RaxML (v. 2.2.3; http://icwww.epfl.ch/~stamatak/index-Dateien/Page443.htm; (41)), and MrBayes (v. 3.2.1; http://mrbayes.csit.fsu.edu/; (42)) The latter was used to determine tree topology and posterior probability values. For PhyML and RaxML, 100 pseudoreplicates were analyzed. For MrBayes,

1×10^6 generations were used and burnin values were assessed by removing trees before a graphically determined plateau. Convergence was determined by ensuring a splits frequency less than 0.1 in all cases.

Antibodies, Cells, and Reagents -- All chemicals used were purchased from commercial sources. Rabbit polyclonal antibodies to human ELMOD1 were generated by immunization of rabbits with a purified, recombinant fusion protein of human ELMOD1 tagged at the C-terminus with maltose binding protein, ELMOD1-MBP. Immunizations and sera collections were performed by Strategic Biosolutions. Other antibodies used were mouse monoclonals GM130 (BD Biosciences), β-tubulin (Sigma), SC35 (BD Biosciences) and rabbit polyclonals raised against Arf1 (43) or ATGL (Cell Signaling Technologies).

Cloning and Plasmids -- The plasmids directing the expression of ELMOD1-myc/His and ELMOD2-myc/His were previously described (3) and plasmids for the expression of ELMOD1 and ELMOD2 mutants were derived from these plasmids using the QuikChange Site-Directed Mutagenesis Kit (Stratagene). All mutations were confirmed by DNA sequencing to ensure the desired mutation was incorporated and that others were not. Plasmids for the bacterial expression of trigger factor fusions of ELMOD1 and ELMOD2 were constructed using the pCold™ TF vector (Takara Bio Inc.). The Tet-on inducible expression plasmid for ELMOD1-HA for lentiviral infection was constructed from ELMOD1-myc/His using the tCMV/GFP/Ubi/rtTA2SM2 expression plasmid (Emory Viral Vector Core) and the expression plasmid for ELMOD1(R174K)-HA was derived from this plasmid. Lentiviruses were made by the Emory Viral Vector Core. The plasmid used for the bacterial expression of GST-GGA3 was a kind gift from James Casanova (University of Virginia) (44).

Preparation of Recombinant Proteins -- Purified, recombinant Arl2 was prepared as previously described (45). Expression plasmid for GST-GGA3 was transformed into *E. coli* BL21(DE3) and a single colony was picked into LB medium. Cultures were grown at 37°C until A_{600} = 0.6 when they were induced with 1mM isopropyl 1-thio-β-D-galactopyranoside for 3.5

hours. Cells were then harvested and lysed by multiple passes through a French press. GST-GGA3 Sepharose beads were made by incubating lysate with Glutathione Sepharose 4B beads (GE Healthcare) for 1 hour at 4°C with rocking. GST-GGA3 conjugated beads were spun, washed, and stored at -80°C for no more than 30 days. Plasmids directing expression of trigger factor fusions of ELMOD1 and ELMOD2 were transformed into *E. coli* BL21(DE3) and a single colony was picked into LB medium. Cultures were grown at 37°C until A_{600} = 0.4 when they were cooled to 15°C for 30 minutes. Protein expression was induced with 0.5mM 1-thio-β-D-galactopyranoside at 15°C for 16 hours. Cells were then harvested and lysed by multiple passes through a French press and protein was purified using a Ni Sepharose column.

Cell Culture and Immunofluorescence -- HeLa and NRK cells were grown in Dulbecco's modified Eagle's medium containing 10% fetal calf serum (GIBCO). Cells were transfected with Lipofectamine 2000 according to the manufacturer's directions (Invitrogen) for exogenous expression. NRK cells were transfected with Dharmafect 2 and Dharmacon OnTarget Plus Smartpool directed against rat ELMOD1 according to manufacturer's directions (Dharmacon). HeLa cell lines capable of the inducible expression of ELMOD1-HA and ELMOD1(R174K)-HA were generated by infecting cells with ELMOD1-HA or ELMOD1(R174K)-HA lentivirus. Protein expression was induced with 2 μg/mL doxycycline. Where indicated, HeLa cells were treated with 10 μM Brefeldin A (BFA) for 10 minutes at 37°C. For immunofluorescence, cells were fixed using 2% paraformaldehyde at room temperature for 15 minutes, washed four times in PBS, and then permeabilized with 0.05% saponin for 30 min at room temperature in blocking buffer containing 1% BSA in PBS. Cells were incubated in primary antibody overnight in blocking buffer, washed four times with a solution of 0.05% saponin in PBS (wash buffer) and labeled with Alexa Fluor 488 and Alexa Fluor 594 secondary antibodies (Invitrogen) at room temperature for one hour in blocking buffer. Cells were then washed twice and labeled with 1 μM Hoechst nuclear stain for five minutes in wash buffer. Cells were washed two more times with wash buffer then once with PBS before being mounted with Mowiol (46).

GAP Assays -- HeLa cell lysates were prepared from cells over-expressing ELMOD1-myc/His or ELMOD2-myc/His or their respective mutants and from mock transfected cells by incubating cells in 25mM HEPES pH 7.4, 100mM NaCl, 1% CHAPS on ice for 15 minutes followed by centrifugation at 14,000xg. The assay was performed as previously described (3) using recombinant Arl2 as a substrate and HeLa lysate or purified, recombinant, trigger factor fusion proteins as a source of GAP. Briefly, recombinant Arl2 was loaded with [γ-^{32}P]GTP at 30°C for 15 minutes in 25mM HEPES, pH 7.4, 100mM NaCl, 2.5mM $MgCl_2$, 1mM dithiothreitol, ~2μM Arl2, and ~0.3 μCi/μL [γ-^{32}P]GTP (6000 Ci/mmol; PerkinElmer Life Sciences). HeLa lysate (25 μL, 20 μg) or trigger factor fusion protein (25 μL, 20 μg TF-ELMOD1 or 2 μg TF-ELMOD2) was then mixed with 20 μL of reaction buffer (62.5 mM HEPES, pH 7.4, 6.25 mM $MgCl_2$, 2.5mM dithiothreitol, 4.2mM ATP, and 2.5mM GTP) on ice. The reaction was started by adding 5 μL of pre-loaded Arl2-[γ-^{32}P]GTP to the HeLa lysate in the reaction mixture, briefly vortexing, and placing in a 30°C water bath. The reaction was carried out for 4 minutes at which time it was stopped by the addition of 750 μL of a suspension of ice-cold activated charcoal (5% in 50 mM NaH_2PO_4). The charcoal was pelleted and amount of $^{32}P_i$ in 400 μL of supernatant was determined by scintillation counting. In a parallel set of triplicate tubes, an equal amount of [γ-^{32}P]GTP to that used in the assay was incubated in the absence of Arl2 or cell lysates and treated with charcoal as described. The resulting free $^{32}P_i$ was quantified and subtracted from each value in the GAP assay as it reflects the level of GTP hydrolyzed prior to use in the assay.

GST-GGA3 Pull-down Assay for Activated Arf – ELMOD1-HA or ELMOD1(R174K)-HA was expressed in HeLa cells infected with lentivirus by induction with doxycycline. Levels of activated Arf in cell lysates were determined using a GST fusion of the Arf binding domain of the adaptor protein GGA3 as previously described (47). The levels of activated Arf in the pull-downs were determined by Western blotting with a polyclonal antibody against Arf1 (43). The level of ELMOD1 expression was determined by loading 4% of cleared starting lysate and was also

immunoblotted using our polyclonal ELMOD1 antibody. Cleared lysate was also immunoblotted for Arf1 and with a monoclonal antibody against β-tubulin as a loading control.

NRK cell fractionation and lipid droplet purification -- For cell fractionation, NRK cells were lysed via glass/glass Dounce homogenizer (40 strokes) in 10mM Tris-MOPS pH 7.4, 1mM EGTA/Tris, 200mM sucrose, protease inhibitor cocktail (Sigma). Cell homogenates were spun at 600x*g* for 10 minutes at 4°C and supernatants collected as post nuclear supernatants (PNS). PNS was spun at 11,000x*g* for 10 minutes at 4°C and the supernatant and pellet were collected as S11 and P11, respectively. The S11 was then spun at 100,000x*g* for 1 hour at 4°C and the supernatant and pellet were collected as S100 and P100. The protocol for lipid droplet purification was adapted from (48), HeLa cells were lysed via Potter-Elvehjem homogenizer with 8 strokes by hand in buffer (20mM Tris-HCl pH 7.4, 1mM EDTA, and protease inhibitor cocktail (Sigma)). Homogenate was spun at 1,000x*g* for 10 minutes at 4°C. The post-nuclear supernatant was collected and a solution of 60% sucrose in the same buffer was added to bring the final concentration of sucrose to 20%, which was then overlaid with 5mL of 5% sucrose and 6mL of 0% sucrose all in the same buffer. The gradient was spun at 28,000x*g* for 30 minutes at 4°C with no braking and 1mL fractions were collected. Fractions with lipid droplets were determined by immunoblot of fractions using an antibody against the lipid droplet marker ATGL.

ELMOD1 Knockdown -- HeLa or NRK cells were transfected with each of six pSUPER-based (49) constructs targeting the coding sequence of human ELMOD1 or ON-TARGET *plus* SMART pools targeting human and rat ELMOD1 (Dharmacon L-013812-01 and L-0-101035-02) according to manufacturer's directions. Cell lysates were prepared after 24, 48, or 72 hours by incubating cells in 25mM HEPES pH 7.4, 100mM NaCl, 1% CHAPS on ice for 15 minutes followed by centrifugation at 14,000xg. The level of endogenous ELMOD1 expression was determined by immunoblot using our polyclonal ELMOD1 antibody.

RESULTS

Phylogenetic analysis of the ELMO family of proteins To examine the distribution of ELMO family members among eukaryotes, we sampled genomic databases that should represent the full span of eukaryotic diversity (36,37). We identified ELMO domain-containing family members in species from every eukaryotic supergroup examined, suggesting that the family dates back to the last eukaryotic common ancestor (LECA). We failed to identify homologs in *Acanthamoeba castellanii* and *Takifugu rubripes*, which may be a matter of incompleteness of the database. However, we also failed to identify ELMOD homologs in the more complete databases of the parasitic *Plasmodium vivax* and *Entamoeba histolytica*. Although several fungi examined encoded one or more ELMO domain-containing family members, we did not identify any in the well-studied yeasts *Saccharomyces cerevisiae* or *Saccharomyces pombe*.

Within the human ELMO family there is a clear distinction between ELMO proteins (ELMOs) and ELMO domain proteins (ELMODs) in both their domain architecture (see Fig. 1) and function in cells (see above). To determine the distribution of each of these two functionally distinct subgroups, we performed a thorough phylogenetic analysis of the family of ELMO domain containing proteins. A total of 71 genes from 24 taxa were used in a maximum likelihood (ML) analysis using PhyML and RAxML and a Bayesian analysis using MrBayes, as described under Experimental Procedures. These three methods produced similar phylogenetic trees represented by the best Bayesian topology in Figure 2. A distinct, moderately supported clade (support values of 0.98/57/70) clustered various holozoan sequences with all three of the human ELMOs, suggesting that ELMOs represent a sub-family within the ELMODs. The tree also suggests that the ELMO sub-family includes fungi with support values of 1.0/58/62.

The clustering of ELMOs as a sub-family was further supported by the domain architecture of the proteins within this group. In addition to the ELMO domain, each protein contained the DUF3361 and PH domains found in each of the three human ELMOs, ELMO1-3. DUF3361 was not found outside of the ELMOD family but we cannot determine if the same is true of the ELMOD associated PH domain, due to the large number of PH domains and limited

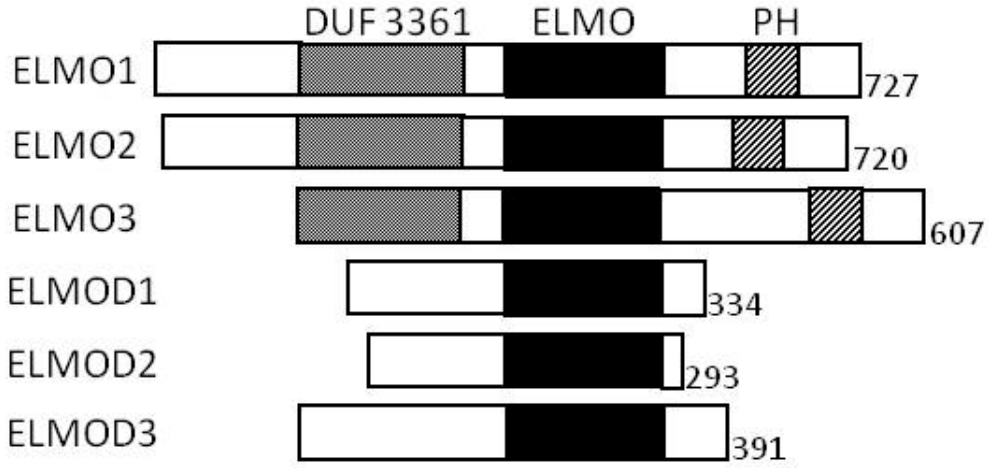

Figure 1: The six human ELMO domain-containing family members are equally divided into three ELMO and three ELMOD proteins. Each member of the family contains the ELMO domain (solid black). The three ELMOs also contain the domain of unknown function (DUF) 3361 (gray shading) and a pleckstrin homology (PH) domain (hatched). The presence of DUF3361 and PH domains in ELMO proteins is highly conserved in opisthokonts.

sequence conservation among them. The presence of the PH domain is strongly correlated with that of DUF3361 in the ELMO sub-family as 20 out of 23 proteins clustering as ELMO homologs by phylogenetic analysis had both domains. This correlation and the divergence of the ELMO domain are of considerable interest and suggest a possible functional relationship between these domains. DUF3361 is found only in proteins within the ELMO sub-family with two notable exceptions. One of the five ELMOD family members (ElmoD_A) in the apusomonad *T. trahens*, a putative sister-group to the Opisthokonta supergroup (50,51), and one of six ELMOD family members (ElmoA) in the amoebozoan *D. discoideum* contains DUF3361 but no PH domain. These proteins did not cluster with the ELMO sub-family, but no strongly supported nodes separate them. Interestingly, however, the next closest, albeit unsupported, branches to the ELMO sub-family are also from *T. trahens* and *D. discoideum*. Together these raise the possibility that ELMOs may also be found in amoebas and that their origin may lay within the Unikonts, i.e. the group of opisthokonts and amoebozoans. Regardless, due to the species limitation of the ELMO sub-family and because the majority of the remaining proteins (which span the breadth of sampled eukaryotic diversity) contain only the ELMO domain, we speculate that the remaining proteins represent the more ancient form of the ELMO domain containing family and will refer to these proteins (those that did not resolve with the fungal or animal ELMOs) as ELMODs.

We were interested to see the resolution of the ELMOs, for which we have the most functional information, into a distinct phylogenetic group so we further pursued this sub-family with a more specific analysis of the ELMO sub-family alone. Fungi and more basal metazoan lineages (e.g. insects and sponges) contained only a single ELMO sub-family protein while in vertebrates, including mammals and fish, an expansion of the sub-family was observed. Thus, to further study this gene duplication, we sampled additional metazoan genomes and performed a phylogenetic analysis limited to metazoan ELMO proteins. This revealed three distinct and well supported clades classified as ELMO1, ELMO2 and ELMO3 based on three human ELMO sequences as landmarks (Fig. 3). The ELMO1 and ELMO2 clades are clearly defined and span

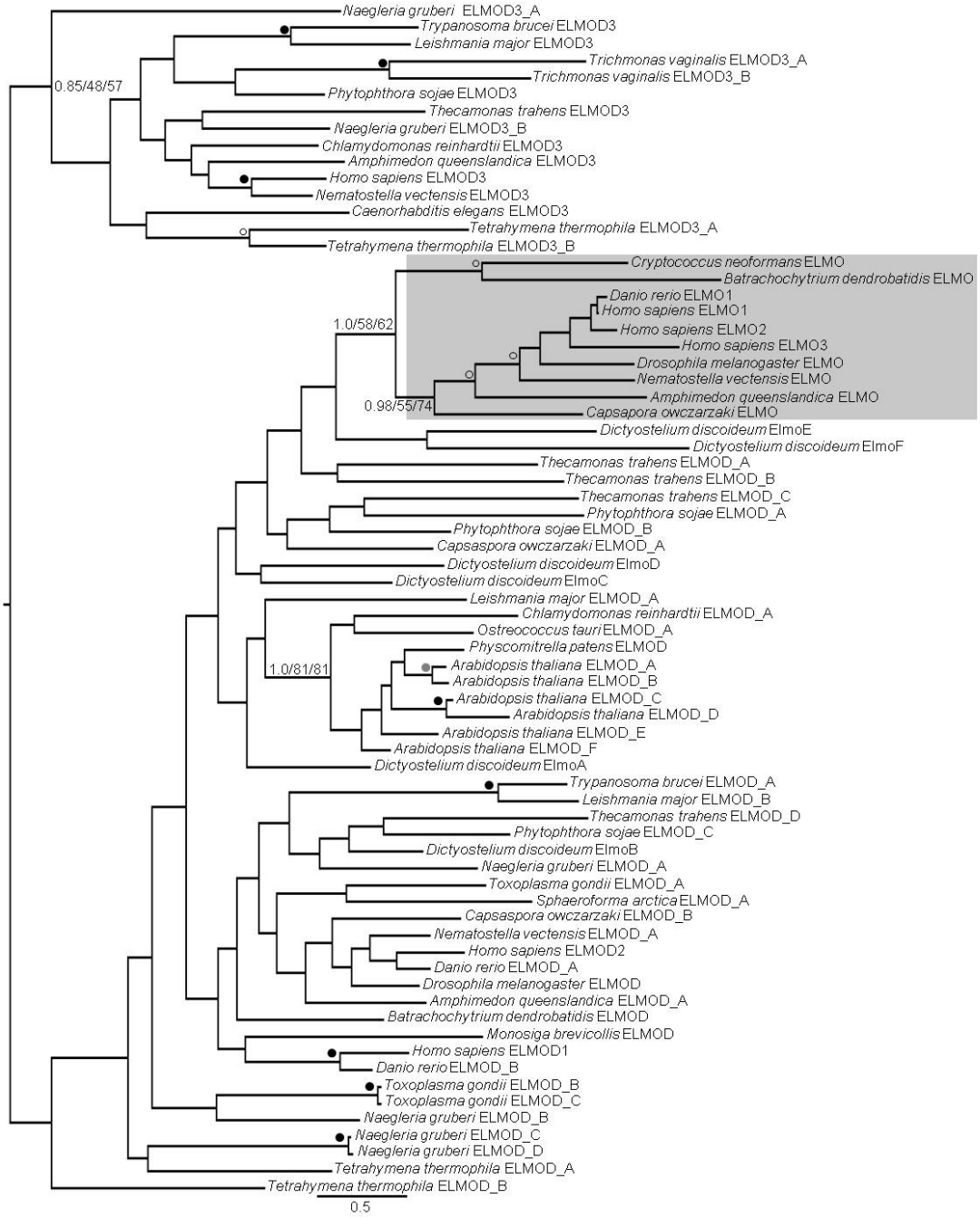
Naegleria gruberi ELMOD3_A
Trypanosoma brucei ELMOD3
Leishmania major ELMOD3
Trichmonas vaginalis ELMOD3_A
Trichmonas vaginalis ELMOD3_B
0.85/48/57
Phytophthora sojae ELMOD3
Thecamonas trahens ELMOD3
Naegleria gruberi ELMOD3_B
Chlamydomonas reinhardtii ELMOD3
Amphimedon queenslandica ELMOD3
Homo sapiens ELMOD3
Nematostella vectensis ELMOD3
Caenorhabditis elegans ELMOD3
Tetrahymena thermophila ELMOD3_A
Tetrahymena thermophila ELMOD3_B
Cryptococcus neoformans ELMO
Batrachochytrium dendrobatidis ELMO
Danio rerio ELMO1
Homo sapiens ELMO1
1.0/58/62
Homo sapiens ELMO2
Homo sapiens ELMO3
Drosophila melanogaster ELMO
Nematostella vectensis ELMO
Amphimedon queenslandica ELMO
0.98/55/74
Capsapora owczarzaki ELMO
Dictyostelium discoideum ElmoE
Dictyostelium discoideum ElmoF
Thecamonas trahens ELMOD_A
Thecamonas trahens ELMOD_B
Thecamonas trahens ELMOD_C
Phytophthora sojae ELMOD_A
Phytophthora sojae ELMOD_B
Capsaspora owczarzaki ELMOD_A
Dictyostelium discoideum ElmoD
Dictyostelium discoideum ElmoC
Leishmania major ELMOD_A
Chlamydomonas reinhardtii ELMOD_A
Ostreococcus tauri ELMOD_A
Physcomitrella patens ELMOD
1.0/81/81
Arabidopsis thaliana ELMOD_A
Arabidopsis thaliana ELMOD_B
Arabidopsis thaliana ELMOD_C
Arabidopsis thaliana ELMOD_D
Arabidopsis thaliana ELMOD_E
Arabidopsis thaliana ELMOD_F
Dictyostelium discoideum ElmoA
Trypanosoma brucei ELMOD_A
Leishmania major ELMOD_B
Thecamonas trahens ELMOD_D
Phytophthora sojae ELMOD_C
Dictyostelium discoideum ElmoB
Naegleria gruberi ELMOD_A
Toxoplasma gondii ELMOD_A
Sphaeroforma arctica ELMOD_A
Capsaspora owczarzaki ELMOD_B
Nematostella vectensis ELMOD_A
Homo sapiens ELMOD2
Danio rerio ELMOD_A
Drosophila melanogaster ELMOD
Amphimedon queenslandica ELMOD_A
Batrachochytrium dendrobatidis ELMOD
Monosiga brevicollis ELMOD
Homo sapiens ELMOD1
Danio rerio ELMOD_B
Toxoplasma gondii ELMOD_B
Toxoplasma gondii ELMOD_C
Naegleria gruberi ELMOD_B
Naegleria gruberi ELMOD_C
Naegleria gruberi ELMOD_D
Tetrahymena thermophila ELMOD_A
Tetrahymena thermophila ELMOD_B
0.5

Figure 2: ELMOs cluster into a distinct phylogenetic sub-family. Isolated ELMO domains from ELMO family members spanning the diversity of eukaryotic evolution were collected for phylogenetic analysis using MrBayes, PhyML, and RaxML, as described under Experimental Procedures. The tree shows the best Bayesian topology and is rooted to highlight the separation of the ELMOD3 and ELMO clusters. Support values for the relevant nodes are provided and other nodes with strong (≥0.95/90/90), robust (≥0.9/80/80), or moderate (≥0.8/50/50) support are indicated with black, grey, and white dots, respectively. Gene names were assigned with either ELMO or ELMOD based on clustering with the human sub-families except for genes with established nomenclature from human and *Dictyostelium discoideum*. The ELMO sub-family is shown shaded. Scale bar indicates number of substitutions per site.

---

the diversity of the sampled vertebrates. The clustering of ELMO3 more closely to the single ELMOs from basal metazoa, if taken at face value, would suggest that ELMO3, which is only found in mammals, is the more ancient form of the ELMO sub-family and that ELMO3 would have been lost multiple times in higher eukaryotes including fish, amphibian and bird lineages. However, it is also possible, and perhaps more likely, that the ELMO3 cluster is simply more divergent and clustering with basal ELMOs as the result of long branch attraction.

In the large-scale analysis of ELMOD containing proteins (Fig 2), we did not observe significant resolution within the backbone of the ELMODs in the phylogenetic analysis. Interestingly, though not well supported (0.85/57/48), human ELMOD3 resolved differently than human ELMOD1 and ELMOD2 in a clade that contains the diversity of eukaryotes sampled. Thus, the ELMOD3 clade may represent a deep evolutionary split and raises the possibility of two ancestral ELMOD proteins present in the LECA. We also recovered a robustly supported clade of plant ELMODs (1.0/81/81) and consistently observed an expansion of the ELMOD family in higher plants with six members in Arabidopsis. Despite the fact that ELMO proteins (ELMOs) were discovered first and are currently better understood functionally, our evidence that the ELMODs arose much earlier in eukaryotic evolution, are present in every eukaryotic supergroup sampled, are more divergent in sequence, and that the ELMOs are proposed to have diverged from them, lead us to conclude that the most appropriate name of this family is ELMOD and not ELMO. This nomenclature also helps avoid confusion if we can refer to the ELMO clade

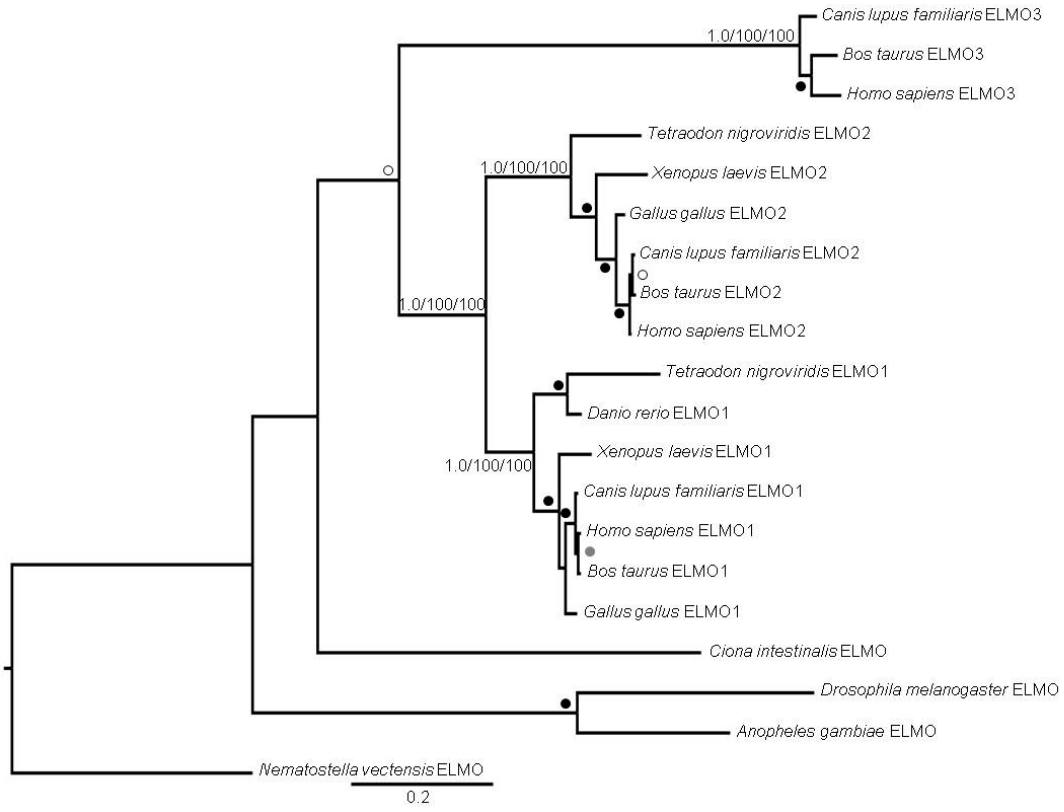

Figure 3: The ELMO sub-family is further divided into three distinct phylogenetic clades. Full-length sequences of ELMO sub-family members from metazoa were collected for phylogenetic analysis using MrBayes, PhyML, and RaxML. The tree shows the best Bayesian topology and is rooted on the basal organism of the analysis. Support values for the relevant nodes are provided and other nodes with strong (≥0.95/90/90), robust (≥0.9/80/80), or moderate (≥0.8/50/50) support are indicated with black, grey, and white dots, respectively. Gene names were assigned ELMO1, ELMO2, or ELMO3 based on clustering with the three human ELMOs. Scale bar indicates number of substitutions per site.

within the ELMOD family and not within the ELMO family. We will adhere to this nomenclature below in efforts to minimize confusion.

Identification of the GAP domain of the ELMODs Our previous work indicated that human ELMOD2 exhibited GAP activity against Arl2, Arl3, and Arf1 and ELMOD1 was active against Arl2 using *in vitro* GAP assays, while we failed to detect Arl2 GAP activity for any of the three human ELMOs or ELMOD3 (3). Because the ELMO proteins per se appear to be lineage-specific and derived versions of the larger ELMOD family, and because all other members of that family are composed of the ELMO domain alone, we speculated that it was this domain that contained the GAP activity. We next aligned sequences of ELMO domains from all ELMODs identified by the unbiased sorting of the phylogenetic analysis in an effort to identify key residues within the GAP domain. The region with the highest level of conservation consisted of a stretch of 26 residues with 13 very highly conserved sites. This putative GAP domain of the ELMODs has a consensus sequence of $WX_3G(F/W)QX_3PXTD(F/L)RGXGX_3LX_2L$ (Fig. 4). This consensus bears no obvious homology to previously described Arf GAP or other Ras superfamily GAP domains. Of particular interest was the presence of a very highly conserved arginine residue toward the middle of the consensus sequence. A mechanism frequently used by GAPs of the Ras superfamily uses an arginine residue that is essential for efficient GAP activity known as the "catalytic arginine." Thus, based upon sequence alignments of members of the ELMOD cluster we have identified a putative GAP domain as well as an arginine residue that is predicted to be critical to GAP activity. When alignments included both ELMOD and ELMO proteins (Fig. 5) we note a much lower level of sequence conservation in this region of ELMOs, including the absence of the highly conserved arginine, identified in the ELMODs.

Arginine mutations affect the biochemical GAP activity of ELMODs in vitro Recombinant human ELMOD2 was shown to have GAP activity against the Arf family members Arl2, Arl3, and Arf1 using an *in vitro* GAP assay, while ELMOD1 was only tested against Arl2 in the earlier study (3). We used a variation of this assay to test the importance of the putative

Figure 4: Sequence alignment of the ELMODs reveals a highly conserved motif that includes a central arginine residue. Sequences representing the diversity of eukaryotic ELMO domains from the ELMODs were aligned using MUSCLE. The region with the highest level of conservation consisted of a stretch of 26 residues (gray shading) with 13 very highly conserved sites (bold text). The same consensus sequence was obtained when all ELMOD sequences (shown in Figure 2) were used in the alignment. An (*) indicates a conserved residue with two possible identities (e.g. F/W or F/L). Gene names were assigned with prefix abbreviations to indicate genus and species (see Table S1).

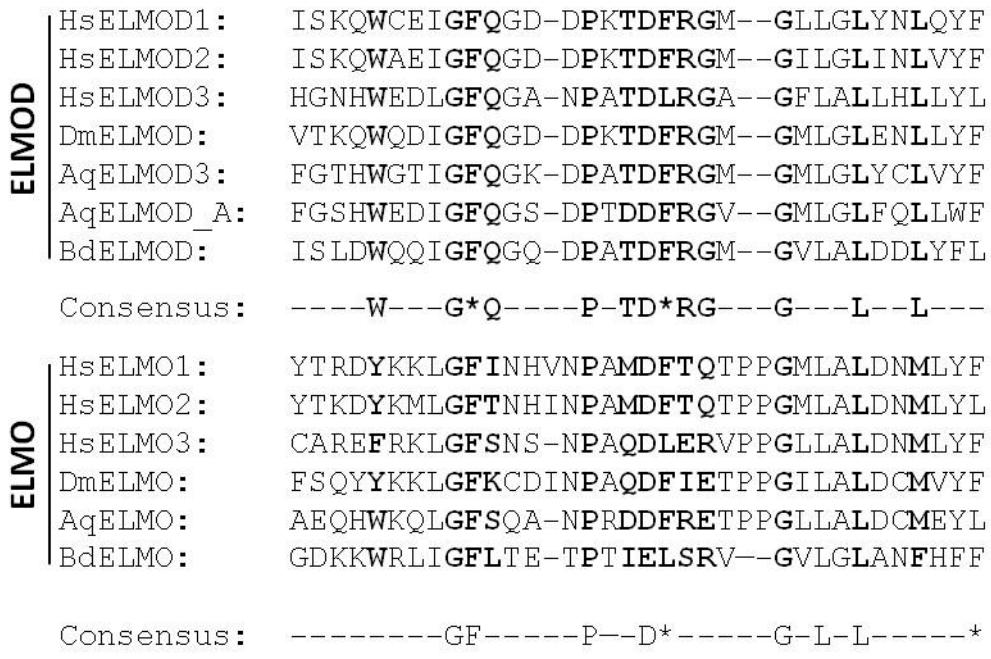

Figure 5: The putative catalytic arginine and some of the other residues within the putative GAP domain of the ELMODs (top) are not conserved in members of the ELMO sub-family (bottom). The ELMO domains from representative members of opisthokont ELMODs and the ELMO sub-family were aligned using MUSCLE. The putative GAP motif of ELMOD is indicated by bold text in the sequences from both sub-families to highlight the differences between ELMOD and ELMO in this region. Most notably, the putative catalytic arginine residue is not conserved in ELMO sub-family members. Consensus sequences of all ELMOD sub-family members analyzed in Fig. 2 are shown in the middle and the effect on this consensus of including the ELMO sub-family members shown is included in the consensus at the bottom. Gene names were assigned with prefix abbreviations to indicate genus and species (see Table S1).

catalytic arginine residue to the GAP activity of the ELMODs. Lysates from HeLa cells expressing ELMOD1 or ELMOD2 or their corresponding arginine mutants, tagged at the C-terminus with c-myc and His6 epitopes, were used as a source of GAP in the assays. HeLa lysates from cells expressing ELMOD1-myc/his or ELMOD2-myc/his had Arl2 GAP activity that was several (~3-5) fold higher than from mock transfected HeLa cells (Fig. 6A). Note that the Arl2 GAP activity present in controls is not solely the result of endogenous Arl2 GAP activity. The substrate in the assay, [γ-^{32}P]GTP, is susceptible to hydrolysis, e.g., by nucleotidases found in all cells. High concentrations of non-radioactive GTP and ATP are included in the GAP assay in efforts to minimize the contributions of this non-GAP mediated hydrolysis to the background, control levels, but we know that suppression is incomplete (3). Thus, the fold stimulation of Arl2 GAP activity resulting from expression of ELMOD1-myc/his or ELMOD2-myc/his seen in HeLa cell lysates is likely considerably greater than the ~3-5 fold increases shown in Fig. 6A, but for technical reasons a more accurate determination of fold increases in activity of total cell lysates is not possible in this assay.

To determine if the most highly conserved, homologous arginines in ELMOD1 and ELMOD2 were important to Arl2 GAP activity, we generated plasmids directing expression of the conservative arginine to lysine mutants for ELMOD1(R174K) and ELMOD2(R167K) in pCDNA3.1-myc/his and for ELMOD1(R174K) in lentiviral vectors. Expression of ELMOD1(R174K)-myc/his or ELMOD2(R167K)-myc/his by transient transfection of HeLa cells led to similar levels of expression as the wild-type proteins (Fig. 6B). We consistently have found that in the same vector(s) ELMOD1 is expressed to higher levels than is ELMOD2. When the cell lysates were assayed in the Arl2 GAP assay, we found that each of the arginine to lysine mutations was sufficient to completely ablate the increased GAP activity associated with ELMOD expression (Fig. 6A).

HeLa cells were also transduced with high titer stocks of lentiviruses that direct expression of ELMOD1 with a C-terminal HA epitope tag (ELMOD1-HA) or its arginine mutant,

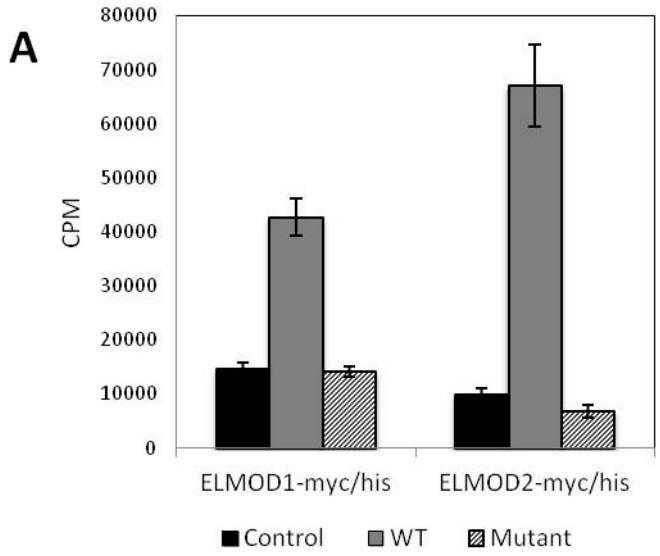
A
80000
70000
60000
50000
40000
30000
20000
10000
0
CPM
ELMOD1-myc/his
ELMOD2-myc/his
Control
WT
Mutant

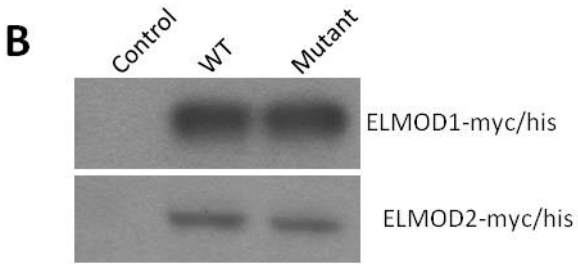
B
Control
WT
Mutant
ELMOD1-myc/his
ELMOD2-myc/his

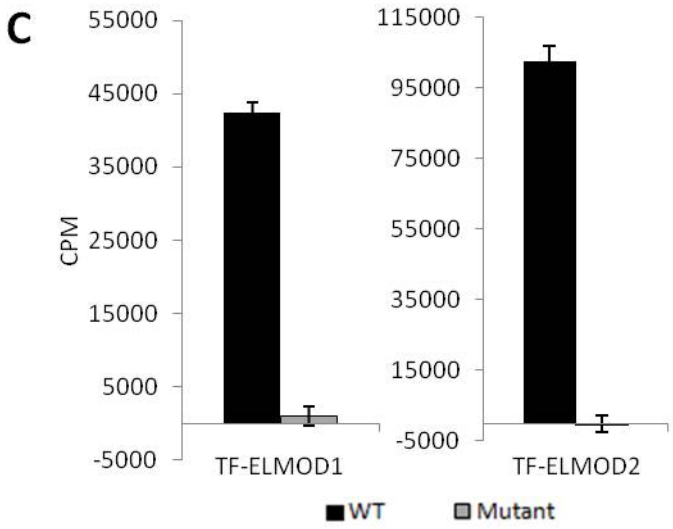
C
55000
45000
35000
25000
15000
5000
-5000
CPM
115000
95000
75000
55000
35000
15000
-5000
TF-ELMOD1
TF-ELMOD2
WT
Mutant

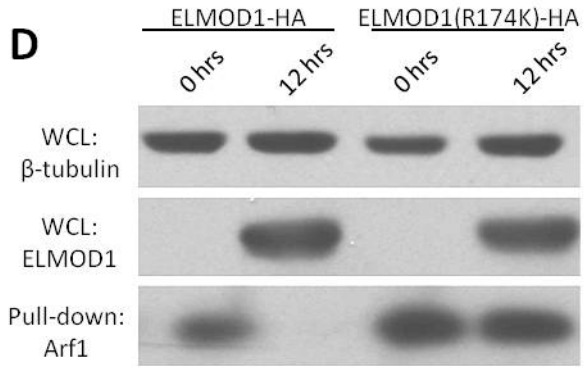

Figure 6: Mutation of the putative catalytic arginine residue reduces GAP activity of ELMOD1-myc/his and ELMOD2-myc/his in *in vitro* and cell-based assays. A. Arginine mutants of ELMOD1-myc/his or ELMOD2-myc/his have lost activity in *in vitro* Arl2 GAP assays. HeLa cells were transiently transfected with no DNA (control) or plasmid encoding ELMOD1-myc/his, ELMOD2-myc/his, or their corresponding arginine mutants (ELMOD1(R174K)-myc/his or ELMOD2(R167K)-myc/his, respectively) and 16 hours later cells were collected for assay. Whole cell lysates (20μg protein) were assayed for Arl2 GAP activity, as described under Experimental Procedures. Data shown are the averages from three independent assays, each performed in triplicate and bars represent one standard deviation. B. Wild type and arginine mutants are each expressed to the same levels. Immunoblots of HeLa lysates from control cells and those expressing ELMOD1-myc/his, ELMOD2-myc/his, or their corresponding arginine mutants show equal expression of wild type and mutant protein. Lysates from ELMOD1-myc/his cells (10 μg total cell protein) and ELMOD2-myc/his cells (20 μg total cell protein) were analyzed by immunoblot with ELMOD1 and ELMOD2 antibodies, respectively. Note that while each wild type/mutant pair expressed to the same levels, ELMOD1 expressed to roughly 10 times the levels seen for ELMOD2. For this reason, the immunoblot shown in the bottom panel was exposed for longer times than that shown on the top. C. Arginine mutants of purified recombinant TF-ELMOD1 or TF-ELMOD2 have lost activity in *in vitro* Arl2 GAP assays. Purified proteins were assayed for Arl2 GAP activity, as described under Experimental Procedures. Data shown are from a single experiment representative of at least three repetitions performed in duplicate and bars represent one standard deviation. D. ELMOD1-HA but not ELMOD1(R174K)-HA lowers levels of activated Arf1 pulled down from HeLa cell lysates. HeLa cells were previously transduced with lentiviruses carrying ELMOD1 proteins whose expression was induced by doxycycline (2 μg/mL for 0 or 12 hours). Lysates were prepared and the GST-GGA3 pull-down for activated Arf (Arf-GTP) was performed, as described under Experimental Procedures. HeLa whole cell lysate (WCL; 20 μg) was analyzed by immunoblot using antibodies specific for β-tubulin to show equal protein loading (top panel) and ELMOD1 (middle panel) to show equal expression of wild type and mutant proteins. The levels of Arf1 from pull-downs were determined by immunoblot with our Arf1-specific antibody (bottom panel).

ELMOD1 (R174K)-HA, under control of the tet-ON promoter. In this case, controls were cells grown in the absence of doxycycline and protein expression was achieved by exposure to 2 μg/mL doxycycline for 16 hours. The levels of induced protein expression achieved were lower than those seen after transient transfections but were the same between ELMOD1-HA and ELMOD1 (R174K)-HA (Fig. 6). We found lower levels of Arl2 GAP activity in HeLa lysates with viral expression than transients but again the mutation of arginine 174 to lysine was sufficient to eliminate the increased Arl2 GAP activity (data not shown). Thus, mutation of the putative catalytic arginine is sufficient to ablate Arl2 GAP activity of ELMOD1-myc/his, ELMOD2-myc/his, or ELMOD1-HA in *in vitro* assays.

To confirm that the assayed Arl2 GAP activities were the direct result of ELMOD protein and that mutation of the conserved arginine residues directly affected this activity, we generated purified recombinant protein stocks of ELMOD1 and ELMOD2 and their corresponding arginine mutants. Initial attempts to generate soluble recombinant stocks were unsuccessful as a number of constructs and fusion proteins were almost entirely insoluble. Fusion at the N-terminus with the prokaryotic chaperone Trigger Factor (TF) increased solubility allowing for the expression and purification of milligram quantities of recombinant proteins. TF-ELMOD1 and TF-ELMOD2 exhibited detectable Arl2 GAP activity (Fig. 6C) but their specific activities were estimated to be less than 0.1% of ELMOD2 purified from bovine testes (3). Despite the low specific activity, the high solubility and ease of purification from bacteria allowed us to use relatively high concentrations of the TF fusion proteins in Arl2 GAP assays and without the concerns of other HeLa proteins contributing, directly or indirectly, to activities. No Arl2 GAP activity was detected for TF-ELMOD1 (R174K) or TF-ELMOD2 (R167K) (Fig. 6C). Thus, loss of Arl2 GAP activity is a direct consequence of mutation of the conserved arginine and not the result of some indirect effect.

The effects of mutation of the putative catalytic arginine residue were also examined using a cell-based assay for Arf GAP activity developed in the laboratory of James Casanova

(University of Virginia). Briefly, a GST fusion of the Arf binding domain of the Arf-dependent adaptor GGA3 was used to selectively precipitate endogenous, activated Arfs (Arf-GTP) from cell lysates to estimate the level of activated Arf under different conditions. We used the doxycycline-inducible lentiviral expression system for ELMOD1-HA or ELMOD1(R174K)-HA in HeLa cells to compare activated Arf levels of control cells to those in cells expressing ELMOD1-HA. Expression of ELMOD1-HA substantially reduced the levels of activated Arf1 that could be brought down with GST-GGA3 (Fig. 6D, bottom panel), consistent with the recombinant protein acting in cells as an Arf1 GAP. We used our Arf-specific antisera to test for specificity amongst the soluble Arfs and found that the expression of ELMOD1-HA led to clear decreases in the levels of activated Arf1 or Arf3, the most abundantly expressed Arfs in most cell lines, but technical concerns and lower levels of endogenous protein expression limited definitive answers as to effects on Arf4 or Arf5. We believe that the expressed ELMOD1 is acting directly on Arfs in cells but cannot rule out less direct mechanisms of action in reducing cellular Arf activities. Nevertheless, this is the first evidence to suggest that an ELMO domain containing protein demonstrates GAP activity against Arfs in cells.

We next used the same assay and inducible lentiviral expression system to assess GAP activities from cell lysates expressing ELMOD1(R174K)-HA. Expression of ELMOD1(R174K)-HA to the same level as ELMOD1-HA had little to no effect on the amount of activated Arf1 brought down by GST-GGA3, in comparison to uninduced control lysates (Fig. 6D). Thus, the GAP activity of ELMOD1(R174K) mutants against purified recombinant Arl2 and endogenous Arf1 were considerably lower than that of tagged ELMOD1 against the same proteins in the same assays, suggesting that the putative catalytic arginine residue is critical for these activities.

Expression of ELMOD2-HA in lentivirus-infected HeLa cells with doxycycline induction had no effect on cellular levels of activated Arf in this assay. ELMOD2-HA was expressed to substantially lower levels than ELMOD1-HA. Thus, it is unclear whether expression levels of ELMOD2-HA were insufficient to detect a change in the levels of activated Arf, ELMOD2-HA

did not localize to regions of the cell containing high levels of activated Arfs, or whether ELMOD2-HA did not exhibit Arf GAP activity when expressed in cells under these conditions.

ELMOD1-HA and ELMOD1(R174K)-HA display different phenotypes when expressed in HeLa cells. We next used our inducible lentiviral expression system in efforts to determine the cellular location of ELMOD1 (about which nothing is currently known) as well as effects of protein over-expression on cell functions. Human ELMOD1-HA expression was induced and HeLa cells were fixed at the earliest times after detection of protein expression, in an effort to minimize artifacts resulting from over-expression. We observed that at early times of expression (e.g., 3 hr) there was a strong increase in the perinuclear staining with either our ELMOD1 rabbit polyclonal antibody or a commercial HA monoclonal antibody (Covance). Indeed, images obtained from these antibodies were superimposable, indicating that the induced protein was being identified by each. The perinuclear compartment to which ELMOD1-HA localized at early times of expression was identified as Golgi by double labeling with at least 15 markers of different organelles (e.g., LAMP1, EEA1, transferrin receptor, TOM20, calnexin, etc.). The most extensive overlap in staining was clearly between ELMOD1-HA and markers of the Golgi, e.g., GM130 (Fig. 7A; middle row).

The same procedure was carried out in HeLa cells expressing ELMOD1(R174K)-HA and we saw the same pattern of Golgi localization at early times (~3-5 hrs) of protein expression (Fig. 7B; middle panel). Thus, mutation of arginine 174 did not visibly alter the localization of ELMOD1 to the Golgi at early times in its expression. At later times (>6 hrs) we noted that both ELMOD1-HA and ELMOD1(R174K)-HA localization to the Golgi became less evident as the staining throughout the cell increased. At these and later times of expression of the two ELMOD1 proteins, the staining of Golgi markers began to diverge in appearance as the Golgi itself was altered by expression of ELMOD1-HA but not the R174K mutant.

Because Arfs also localize to the Golgi and we found earlier that ELMOD1 acts on Arfs in cells we speculated that its presence at that organelle might be responsible for changes in the

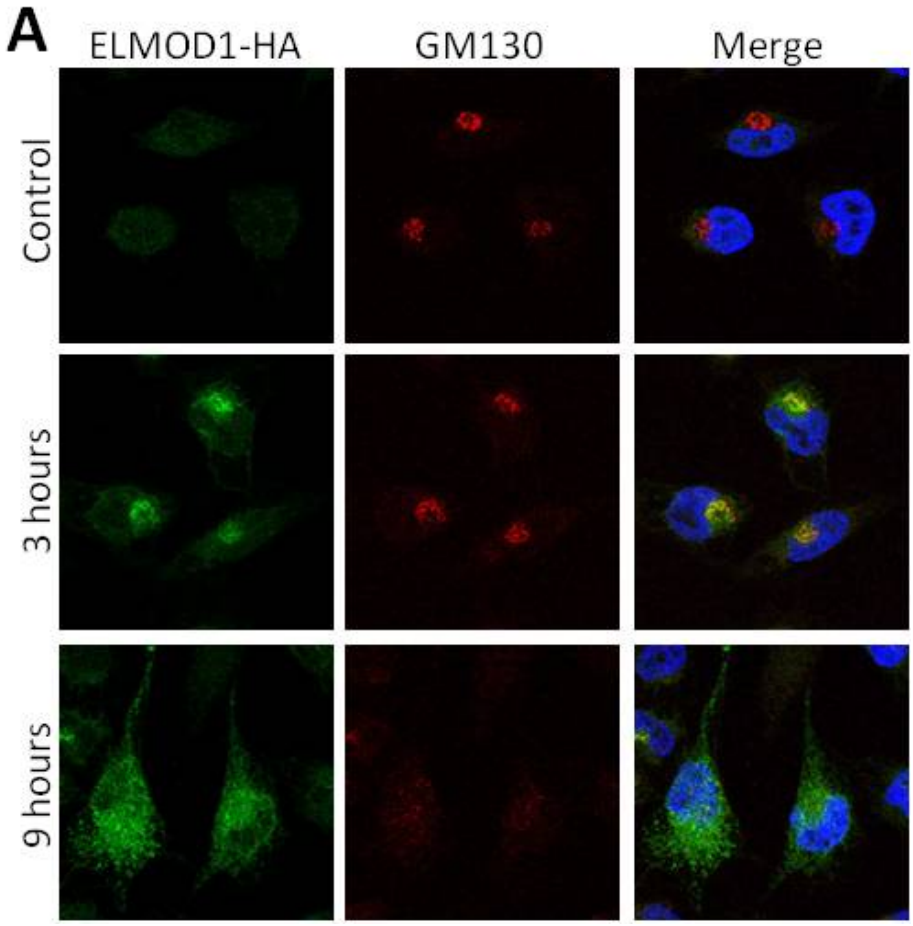

Figure 7: Over-expression of ELMOD1-HA alters Golgi morphology but this phenotype is absent for ELMOD1(R174K)-HA. Expression of ELMOD1-HA (A) or ELMOD1(R174K)-HA (B) was induced in lentivirus infected HeLa cells with doxycycline (2 μg/mL) for the given times. Note that ELMOD1-HA localizes to the Golgi at early times (3 hours; middle row) and disrupts Golgi morphology at later times (9 hours; bottom row) of expression but while localization is retained, the effect on Golgi morphology is lost with ELMOD1(R174K)-HA. (C) Uninfected cells were treated with 10 μM Brefeldin A (BFA) for 10 minutes as indicated. Cells were fixed and stained, as described under Experimental Procedures, using antibodies directed against ELMOD1 and GM130, a Golgi marker. Representative cells are shown for each condition.

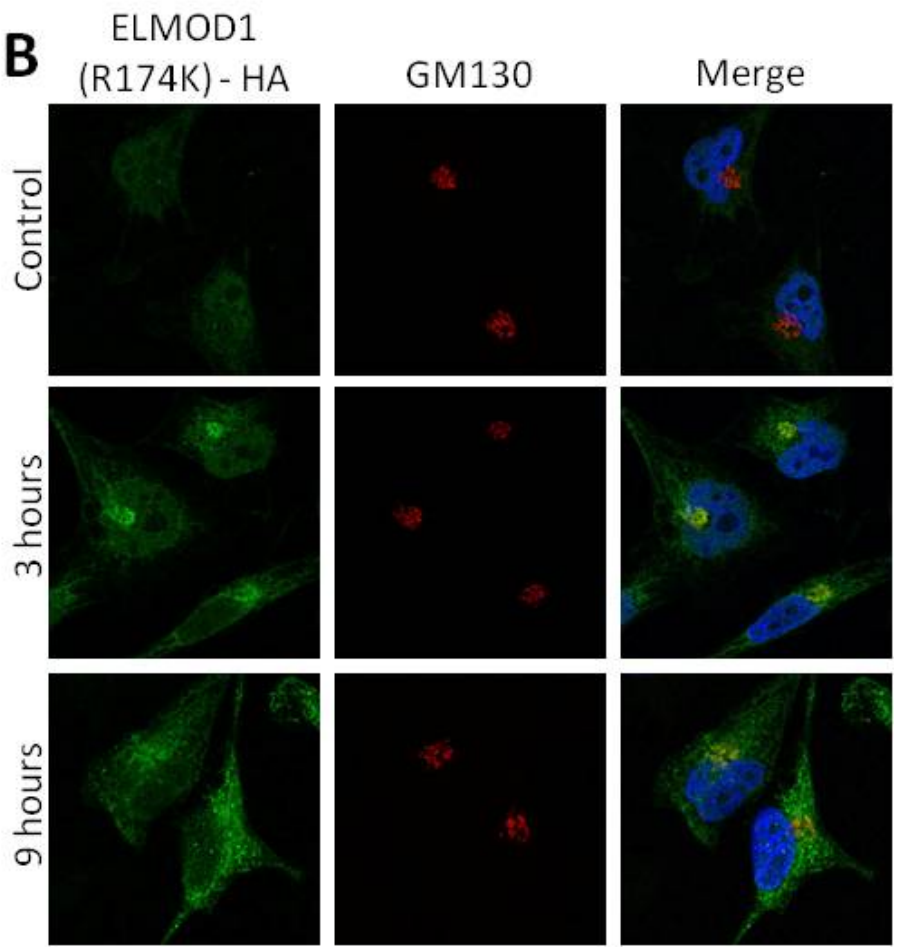
B
ELMOD1
(R174K) - HA
GM130
Merge
Control
3 hours
9 hours

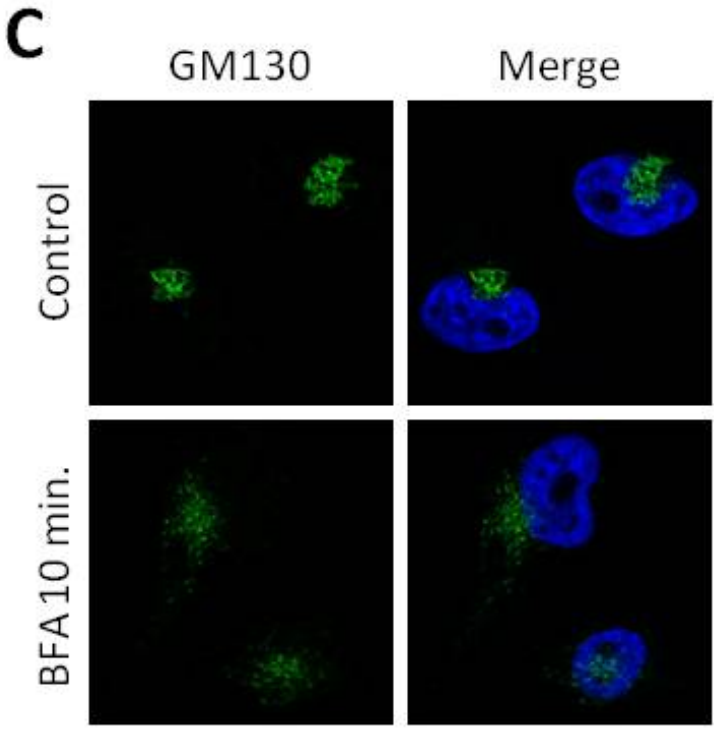
C
GM130
Merge
Control
BFA 10 min.

organelle itself. To determine whether expression of ELMOD1 had an effect on membranes of the secretory pathway we performed double labeling for ELMOD1 and markers of membrane bound organelles at different times after expression. While most of these markers displayed no evident differences, the Golgi was strongly perturbed in cells expressing ELMOD1-HA. GM130 staining was more diffuse and peripheral (Fig 7A; bottom panel). This was also true of other Golgi markers examined, including β-COP, giantin and TGN46 and consistent with the conclusion that ELMOD1-HA expression caused the breakdown of cis-, medial- and trans-Golgi compartments. This effect was somewhat reminiscent of the effects of BFA (Fig 7C), a specific inhibitor of some Arf GEFs, on the Golgi that result from the lowering of cellular Arf-GTP levels. There were subtle differences in the phenotypes of BFA treatment and expression of ELMOD1-HA. The early Golgi marker GM130 adopts a more punctate phenotype with BFA treatment whereas GM130 staining appears more diffuse with some tubular elements with expression of ELMOD1-HA (compare Fig 7B bottom row to Fig 7C). The effects of ELMOD1-HA expression on Golgi morphology is also similar to that reported from over-expression of the Arf GAP, ArfGAP1 (52,53), which is consistent with our evidence (see above) that ELMOD1-HA lowers activated Arf levels in cells.

Finally, we investigated the ability of ELMOD1(R174K)-HA to alter Golgi morphology. At comparable times and levels of expression to ELMOD1-HA we found that the arginine mutant had no discernible effect on the Golgi or the staining of GM130, TGN46, or β-COP (Fig 7B; bottom panel). No effect on Golgi morphology was observed even at times of ELMOD1(R174K)-HA expression up to 48 hours. Thus, arginine 174 of ELMOD1 is critical to GAP activity *in vitro*, Arf GAP activity in cells, and the changes in Golgi integrity and recruitment to the Golgi of the Arf-dependent adaptor COPI when over-expressed in cultured cells. These data are consistent with R174 of ELMOD1 acting as a catalytic arginine in GAP reactions and with Arfs being potential targets of ELMOD1 in cells and/or, ELMOD1 being an effector of Arfs in cells.

We emphasize that the staining of ELMOD1-HA and ELMOD1(R174K)-HA at the Golgi was transient and that the R174K mutant is deficient in effects on Golgi morphology and associated proteins. However, at later times of expression both proteins were seen accumulating in quite distinct structures that could not be identified initially but which were striking in appearance (see below). These results led us to define to the extent technically possible with existing reagents the location of endogenous ELMOD1 and exogenously expressed ELMOD1-HA.

Cellular localization of endogenous and epitope tagged ELMOD1 Using rabbit polyclonal antibodies raised against recombinant human ELMOD1, we investigated the cellular localizations of endogenous and epitope tagged, exogenous ELMOD1 in cultured cells. The only staining we describe in this report is that which is seen with immune but not pre-immune serum (from the same rabbit) and is competable with excess antigen in immunoblots and with immunofluorescence (Fig. 8A). In several cell lines (including HeLa, COS-7, and, most prominently, NRK cells) there was strong nuclear staining for endogenous ELMOD1 with distinct puncta that co-stained with a marker of nuclear speckles, SC35 (Fig. 8B). No other specific staining was detected for endogenous ELMOD1, but cellular fractionation experiments from NRK cells revealed that ELMOD1 is predominantly found in the 100,000x*g* supernatant, consistent with it being a soluble protein (Fig. 8C). By comparison of purified, recombinant ELMOD1 to total cell lysates or cell fractions we have noted that ELMOD1 is expressed to very low levels in each of the cell lines tested, limiting our ability to identify all cellular localizations of endogenous ELMOD1 by indirect immunofluorescence or cell fractionation. We estimate that our ELMOD1 antibody can detect as little as a few nanograms of ELMOD1 in a lane of an immunoblot and reacts with cell lines derived from human, mouse, rat, and monkey but detection in whole cell homogenates is weak at best. Thus, in these cell lines ELMOD1 is typically expressed to less than 0.01% of total cell protein.

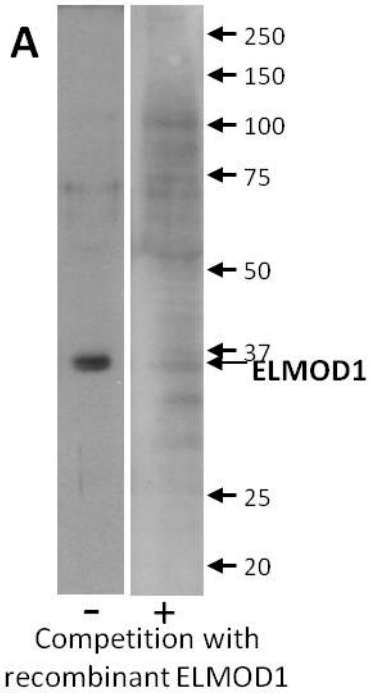
A
250
150
100
75
50
37
ELMOD1
25
20
-
+
Competition with
recombinant ELMOD1

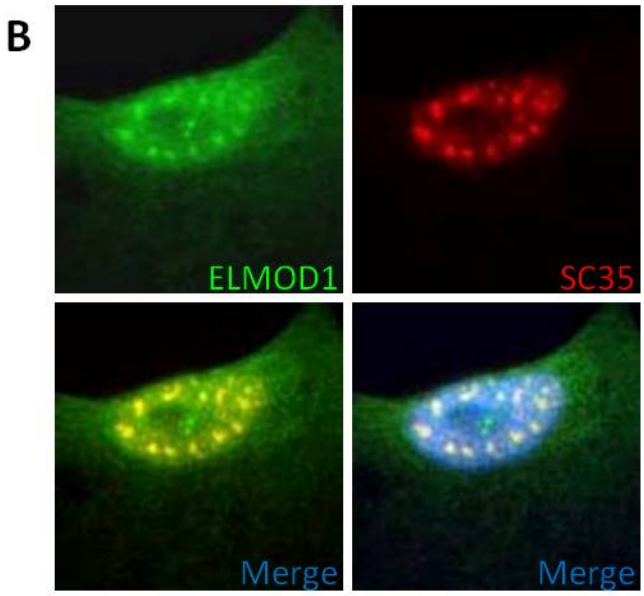
B
ELMOD1
SC35
Merge
Merge

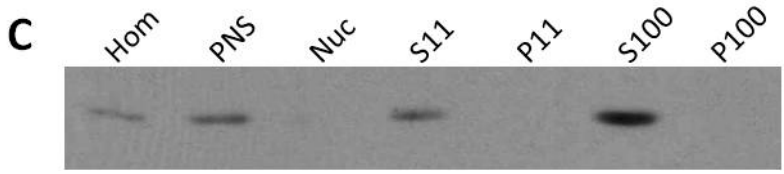
C
Hom
PNS
Nuc
S11
P11
S100
P100

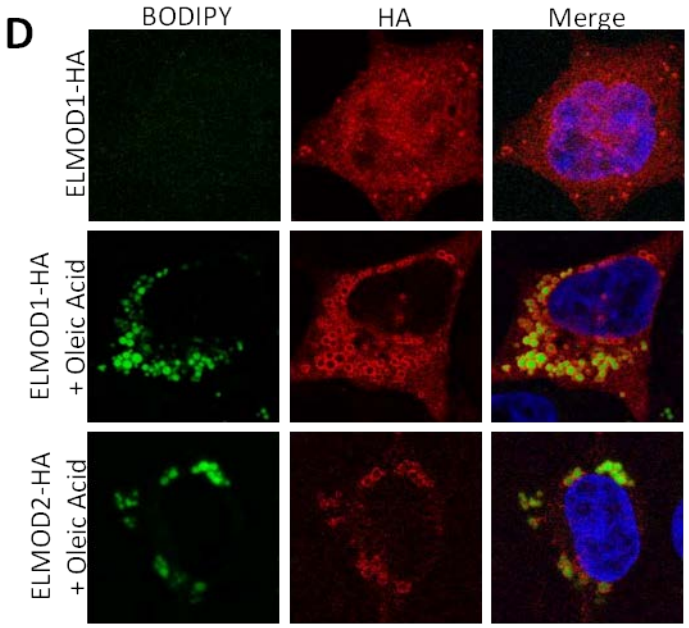

Figure 8: Cellular localization of endogenous ELMOD1 and exogenous ELMOD1-HA or ELMOD2-HA. A. Rabbit polyclonal antibody directed against ELMOD1 detects a single prominent band in immunoblots that is effectively competed with antigen. Total cell lysate from NRK cells (20 µg) was analyzed by immunoblot using our ELMOD1 antibody with (right) and without (left) competition with antigen. B. NRK cells were fixed and permeabilized as described under Experimental Procedures before developing with antibodies to ELMOD1 (top left panel) or SC35 (top right panel), a marker for nuclear speckles. C. Endogenous ELMOD1 is predominantly found in the supernatant (S100) after centrifugation at 100,000x*g*. NRK cells were lysed with a Dounce homogenizer, as described under Experimental Procedures, in the absence of detergent before being subjected differential centrifugation. Equal protein (20 µg) from each fraction was analyzed by immunoblot using ELMOD1 antibody. D. ELMOD1-HA localizes to ring-like structures seen throughout the cytosol and predominantly after nine hours of induction (2µg/mL doxycycline) or longer (top row; 16 hr of induction). Small droplets can be seen with staining for HA in the top panel but co-staining with BODIPY is not evident due to its rapid photobleaching. ELMOD1-HA positive ring structures increase in size and number with treatment of cells with oleic acid (300µM, 6 hr), which induces biosynthesis of lipid droplets (middle panel). Note that the increased staining of BODIPY is easily captured after oleate treatment (middle row, left panel). ELMOD2-HA also localizes to oleic acid induced lipid droplets (bottom row). Cells were fixed in paraformaldehyde and stained with antibody specific for the HA epitope and with BODIPY 493/503 to stain lipid droplets, as described under Experimental Procedures.

When expressed using our lentiviral expression system in HeLa cells, ELMOD1-HA localized predominantly to the Golgi at early time points (Fig. 7A; middle row). At later time points, ELMOD1-HA adopted a more diffuse reticular staining pattern reminiscent of ER localization (Fig. 7A; bottom row), but co-staining with several markers of the ER (including calnexin and BiP) did not display extensive overlap (data not shown). At similar times of protein expression ELMOD1-HA also localized to ring-like structures throughout the cytosol. After failing to find markers of the secretory or endocytic pathways that also stained these structures we suspected that they might be lipid droplets, which are found in every cell line but differ in size and abundance with conditions. Lipid droplets increase in size and number upon treatment of cells with oleic acid (300 μM), which promotes their biosynthesis ((48); see Fig. 8D). We found that oleic acid treatment of HeLa cells increased the size and number of ELMOD1-HA positive ring structures and that these were also stained by the lipid droplet dye, BODIPY 493/503 (e.g. see Fig. 8D, middle row). BODIPY 493/503 staining of cells that were not treated is more variable due to the rapid photobleaching of the dye but is strongly increased by oleic acid. Note that while ELMOD1-HA staining was limited to the surface of the droplets, BODIPY 493/503 stains neutral lipids and thus more the interior of the lipid droplet. It is clear from Fig. 8D that the ring structures identified by the presence of ELMOD1 are positive for BODIPY 493/503. Finally, to confirm that ELMOD1-HA was specifically localizing to lipid droplets we purified lipid droplets from HeLa cells, using a previously established procedure (48). ELMOD1-HA was found to be enriched in this preparation as detected by immunoblotting of purified lipid droplets (data not shown). Despite the strong evidence supporting association of ELMOD1-HA with lipid droplets, we were unable to detect endogenous ELMOD1 in purified lipid droplet preparations from HeLa cells or by immunofluorescence with our ELMOD1 antibodies (data not shown), possibly due to low levels of endogenous protein expression. No changes in the number or size of lipid droplets were evident upon expression of ELMOD1-HA or ELMOD2-HA either with or without oleate treatment of HeLa cells.

Because several proteomics studies of purified lipid droplets detected ELMOD2 as a constituent of these organelles (54,55), we also tested whether ELMOD2 localized to lipid droplets. Expression of ELMOD2-HA using our inducible lentiviral expression system showed strong localization to lipid droplets that was further stimulated by treatment of cells with oleic acid (Fig. 8D; bottom row). Endogenous ELMOD2 was also detected by immunoblot of purified lipid droplets using our ELMOD2 antibody (data not shown) but we did not observe staining of endogenous ELMOD2 on lipid droplets of fixed HeLa cells by immunofluorescence. We were further limited in our ability to test for ELMOD2 on lipid droplets in other cell lines because our ELMOD2 antibody appears to be specific to the human and monkey (e.g., COS-7 cells) proteins.

In attempts to provide mechanistic insight into the subcellular localization of ELMOD1 in cells, we performed ELMOD1 knock down in NRK cells or HeLa cells. We constructed a total of six different pSUPER-based plasmids and purchased the Dharmacon Smart Pool siRNAs directed against rat or human ELMOD1. These assays were complicated by the decrease in levels of ELMOD1 protein that correlated with the cells approaching confluence, more readily seen in HeLa than NRK cells. However, none of these reagents gave consistent knockdown of ELMOD1 protein.

DISCUSSION

In this study, we identified and performed initial characterization of the GAP domain of ELMODs, a novel group of GAPs with wider specificity for Arf family GTPases than previously described for the family of Arf GAPs (27). A highly conserved arginine residue within the GAP domain was critically important to the GAP activity of ELMOD1 and ELMOD2 *in vitro* and for the phenotype of epitope tagged ELMOD1 expression in HeLa cells. Studies in HeLa cells of exogenous, epitope tagged protein provide initial evidence of a biological function for ELMOD1 as an Arf family GAP at the Golgi, more likely involving Arfs than Arl2, based upon the known cellular localizations and functions of these GTPases. Homology searching identified ELMOD

containing proteins in genomes from taxa spanning the diversity of eukaryotes. Phylogenetic analysis of these proteins suggested that the majority of the protein family consists of the ELMODs for which homologs were found in the breadth of sampled eukaryotic diversity. By contrast, the ELMOs, for which we currently have the most functional information, represent a distinct sub-family, most likely restricted to the supergroup Opisthokonta. Thus, the ELMODs represent the more ancient form of the family and were likely present in the LECA, whereas the ELMO sub-family is a much more recent evolutionary development. We also describe localization of endogenous and over-expressed ELMOD1 in a few cultured cell lines. The diversity of cellular locations for ELMOD1 is consistent with the diversity of actions of both Arfs and Arls and supports the hypothesis that it functions in cells as a GAP and potential effector for one or more Arf family members. These findings offer initial insights into an evolutionarily conserved family of proteins that is predicted to provide the basis for further characterization of their biological functions.

We used the unbiased sorting of the Arf family GAP ELMODs and segregation of the ELMOs, which lack the Arf family GAP activities, in our phylogenetic analysis and sequence alignments to identify the putative GAP domain within the ELMODs. A single region of very high conservation was identified with a consensus sequence $WX_3G(F/W)QX_3PXTD(F/L)$**R**$GXGX_3LX_2L$. A notable feature of this region was the presence of a very highly conserved arginine residue that was not conserved in the ELMO sub-family. All of the known Arf family GAPs and many, but not all, other GAPs of small regulatory GTPases use a mechanism known as a "catalytic arginine" residue to confer GAP activity. The arginine side chain stabilizes the transition state through interactions with the gamma phosphate of the bound GTP and can increase rates of hydrolysis by several orders of magnitude (28). Consequently, mutation of this arginine residue is generally sufficient to reduce GAP activity by several orders of magnitude. We used a variety of *in vitro* and cell-based assays to determine the importance of the conserved arginine residue. The conserved arginine residue was essential for

efficient *in vitro* GAP activity of ELMOD1 and ELMOD2, as even a minimal R→K mutation was sufficient to lower GAP activities to undetectable levels. These findings support our hypothesis that the conserved region is the GAP domain and offer initial characterization of the ELMOD GAP domain. Highly charged arginine residues are likely to be on the protein surface and not required for protein folding. The findings that the point mutant is expressed to the same levels and localizes as the wild type protein are consistent with the point mutant folding properly and thus the loss of cellular activities is consistent with the loss of the biochemical GAP activity. Loss of *in vitro* Arl2 GAP activity of the point mutants of recombinant TF-ELMOD1 and TF-ELMOD2 more directly indicates that the conserved arginine is critical for the biochemical GAP activity and precludes the possibility that our observations in HeLa lysates were the result of indirect effects. Nevertheless, confirmation that ELMODs use the catalytic arginine mechanism of GTP hydrolysis described for other GAPs or that R174 of ELMOD1 or R167 of ELMOD2 are directly involved in catalysis will require more detailed enzymatic and structural work. We speculate that the drastically lower specific activity of TF-ELMOD1 and TF-ELMOD2 compared to epitope tagged protein expressed in HeLa lysates (<0.1%) is due to the lack of an obligate binding partner(s). ELMOD2 required detergent addition at late stages in its purification from bovine testes, to resolve it from other proteins, and the GAP activity became less stable under these conditions (3). Preliminary data from quantitative co-immunoprecipitation experiments of ELMOD1-HA in HeLa cells using stable isotope labeling reproducibly showed enrichment of the non-opioid σ receptor 1 (SIGMAR1) to near stoichiometric levels (M. East and R. A. Kahn, unpublished observations). Members of the ELMO sub-family from several species also require DOCK180 obligate binding partners for their activity *in vitro* and in cells (1,2,5,14). Thus, it is likely that our problems with solubility and with reduced GAP activity of recombinant ELMODs is the result of a missing obligate binding partner, though preliminary testing of co-expression with SIGMAR1 failed to remedy this situation.

ELMOD2 was the first mammalian GAP identified for any of the Arl proteins that make up the bulk of the Arf family of regulatory GTPases. Of particular interest was that ELMOD2 (3) and ELMOD1 (this study) possess GAP activity for both Arls and Arfs, offering the first evidence for cross talk between these two functionally distinct groups of regulatory GTPases. Because every other known Arf GAP uses the canonical arginine finger Arf GAP domain and presumably catalytic mechanism, the GAP domain of the ELMODs represents both a novel Arf GAP domain and a founding member of a novel group of Arl GAPs. Only one other protein, RP2, has been found to share Arl3 GAP activity (24,56,57) and ELMODs do not share any extensive sequence homology or similarity and, thus, likely represent functionally and structurally distinct Arf family GAPs. We note that the Arl2 binding partner cofactor D and the RP2 homolog cofactor C have been implicated as GAPs for tubulin at the completion of the regulated folding reaction (58,59) and that the binding of Arl2 can modulate this step but this is a quite different process from the regulation of signaling GTPase by its GAPs.

At early times of ELMOD1-HA expression in HeLa cells using our lentiviral inducible expression system, ELMOD1-HA localized predominantly to the Golgi. Shortly thereafter the morphology of the cis-, medial-, and trans-Golgi compartments were altered. This phenotype was reminiscent of the over-expression of the well-characterized Golgi Arf GAP, ArfGAP1, and of treatment with cells with BFA, an inhibitor of Arf activation. Although Golgi morphology is disrupted in cells treated with BFA and in cells expressing ELMOD1-HA, the two phenotypes are distinct from one another. In BFA treated cells, GM130 staining adopted a more punctate staining pattern while GM130 staining was more diffuse with some tubular elements when ELMOD1-HA was expressed. These differences are consistent with the two proposed mechanisms of BFA and ELMOD1-HA as inhibitors of Arf GEFs and as an Arf GAP, respectively. Because of the previously established roles for Arfs in maintenance of Golgi integrity (e.g., as seen by effects of BFA) and together with our findings that ELMOD1-HA lowers cellular levels of activated Arf in HeLa cells (using the GST-GGA3 pull-down assay) these data suggest a role for ELMOD1 at the

Golgi as an Arf GAP. The model for the function of ELMOD1 in cells as an Arf family GAP is further supported by studies of the catalytic arginine mutant ELMOD1(R174K)-HA in the same assays. Expression of ELMOD1(R174K)-HA had no effect on Golgi morphology and did not affect cellular levels of activated Arf. These data suggest that the disruption of Golgi morphology by ELMOD1 is tightly linked to its Arf GAP activity and, thus, loss of Golgi morphology is the result of an over-abundance of GAP activity at the Golgi. However, this model is weakened by the incomplete testing of substrate specificities of ELMODs as Arf family GAPs and the roles of other family members (including but not limited to Arl1, Arl3, Arl5, Arl8, and Arfrp1) in maintenance of Golgi morphology. The model for the function of ELMOD1 as an Arf GAP at the Golgi is further limited by the fact that it is based solely on results from protein over-expression. Attempts to localize endogenous ELMOD1 to the Golgi by indirect immunofluorescence have been unsuccessful though it is unclear whether this is due to low levels of ELMOD1 expression in cultured mammalian cells and/or to limits of sensitivity of our ELMOD1 antibody. In addition, while we have found ELMOD1 to possess Arf1 GAP activity both *in vitro* and in cultured cells, we have not yet tested it for GAP activity against several other Arf family members that are known to localize to the Golgi. Characterization of the specificities, functions, and locations of ELMODs as GAPs and potential effectors (60) for Arf family members will clearly require additional testing.

ELMOD protein homologs were identified in nearly all genomes examined; a sampling that spans eukaryotic diversity. This extent suggests that the protein family is ancient and builds on the emerging conclusion of a sophisticated membrane-traffic system in the LECA (34,35). Indeed, ELMOD homologs are more conserved in their distribution than several other ancient but patchily distributed proteins recently described (61,62) and reinforces the idea that the proteins likely serve an important cellular function. By contrast, the ELMOs were only found in the Opisthokonta supergroup, with the open possibility of homologs in the apusomonads and

amoebozoa. Regardless of the precise point of origin, this distribution suggests that ELMOs were a more recent evolutionary development and evolved from the more ancient ELMODs.

Our phylogenetic analyses offered some enlightening information regarding the contrasting functions of the human ELMOs, which function as heterodimeric, unconventional Rac1 GEFs, and ELMODs, which are Arf family GAPs. Because ELMOs cluster away from ELMODs in a distinct phylogenetic sub-family, the contrasting functions of the ELMOs and ELMODs may be linked to divergent evolution of the ELMO domain itself, which is the only region of homology between the ELMOs and ELMODs. However, we note that the Rac GEF activity associated with ELMOs is actually found within its binding partner, Dock180 and paralogs, thus the biochemical function of the ELMO domain in the ELMO sub-family has no known function(s). The presence of DUF3361 is consistent with the divergence of the ELMO domain from its ancestral ELMOD as it is found almost exclusively in ELMO sub-family members. Thus, DUF3361 may also play an important role in defining the functions of the ELMO family members and may be functionally linked to the ELMO domain in these proteins. We speculate that ELMOs lost the biochemical GAP activity of their ancestral ELMODs but may have retained the ability to bind Arf family GTPases. If so, they may be effectors of Arf family signaling. This is currently being tested in our laboratory with the development of protein interaction assays that are independent of GAP activity. In this model, ELMOs would be predicted to have adopted a more predominant role as effectors of GTPases whereas the ELMODs retained the biochemical GAP activity. In many cases, a GAP for a given GTPase is able to function as both a terminator of GTPase signaling through its GAP activity and as an effector of GTPase signaling to mediate downstream signaling (63). We speculate that the divergent evolution of ELMO from ELMODs was the result of a specialization in the effector function of these two tasks.

Whether ELMODs function as effectors or terminators of Arf family signaling, or both, requires additional definition of their cellular roles. Only a few clues to this end have appeared in

the literature. The one ELMOD gene in flies (*D. melanogaster*) emerged from a screen of genes whose mutations alter cytokinesis (64) and human ELMOD2 is implicated as a gene linked to idiopathic pulmonary fibrosis (65,66). Two studies in *D. discoideum* also reported that ElmoA regulates actin dynamics and forms a complex with the Dock180 ortholog DockD and Rac1 (29,30). It is unclear whether this protein is an ELMO or ELMOD homolog. It fails to cluster with the other ELMOs, but is not separated from that clade by any supported nodes. It has the domain architecture of ELMOs, but possesses the catalytic arginine of ELMOD proteins. Therefore this protein may provide the first indication of a functional overlap between the two classes of ELMO domain containing proteins. A recent study in mice also linked hearing and balance deficits to two different naturally occurring mutations in ELMOD1 (67). Further analysis of these mice revealed morphological defects in the actin based mechanoelectrical signaling organelles, stereocilia, in both inner and outer hair cells. Stereocilia morphology appeared normal in newborn mice but progressively worsened with age. Thus, ELMOD1 is essential for the maintenance of stereocilia in hair cells. While the function of ELMODs in stereocilia is intriguing and has significant clinical relevance to deafness, ELMODs arose in evolution well before these highly specialized organelles. Thus, we expect to find other fundamental functions of ELMODs in more ubiquitous biological processes. Further experimentation is necessary to determine the function of ELMOD1 in these processes. Thus, the function of the ELMOs in regulating actin dynamics and cell motility may be relevant to ELMOD proteins. ELMOA may also be a useful tool to link the Arf family GAP activity of the ELMODs to the cellular roles of the ELMOs because it has both the conserved GAP domain of the ELMODs and interacts with binding partners essential to the function of ELMOs. We speculate that ELMOs may be Arf family GTPase effectors and similarly that ELMODs may be found capable of regulating actin and cell motility.

Finally, we provide initial data on the localization of endogenous and exogenously expressed ELMOD1 in a few cultured cell lines. While data on the endogenous protein provides

more reliable answers as to the biological contexts, the low levels of endogenous protein expression limited our ability to define locations for ELMOD1. Endogenous ELMOD1 quite prominently stains nuclear speckles, as evidence by its co-localization with the marker SC35, though its function there is particularly obscure as a result of the lack of specific localization of any Arf family members to such structures and the limited functional information linked to these structures. A previous study (68) has found that Dock180 and members of the mammalian ELMO sub-family are found predominantly in the nucleus and immunofluorescence images are consistent with localization of nuclear speckles, though this was not specifically examined in the previous study. Arl2 antibodies also stain the nucleus (though not specifically speckles) and there is one report of a role for Arl2 and BART to act inside the nucleus in STAT signaling (69). Cell fractionation experiments suggest that the majority of endogenous ELMOD1 is soluble. Thus, it is likely that there is a free soluble pool of ELMOD1 that is recruited to its sites of action (e.g. Golgi, nuclear speckles, lipid droplets) in a manner that may parallel the recruitment of one of its proposed substrate GTPases, Arf, which cycles on and off membranes depending on the bound nucleotide (70). When epitope tagged ELMOD1-HA is exogenously expressed in cells, it first localizes to the Golgi then adopts a more disperse reticular staining pattern throughout the cell that is reminiscent of ER staining, although we were unable to find a marker of the ER with extensive overlap. This ER-like staining pattern was not the result of disruption of the Golgi by ELMOD1-HA over-expression since ELMOD1(R174K)-HA, which does not disrupt the Golgi, adopts a similar staining pattern at later times of over-expression. Thus, the ER may be a site of localization and function for ELMOD1. ELMOD1-HA also localized to lipid droplets by immunofluorescence and was detected in purified lipid droplets by immunoblot. It is not clear whether endogenous ELMOD1 localizes to lipid droplets though it was not detected in our purified HeLa lipid droplet preparation and is also absent from the published proteome of lipid droplet preparations (at least one of which was from HeLa cells). Localization to both ER and lipid droplets would be consistent with the proposal that the ER is the site of new lipid droplet

formation (71). The reason for the discrepancies between the localizations of endogenous and exogenously expressed ELMOD1 remains unclear. Exogenously expressed ELMOD1 (WT or epitope tagged) does not appear to localize specifically to nuclear speckles or to the nucleus and we have failed to localize endogenous ELMOD1 to any other organelle. Our polyclonal ELMOD1 antibody may not be sensitive enough to recognize other localizations of the endogenous protein in immunofluorescence experiments given the low levels of expression of endogenous ELMOD1. ELMOD2-HA also localized to lipid droplets by immunofluorescence when over-expressed and endogenous ELMOD2 was detected in purified lipid droplets by immunoblot (Fig. 8C) and in published proteomes (54,55). Several Arf family GTPases have been shown to localize to, and are important for the formation of, lipid droplets; including Arf1(72,73), Arfrp1 (74), and Arl4A (75). Thus, even though our initial testing for effects of ELMOD1 or ELMOD2 over-expression on lipid droplet number or size were negative, we predict that functions for these GAPs will likely be found, and will involve these or other Arf family members.

Together, we conclude that ELMOD1 and ELMOD2, like the members of the Arf family GTPases that serve as substrates for their GAP activities, are ancient cell regulators found at multiple sites in eukaryotic cells and predict that they act on a more diverse array of Arf family GTPases than do the Arf GAPs, making their functional dissection even more difficult but no less important.

REFERENCES

1. Brugnera, E., Haney, L., Grimsley, C., Lu, M., Walk, S. F., Tosello-Trampont, A. C., Macara, I. G., Madhani, H., Fink, G. R., and Ravichandran, K. S. (2002) *Nat Cell Biol* **4**, 574-582

2. Lu, M., Kinchen, J. M., Rossman, K. L., Grimsley, C., deBakker, C., Brugnera, E., Tosello-Trampont, A. C., Haney, L. B., Klingele, D., Sondek, J., Hengartner, M. O., and Ravichandran, K. S. (2004) *Nature structural & molecular biology* **11**, 756-762

3. Bowzard, J. B., Cheng, D., Peng, J., and Kahn, R. A. (2007) *J Biol Chem* **282**, 17568-17580

4. Chung, S., Gumienny, T. L., Hengartner, M. O., and Driscoll, M. (2000) *Nat Cell Biol* **2**, 931-937

5. Gumienny, T. L., Brugnera, E., Tosello-Trampont, A. C., Kinchen, J. M., Haney, L. B., Nishiwaki, K., Walk, S. F., Nemergut, M. E., Macara, I. G., Francis, R., Schedl, T., Qin, Y., Van Aelst, L., Hengartner, M. O., and Ravichandran, K. S. (2001) *Cell* **107**, 27-41

6. Wu, Y. C., Tsai, M. C., Cheng, L. C., Chou, C. J., and Weng, N. Y. (2001) *Developmental cell* **1**, 491-502

7. Zhou, Z., Caron, E., Hartwieg, E., Hall, A., and Horvitz, H. R. (2001) *Dev Cell* **1**, 477-489

8. Elliott, M. R., and Ravichandran, K. S. (2010) *Annals of the New York Academy of Sciences* **1209**, 30-36

9. Elliott, M. R., Zheng, S., Park, D., Woodson, R. I., Reardon, M. A., Juncadella, I. J., Kinchen, J. M., Zhang, J., Lysiak, J. J., and Ravichandran, K. S. (2010) *Nature* **467**, 333-337

10. Shimazaki, A., Tanaka, Y., Shinosaki, T., Ikeda, M., Watada, H., Hirose, T., Kawamori, R., and Maeda, S. (2006) *Kidney international* **70**, 1769-1776

11. Yang, C., and Sorokin, A. (2011) *Cellular signalling* **23**, 99-104

12. Komander, D., Patel, M., Laurin, M., Fradet, N., Pelletier, A., Barford, D., and Cote, J. F. (2008) *Mol Biol Cell* **19**, 4837-4851

13. Sevajol, M., Reiser, J. B., Chouquet, A., Perard, J., Ayala, I., Gans, P., Kleman, J. P., and Housset, D. (2012) *Biochimie* **94**, 823-828

14. Grimsley, C. M., Kinchen, J. M., Tosello-Trampont, A. C., Brugnera, E., Haney, L. B., Lu, M., Chen, Q., Klingele, D., Hengartner, M. O., and Ravichandran, K. S. (2004) *J Biol Chem* **279**, 6087-6097

15. Kahn, R. A., Cherfils, J., Elias, M., Lovering, R. C., Munro, S., and Schurmann, A. (2006) *J Cell Biol* **172**, 645-650

16. Donaldson, J. G., and Jackson, C. L. (2011) *Nat Rev Mol Cell Biol* **12**, 362-375

17. Nie, Z., and Randazzo, P. A. (2006) *J Cell Sci* **119**, 1203-1211

18. Zhou, C., Cunningham, L., Marcus, A. I., Li, Y., and Kahn, R. A. (2006) *Mol Biol Cell* **17**, 2476-2487

19. Li, Y., Wei, Q., Zhang, Y., Ling, K., and Hu, J. *J Cell Biol* **189**, 1039-1051

20. Larkins, C. E., Aviles, G. D., East, M. P., Kahn, R. A., and Caspary, T. (2011) *Mol Biol Cell* **22**, 4694-4703

21. Burd, C. G., Strochlic, T. I., and Gangi Setty, S. R. (2004) *Trends Cell Biol* **14**, 687-694

22. Graham, D. J. (2011) *Curr Biol* **21**, R914-916

23. D'Souza-Schorey, C., and Chavrier, P. (2006) *Nature reviews. Molecular cell biology* **7**, 347-358

24. Veltel, S., Gasper, R., Eisenacher, E., and Wittinghofer, A. (2008) *Nature structural & molecular biology* **15**, 373-380

25. Liu, Y. W., Huang, C. F., Huang, K. B., and Lee, F. J. (2005) *Mol Biol Cell* **16**, 4024-4033

26. Cukierman, E., Huber, I., Rotman, M., and Cassel, D. (1995) *Science* **270**, 1999-2002

27. Kahn, R. A., Bruford, E., Inoue, H., Logsdon, J. M., Jr., Nie, Z., Premont, R. T., Randazzo, P. A., Satake, M., Theibert, A. B., Zapp, M. L., and Cassel, D. (2008) *J Cell Biol* **182**, 1039-1044

28. Scheffzek, K., Ahmadian, M. R., and Wittinghofer, A. (1998) *Trends Biochem Sci* **23**, 257-262

29. Isik, N., Brzostowski, J. A., and Jin, T. (2008) *Developmental cell* **15**, 590-602

30. Para, A., Krischke, M., Merlot, S., Shen, Z., Oberholzer, M., Lee, S., Briggs, S., and Firtel, R. A. (2009) *Mol Biol Cell* **20**, 699-707

31. Brzostowski, J. A., Fey, P., Yan, J., Isik, N., and Jin, T. (2009) *Communicative & integrative biology* **2**, 337-340

32. Adl, S. M., Simpson, A. G., Farmer, M. A., Andersen, R. A., Anderson, O. R., Barta, J. R., Bowser, S. S., Brugerolle, G., Fensome, R. A., Fredericq, S., James, T. Y., Karpov, S., Kugrens, P., Krug, J., Lane, C. E., Lewis, L. A., Lodge, J., Lynn, D. H., Mann, D. G., McCourt, R. M., Mendoza, L., Moestrup, O., Mozley-Standridge, S. E., Nerad, T. A., Shearer, C. A., Smirnov, A. V., Spiegel, F. W., and Taylor, M. F. (2005) *The Journal of eukaryotic microbiology* **52**, 399-451

33. Field, M. C., Gabernet-Castello, C., and Dacks, J. B. (2007) *Advances in experimental medicine and biology* **607**, 84-96

34. Elias, M. (2010) *Molecular membrane biology* **27**, 469-489

35. Dacks, J. B., and Field, M. C. (2007) *Journal of cell science* **120**, 2977-2985

36. Walker, G., Dorrell, R. G., Schlacht, A., and Dacks, J. B. (2011) *Parasitology* **138**, 1638-1663

37. Burki, F., Okamoto, N., Pombert, J. F., and Keeling, P. J. (2012) *Proceedings. Biological sciences / The Royal Society*

38. Edgar, R. C. (2004) *Nucleic acids research* **32**, 1792-1797

39. Abascal, F., Zardoya, R., and Posada, D. (2005) *Bioinformatics* **21**, 2104-2105

40. Guindon, S., and Gascuel, O. (2003) *Systematic biology* **52**, 696-704

41. Stamatakis, A. (2006) *Bioinformatics* **22**, 2688-2690

42. Ronquist, F., and Huelsenbeck, J. P. (2003) *Bioinformatics* **19**, 1572-1574

43. Cavenagh, M. M., Whitney, J. A., Carroll, K., Zhang, C., Boman, A. L., Rosenwald, A. G., Mellman, I., and Kahn, R. A. (1996) *J Biol Chem* **271**, 21767-21774

44. Cuthbert, E. J., Davis, K. K., and Casanova, J. E. (2008) *American journal of physiology. Cell physiology* **294**, C263-270

45. Bowzard, J. B., Sharer, J. D., and Kahn, R. A. (2005) *Methods Enzymol* **404**, 453-467

46. Valnes, K., and Brandtzaeg, P. (1985) *J Histochem Cytochem* **33**, 755-761

47. Austin, C., Boehm, M., and Tooze, S. A. (2002) *Biochemistry* **41**, 4669-4677

48. Brasaemle, D. L., and Wolins, N. E. (2006) *Current protocols in cell biology / editorial board, Juan S. Bonifacino ... [et al.]* **Chapter 3**, Unit 3 15

49. Brummelkamp, T. R., Bernards, R., and Agami, R. (2002) *Science* **296**, 550-553

50. Katz, L. A., Grant, J., Parfrey, L. W., Gant, A., O'Kelly, C. J., Anderson, O. R., Molestina, R. E., and Nerad, T. (2011) *Protist* **162**, 762-773

51. Sebe-Pedros, A., Roger, A. J., Lang, F. B., King, N., and Ruiz-Trillo, I. (2010) *Proc Natl Acad Sci U S A* **107**, 10142-10147

52. Yu, S., and Roth, M. G. (2002) *Mol Biol Cell* **13**, 2559-2570

53. Randazzo, P. A., and Hirsch, D. S. (2004) *Cell Signal* **16**, 401-413

54. Hodges, B. D., and Wu, C. C. (2010) *Journal of lipid research* **51**, 262-273

55. Bouchoux, J., Beilstein, F., Pauquai, T., Guerrera, I. C., Chateau, D., Ly, N., Alqub, M., Klein, C., Chambaz, J., Rousset, M., Lacorte, J. M., Morel, E., and Demignot, S. (2011) *Biology of the cell / under the auspices of the European Cell Biology Organization* **103**, 499-517

56. Kuhnel, K., Veltel, S., Schlichting, I., and Wittinghofer, A. (2006) *Structure* **14**, 367-378

57. Veltel, S., Kravchenko, A., Ismail, S., and Wittinghofer, A. (2008) *FEBS letters* **582**, 2501-2507

58. Tian, G., Bhamidipati, A., Cowan, N. J., and Lewis, S. A. (1999) *J Biol Chem* **274**, 24054-24058

59. Bhamidipati, A., Lewis, S. A., and Cowan, N. J. (2000) *J Cell Biol* **149**, 1087-1096.

60. East, M. P., and Kahn, R. A. *Semin Cell Dev Biol* **22**, 3-9

61. Hirst, J., Barlow, L. D., Francisco, G. C., Sahlender, D. A., Seaman, M. N., Dacks, J. B., and Robinson, M. S. (2011) *PLoS biology* **9**, e1001170

62. Koumandou, V. L., Klute, M. J., Herman, E. K., Nunez-Miguel, R., Dacks, J. B., and Field, M. C. (2011) *Journal of cell science* **124**, 1496-1509

63. East, M. P., and Kahn, R. A. (2011) *Seminars in cell & developmental biology* **22**, 3-9

64. Echard, A., Hickson, G. R., Foley, E., and O'Farrell, P. H. (2004) *Current biology : CB* **14**, 1685-1693

65. Pulkkinen, V., Bruce, S., Rintahaka, J., Hodgson, U., Laitinen, T., Alenius, H., Kinnula, V. L., Myllarniemi, M., Matikainen, S., and Kere, J. (2010) *The FASEB journal : official publication of the Federation of American Societies for Experimental Biology* **24**, 1167-1177

66. Hodgson, U., Pulkkinen, V., Dixon, M., Peyrard-Janvid, M., Rehn, M., Lahermo, P., Ollikainen, V., Salmenkivi, K., Kinnula, V., Kere, J., Tukiainen, P., and Laitinen, T. (2006) *American journal of human genetics* **79**, 149-154

67. Johnson, K. R., Longo-Guess, C. M., and Gagnon, L. H. (2012) *PLoS One* **7**, e36074

68. Yin, J., Haney, L., Walk, S., Zhou, S., Ravichandran, K. S., and Wang, W. (2004) *Arch Biochem Biophys* **429**, 23-29

69. Muromoto, R., Sekine, Y., Imoto, S., Ikeda, O., Okayama, T., Sato, N., and Matsuda, T. (2008) *International immunology* **20**, 395-403

70. Kahn, R. A. (1991) *J Biol Chem* **266**, 15595-15597

71. Kalantari, F., Bergeron, J. J., and Nilsson, T. (2010) *Molecular membrane biology* **27**, 462-468

72. Nakamura, N., Akashi, T., Taneda, T., Kogo, H., Kikuchi, A., and Fujimoto, T. (2004) *Biochem Biophys Res Commun* **322**, 957-965

73. Nakamura, N., Banno, Y., and Tamiya-Koizumi, K. (2005) *Biochem Biophys Res Commun* **335**, 117-123

74. Hommel, A., Hesse, D., Volker, W., Jaschke, A., Moser, M., Engel, T., Bluher, M., Zahn, C., Chadt, A., Ruschke, K., Vogel, H., Kluge, R., Robenek, H., Joost, H. G., and Schurmann, A. *Mol Cell Biol* **30**, 1231-1242

75. Patel, M., Chiang, T. C., Tran, V., Lee, F. J., and Cote, J. F. (2011) *J Biol Chem* **286**, 38969-38979

Acknowledgements: We thank James Olzmann (Stanford University) for helpful discussions and sharing data on the proteomes of different lipid droplet preparations and assistance in purifying lipid droplets from cells and Alex Schlacht (University of Alberta) for his help in the phylogenetic analyses.

FOOTNOTES

* This work was supported by grants from the NIH (RAK; R01-GM090158), AHA (ME; 09PRE2140029), NSERC and AITF (JBD; Discovery grant and New Faculty Award). JBD also acknowledged support from the CRC program. This research project was also supported in part by the Viral Vector and Microscopy Cores of the Emory Neuroscience NINDS Core Facilities grant, P30-NS055077.

[1]To whom all correspondence should be addressed: Richard A. Kahn, Department of Biochemistry, Emory University School of Medicine, 1510 Clifton Road, Atlanta, GA, USA, Tel.: (404) 727-3561; E-mail: rkahn@emory.edu

[2]Department of Cell Biology, Faculty of Medicine and Dentistry, University of Alberta

[3]The abbreviations used are: Arf, ADP-ribosylation factor; Arl, Arf-like protein; ELMO, cell engulfment and motility domain; GAP, GTPase activating protein; GEF, guanine nucleotide exchange factor; LECA, last eukaryotic common ancestor

Organism	Annotation	Abbreviation	Accession #	Gene Location
Homo sapien	HsELMOD1	ELMOD1	NP_061182	
Homo sapien	HsELMOD2	ELMOD2	NP_714913	
Homo sapien	HsELMOD3	ELMOD3	NP_115589	
Homo sapien	HsELMO1	ELMO1	NP_055615	
Homo sapien	HsELMO2	ELMO2	NP_877496	
Homo sapien	HsELMO3	ELMO3	NP_078988	
Danio rerio	DrELMOW	ELMOD_B	NP_001074150.1	
Danio rerio	DrELMOX	ELMOD_A	XP_691971.4	
Danio rerio	DrELMOY	ELMO1	NP_998256.1	
Nematostella vectensis	NvELMOX	ELMOD_A	XP_001628072	
Nematostella vectensis	NvELMOY	ELMOD3	XP_001623228	
Nematostella vectensis	NvELMOZ	ELMO	XP_001627551	
Monosiga brevicollis	MbELMOZ	ELMOD	XP_001745572	
Cryptococcus neoformans	CnELMOZ	ELMO	CNAG_05930.2	
Batrachochytrium dendrobatidis	BdELMOY	ELMOD	BDEG_00507.1	
Batrachochytrium dendrobatidis	BdELMOZ	ELMO	BDEG_04078.1	
Drosophila melanogaster	DmELMOY	ELMOD	NP_649695	
Drosophila melanogaster	DmELMOZ	ELMO	NP_609548	
Caenorhabditis elegans	CeELMOY	ELMOD3	NP_497699	
Dictyostelium discoideum	DdELMOA	ElmoA	XP_642091	
Dictyostelium discoideum	DdELMOB	ElmoB	XP_641287	
Dictyostelium discoideum	DdELMOC	ElmoC	XP_639274	
Dictyostelium discoideum	DdELMOD	ElmoD	XP_640972	
Dictyostelium discoideum	DdELMOE	ElmoE	XP_641578	
Dictyostelium discoideum	DdELMOF	ElmoF	XP_647117	
Trichomonas vaginalis	TvELMOY	ELMOD3_A	XP_001581069	
Trichomonas vaginalis	TvELMOZ	ELMOD3_B	XP_001318953	
Trypanosoma brucei	TbELMOY	ELMOD_A	XP_803577	
Trypanosoma brucei	TbELMOZ	ELMOD3	XP_822839	
Leishmania major	LmELMOX	ELMOD_B	XP_001684191	
Leishmania major	LmELMOY	ELMOD_A	XP_001682746	
Leishmania major	LmELMOZ	ELMOD3	XP_001686726	
Naegleria gruberi	NgELMOU	ELMOD_A	XP_002680121	
Naegleria gruberi	NgELMOV	ELMOD_B	XP_002676984	

Naegleria gruberi	NgELMOW	ELMOD3_B	XP_002675911	
Naegleria gruberi	NgELMOX	ELMOD_C	XP_002670995	
Naegleria gruberi	NgELMOY	ELMOD_D	XP_002668667	
Naegleria gruberi	NgELMOZ	ELMOD3_A	XP_002678333	
Arabidopsis thaliana	AtELMOU	ELMOD_A	NP_567097	
Arabidopsis thaliana	AtELMOV	ELMOD_C	NP_564897	
Arabidopsis thaliana	AtELMOW	ELMOD_F	NP_566211	
Arabidopsis thaliana	AtELMOX	ELMOD_E	NP_171859	
Arabidopsis thaliana	AtELMOY	ELMOD_D	NP_189926	
Arabidopsis thaliana	AtELMOZ	ELMOD_B	NP_566027	
Physcomitrella patens	PpELMOZ	ELMOD	XP_001756777	
Chlamydomonas reinhardtii	CrELMOY	ELMOD3		Chlre4|150490|Chlre2_kg.scaffold_32000043
Chlamydomonas reinhardtii	CrELMOZ	ELMOD_A		Chlre4|21823|fgenesh1_pg.C_scaffold_80000050
Ostreococcus tauri	OtELMOZ	ELMOD_A	XP_003078509	
Toxoplasma gondii	TxgELMOX	ELMOD_B	EEE21379	
Toxoplasma gondii	TxgELMOY	ELMOD_A	EEE22446	
Toxoplasma gondii	TxgELMOZ	ELMOD_C	EEE29665	
Tetrahymena thermophila	TtELMOW	ELMOD_A	XP_001014395.2	
Tetrahymena thermophila	TtELMOX	ELMOD3_B	XP_001033010.1	
Tetrahymena thermophila	TtELMOY	ELMOD_B	XP_001026931.1	
Tetrahymena thermophila	TtELMOZ	ELMOD3_A	XP_001024802.1	
Phytophthora sojae	PsELMOW	ELMOD_C		Physo1_1|137612|estExt_fgenesh1_pg.C_550103
Phytophthora sojae	PsELMOX	ELMOD_B		Physo1_1|128030|estExt_fgenesh1_pg.C_30239
Phytophthora sojae	PsELMOY	ELMOD_A		Physo1_1|128030|estExt_fgenesh1_pg.C_30239
Phytophthora sojae	PsELMOZ	ELMOD3		Physo1_1|133225|estExt_fgenesh1_pg.C_240194
Amphimedon queenslandica	AqELMOX	ELMOD3	XP_003384642	
Amphimedon queenslandica	AqELMOY	ELMOD_A	XP_003387436	
Amphimedon queenslandica	AqELMOZ	ELMO	XP_003386618	
Capsaspora owczarzaki	CoELMOX	ELMOD_A	EFW40932	
Capsaspora owczarzaki	CoELMOY	ELMOD_B	EFW39689	
Capsaspora owczarzaki	CoELMOZ	ELMO	EFW44340	
Thecamonas trahens	TtrELMOV	ELMOD_D	AMSG_00305.1	
Thecamonas trahens	TtrELMOW	ELMOD_C	AMSG_09134.1	
Thecamonas trahens	TtrELMOX	ELMOD_B	AMSG_01964.1	
Thecamonas trahens	TtrELMOY	ELMOD3	AMSG_10099.1	

Thecamonas trahens	TtrELMOZ	ELMOD_A	AMSG_05642.1	
Sphaeroforma arctica	SaELMOZ	ELMOD_A	SARC_01169.1	
Ciona intestinalis	CiELMOZ	ELMO		Cioin2|299311|estExt_fgenesh3_kg.C_1560003
Anopheles gambiae	AgELMOZ	ELMO	XP_320013.2	
Canis lupus familiaris	ClfELMOX	ELMO3	XP_546883	
Canis lupus familiaris	ClfELMOY	ELMO1	XP_852411	
Canis lupus familiaris	ClfELMOZ	ELMO2	XP_866738	
Bos taurus	BtELMOX	ELMO1	NP_001106698	
Bos taurus	BtELMOY	ELMO2	NP_001076860	
Bos taurus	BtELMOZ	ELMO3	NP_001095561	
Tetraodon nigroviridis	TnELMOW	ELMO2	CAF96838	
Tetraodon nigroviridis	TnELMOX	ELMO1	CAG10033	
Xenopus laevis	XlELMOY	ELMO1	NP_001089652.1	
Xenopus laevis	XlELMOZ	ELMO2	NP_001083487.1	
Gallus gallus	GgELMOX	ELMO1	NP_001026165	
Gallus gallus	GgELMOY	ELMO2	XP_417479	
Sampled organisms where no ELMOD family members were found				
Saccharomyces cerevisiae				
Schizosaccharomyces pombe				
Acanthamoeba castellani				
Entamoeba histolytica				
Plasmodium vivax				
Takifugu rubripes				

Table S1: List of taxa and accession numbers for ELMO domain containing proteins used in our analyses.

Chapter III

ELMOD3 is a novel regulator of the actin cytoskeleton through a RhoA dependent mechanism

Michael Patrick East

Department of Biochemistry and Program in Biochemistry, Cell, and Developmental Biology, Emory University, Atlanta GA 30322

Abstract

The human ELMO family of proteins consists of two phylogenetically distinct subgroups including the ELMOs and ELMODs. ELMOs primarily function in complex with DOCK180 as unconventional guanine nucleotide exchange factors for Rac1 at the leading edge of migrating cells. ELMODs are thought to function as GTPase activating proteins for an array of Arf family GTPases. In this study, we used over-expression models of ELMOD3 to identify a novel and unexpected role for ELMOD3 as an activator of RhoA signaling. Expression of epitope tagged ELMOD3 resulted in blebbing of the plasma membrane which was blocked upon inhibition of RhoA signaling at two different steps of the pathway. We also provide initial characterization of the subcellular localization of endogenous ELMOD3 at the trailing edge of migrating cells and in punctate structures associated with the actin cytoskeleton in non-polarized cells. These findings provide the first functional information for ELMOD3 and initial characterization of endogenous ELMOD3 in cultured cell lines.

Introduction

The ELMO family of proteins consists of six members in humans characterized by the presence of the ELMO domain. This family is equally divided into two structurally and phylogenetically distinct subgroups termed ELMOs and ELMO domain containing proteins (ELMODs) [1]. The ELMO proteins are approximately twice as large as the ELMODs and include several domains including Rho and ERM binding domains, a PH domain, two auto-regulatory domains, and the ELMO domain [2-4]. The ELMODs are single domain proteins consisting primarily of the ELMO domain. The only region of sequence homology between the ELMOs and the ELMODs lies within the ELMO domain [5]. A role for this domain was only recently first described as a GTPase activating protein (GAP) domain for Arf family GTPases although only the ELMODs, and not ELMOs, have been shown to possess this activity [1, 5, 6].

The ELMODs are an ancient group of proteins that spans the entire diversity of eukaryotes and dates all the way back to the last eukaryotic common ancestor [1]. We have reported that they are novel GAPs with promiscuous specificities against the six Arf family GTPases tested [5-7] and our current functional models of ELMOD1 and ELMOD2 indicate roles at the Golgi apparatus and in mitochondria, respectively [1](Newman *et. al.* in press). Other cellular locations for ELMOD1 and ELMOD2 include lipid droplets and nuclear speckles (ELMOD1 only) although no functional information is available at either of these locations [1]. Of the three human ELMODs, ELMOD3 is the least well defined. It was only recently discovered to have GAP activity [7] and the specific activity of ELMOD3 for GTPases was orders of magnitude lower than that of ELMOD1 or ELMOD2 for the same GTPases [6]. A mutation in ELMOD3 was linked to deafness in a human family suggesting that ELMOD3 is important in inner ear hair cells and in hearing [7]. In the same study, ELMOD3 specifically localized to stereocilia, the mechanosensory organelles of inner ear hair cells responsible for converting sound waves into electrical impulses for the perception of sound. GFP-ELMOD3 was also recruited to stereocilia in inner ear explants and to cortical actin structures in a confluent monolayer of MDCK cells. Thus, there appears to be a strong link between ELMOD3 and the actin cytoskeleton but the role of ELMOD3 is not understood.

The ELMO proteins were first characterized in *Caenorhabditis elegans* where they were essential for phagocytosis and cell migration [8]. Human ELMO1 and ELMO2 are key regulators of actin dynamics in the cell and function with an obligate binding partner, DOCK180, as unconventional guanine nucleotide exchange factors (GEF) for the Rho family GTPase, Rac1 [9-13]. DOCK180 has intrinsic Rac1 GEF activity *in vitro* but binding to ELMO1 was required for Rac1 GTP loading in cells [10], relieved DOCK180 auto-inhibition [14], and helped DOCK180 stabilize nucleotide free Rac1 [11]. DOCK180 lacks the Dbl homology domain characteristic of other Rac1 GEFs and instead binds to nucleotide free Rac1 to facilitate GTP loading [10, 11].

The DOCK180/ELMO complex is further regulated by auto-inhibition of ELMO via intra-molecular interactions, the Rho family GTPase RhoG, and the Arf family GTPase Arf6 [3, 15-18]. Two domains within ELMO termed the ELMO autoregulatory domain and ELMO inhibitory domain at the N- and C-termini, respectively, interact with each other to adopt an auto-inhibitory conformation [4]. RhoG binds to the Ras-binding domain of ELMO at the N-terminus to alleviate auto-inhibition of ELMO and to promote the translocation of DOCK180/ELMO to the cell surface where it induces Rac1 activation and cell migration [19, 20]. The Arf family GTPase Arf6 and its GEF ARNO have also been shown to be important regulators of the DOCK180/ELMO complex. Activation of Arf6 by ARNO induces Rac1 activation and lamellipodia formation in a DOCK180/ELMO dependent manner [17, 18]. Similar to RhoG, Arf6 is thought to help localize DOCK180/ELMO to the cell surface [21] but the mechanism and whether Arf6 or ARNO interacts with either protein is not known.

Rho family GTPases are key regulators of actin dynamics and cell migration. Rac1 and RhoA are among the best understood Rho family GTPases and regulate key functions at the leading and trailing edges of migrating cells, respectively [22, 23]. Compartmentalization of Rac1 and RhoA is essential because they induce opposing phenotypes and have an antagonistic relationship with each other [24]. Activation of Rac1 induces localized polymerization of actin via the Arp2/3 complex and generates the protrusive force required for membrane ruffling and lamellipodia formation at the leading edge of the cell. The DOCK180/ELMO complex is an important regulator of these Rac1 mediated processes [16]. RhoA functions primarily at the rear of migrating cells and in the generation and stabilization of actin stress fibers. RhoA activates actomyosin contraction at the trailing edge to generate the force required to pull the cell rear along during migration and for retraction of the cell tail [25, 26]. Actomyosin contraction is stimulated via RhoA activation leading to activation of Rho kinase (ROCK) which activates myosin light chain (MLC) and myosin motor activity [27]. Myosin motors cross-link highly

bundled actin stress fibers and the motor activity generates the pulling force. Stress fiber formation appears to require both activation of ROCK and another effector of RhoA, mDia1 [27]. RhoA is also essential for the amoeboid like motility of tumor cells using plasma membrane blebbing protrusions in place of lamellipodia for directed motility during cell invasion [28-32]. The RhoA/ROCK/MLC cascade comprises the core machinery involved in plasma membrane blebbing as up-regulation of this pathway at virtually any step is sufficient to cause plasma membrane blebbing [33].

In this study, we provide initial characterization of the cellular function of ELMOD3 as a novel regulator of the actin cytoskeleton through a RhoA dependent pathway. We also describe the subcellular localization of endogenous ELMOD3 in cultured cells at the trailing edge of migrating cells and in punctate structures associated with the actin cytoskeleton. The results of this study provide the first functional information for ELMOD3 and offer insight into a potential role for ELMOD3 as a novel activator of RhoA.

Materials and Methods

Antibodies, Cells, and Reagents

All chemicals used were purchased from commercial sources. Rabbit polyclonal antibody to ELMOD3 was purchased from Sigma (Cat# HPA012126). Rhodamine phalloidin was from Life Technologies. Other antibodies used included mouse monoclonal antibodies to β-tubulin (Sigma) and the HA (Covance) and myc (Life Technologies) epitopes. Mouse embryonic fibroblasts (MEFs) were generously provided by Tamara Caspary (Emory University). All other cell lines including HeLa (human cervix epithelial cells), Cos7 (African green monkey kidney fibroblast), NRK (rat kidney epithelial cells), SF295 (human glioblastoma), and NIH3T3 (mouse embryo fibroblast) cells were from the ATCC.

Antigen competition was performed using purified recombinant ELMOD3 tagged at the N-terminus with either GST or trigger factor as indicated [34]. Primary antibody was incubated in PBS or with 20 µg antigen per µL of antibody on ice for three hours. Antibody solutions were then diluted directly in Blotto for immunoblot experiments or in blocking buffer for immunofluorescence experiments.

Cloning and Plasmids

All constructs for ELMOD3 used in this study encode human ELMOD3 isoform B (NCBI Reference Sequence: NP_001128493.1) which encodes a protein of 381 residues. The plasmids directing the expression of human ELMOD3-HA, ELMOD3(L265S)-HA, and GFP-ELMOD3 were kind gifts from Saima Riazuddin (Cincinnati Children's Hospital). The plasmid for ELMOD3(R211K)-HA was derived from these plasmids using the QuikChange site-directed mutagenesis kit by the Emory Cloning Core. The plasmid for mammalian expression of human GST-ELMOD3 was previously described [6]. The plasmid for bacterial expression of trigger factor fusion of ELMOD3 was constructed using the pCold^{TM} TF vector (Takara Bio Inc.). The plasmid for expression of HA-RhoA(F30L) was a kind gift from Richard Cerione (Cornell University). Plasmids for the mammalian expression of myc-RhoA and myc-RhoA(T19N) were gifts from Keith Burridge (University of North Carolina). Each plasmid was confirmed by DNA sequencing.

Cell Culture and Immunofluorescence

HeLa cells and MEFs were grown in Dulbecco's modified Eagle's medium containing 10% fetal calf serum (Atlanta Biologicals). Cells were transfected with Lipofectamine PLUS according to the manufacturer's directions (Life Technologies) for exogenous expression. Where indicated, HeLa cells were treated with 10 µM Y-27632, a ROCK inhibitor, in cell culture medium for three hours at 37°C, with one unit / mL of Rho activator I (Cytoskeleton Inc) in cell

culture medium for 30 minutes at 37°C, with 1 µg/mL Cytochalasin D in cell culture medium for one hour at 37°C, or with 50 µg/mL cycloheximide in cell culture medium for 16 hours at 37°C. For immunofluorescence, cells were fixed using 2% paraformaldehyde at room temperature for 15 minutes, washed four times in PBS, and then permeabilized with 0.05% saponin for 30 min at room temperature in blocking buffer containing 1% BSA in PBS. Cells were incubated in primary antibody overnight in blocking buffer, washed four times with a solution of 0.05% saponin in PBS (wash buffer) and labeled with Alexa Fluor 488 and/or Alexa Fluor 594 secondary antibodies (Life Technologies) at room temperature for one hour in blocking buffer. Cells were then washed twice and labeled with 1 µM Hoechst nuclear stain for five minutes in wash buffer. Cells were washed two more times with wash buffer then once with PBS before being mounted with Prolong Antifade (Life Technologies) [35]. Images shown are representative of the population or, where indicated, of the population of cells with a given phenotype.

RESULTS

ELMOD3 is associated with the actin cytoskeleton

We used a commercially available polyclonal antibody against ELMOD3 to determine the subcellular localization of endogenous ELMOD3. The antibody was first characterized by immunoblot using lysates from cell lines from a variety of species (Fig 1: Left panel). Two prominent bands with apparent molecular weights of ~60 and ~65 kDa were observed, whose intensities varied in the different cell line examined. Both of these bands were strongly reduced or ablated upon prior incubation of primary antibody with purified recombinant GST-ELMOD3 (Fig 1: Right panel). The antibody also recognized ectopic ELMOD3-HA from HeLa lysate and this band was also markedly reduced upon antigen competition. These data suggest that the two bands at 60 and 65 kDa represent endogenous ELMOD3 or share an epitope with a dominant one

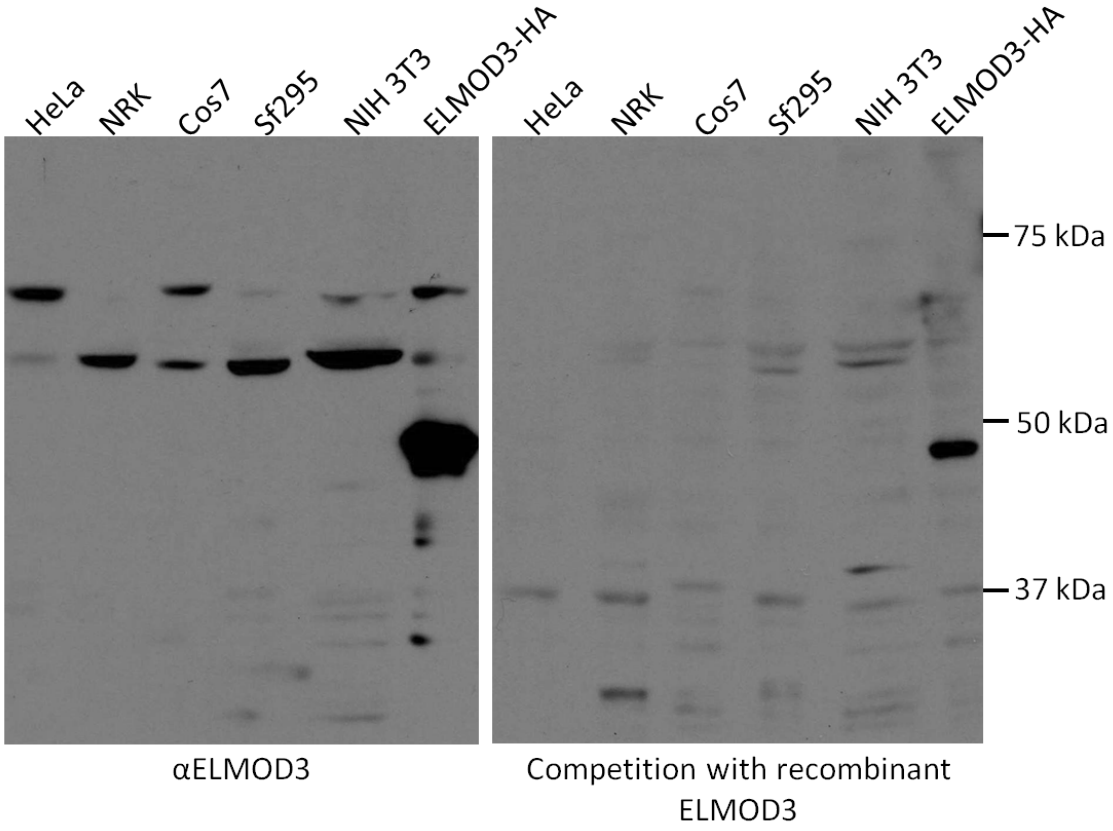

Figure 1: ELMOD3 migrates at a higher than expected apparent molecular weight on SDS gels. A rabbit polyclonal antibody directed against ELMOD3 detects two prominent bands in immunoblots that are effectively competed with purified recombinant GST-ELMOD3. Total cell lysate from various cell lysates (20 µg) was analyzed by immunoblot using our ELMOD3 antibody with (right) and without (left) competition with antigen, as described under Materials and Methods. ELMOD3 tagged at the C-terminus with HA (ELMOD3-HA) in HeLa lysate (10 µg) ran at the predicted molecular weight of ~48 kDa.

in ELMOD3. The two bands may represent the A and B isoforms of ELMOD3 that differ in length by 10 amino acids and have distinct C-termini. The apparent molecular weights of endogenous ELMOD3 differed greatly from both the predicted molecular weight of ELMOD3 (~43 kDa) and the apparent molecular weight of ectopically expressed ELMOD3-HA from HeLa lysate (~48kDa). Genomic analysis by the Riazuddin lab [7] were consistent with sequences deposited in GenBank suggesting that this size difference is not the result of an incomplete coding region or missing exon in the ELMOD3-HA expression vector.

We next used the ELMOD3 antibody to determine the subcellular localization of endogenous ELMOD3 in mouse embryonic fibroblasts (MEFs) (Fig 2 and 3). Staining of endogenous ELMOD3 displayed distinct organizations in polarized and non-polarized cells. In polarized, migrating cells (Fig 2: top row), ELMOD3 staining localized predominantly to the plasma membrane at the trailing edge of the cell indicated by the long actin tail stained by rhodamine-phalloidin (arrowheads). ELMOD3 puncta were also observed throughout the cell body. Similar staining patterns of puncta throughout and predominant trailing edge profiles were observed in other cell lines including MDCK, NIH-3T3, and SF295 (data not shown). Pre-incubation of primary antibody with purified recombinant TF-ELMOD3 substantially reduced signal intensity for ELMOD3 staining at the trailing edge and in puncta (Fig 2: bottom row). Thus, both the trailing edge and punctate staining pattern is specific to ELMOD3 and represents the subcellular localization of ELMOD3. Virtually all cells in each cell line examined contained ELMOD3 puncta and the majority of NIH-3T3, contact naïve MDCK, and SF295 cells displayed trailing edge localization. Staining of endogenous ELMOD3 in non-polarized MEFs primarily displayed discreet puncta that often aligned into linear organizations in the cell body (Fig 3). Co-staining with rhodamine-phalloidin revealed an association between the linear arrays of ELMOD3 puncta and actin stress fibers. A similar staining pattern for endogenous ELMOD3 was also observed in HeLa cells (Fig 5: top row) and treatment of HeLa cells with the actin de-

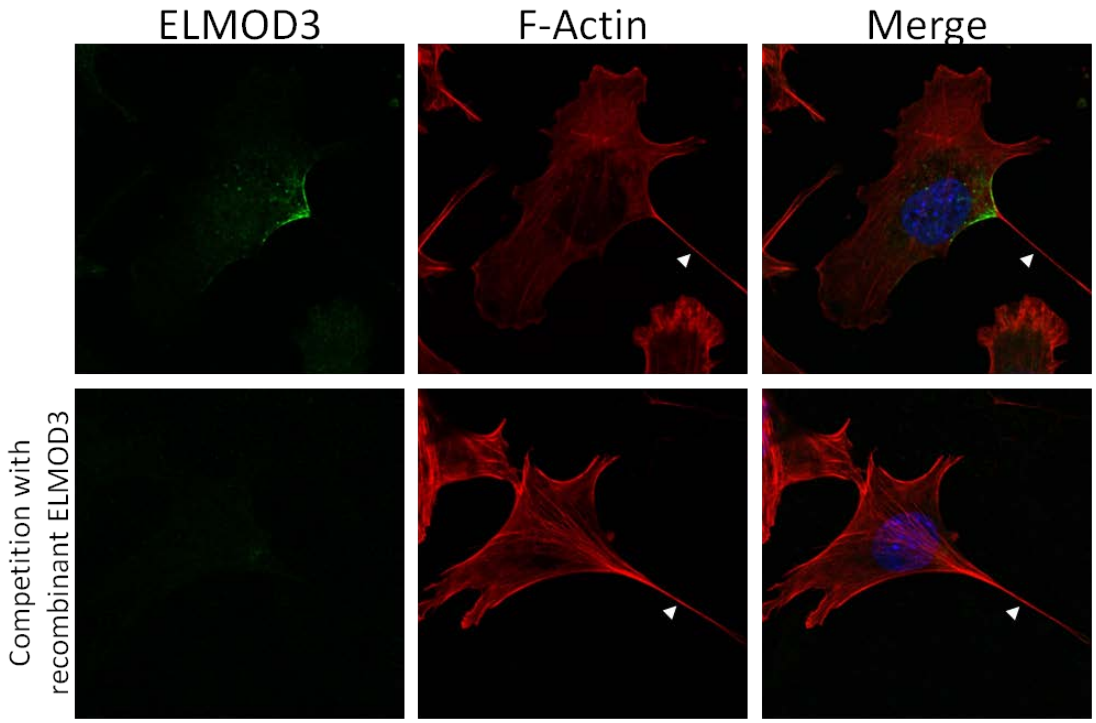

Figure 2: Endogenous ELMOD3 localizes to the trailing edge of migrating mouse embryonic fibroblasts (MEFs). MEFs were fixed and permeabilized as described in Materials and Methods before being developed with a rabbit polyclonal antibody to ELMOD3 (left panel) and with rhodamine-phalloidin to stain f-actin (middle panel) with (bottom row) or without (top row) competition with purified recombinant trigger factor-ELMOD3 (TF-ELMOD3). Migrating cells were identified by the presence of an actin tail (white arrowhead).

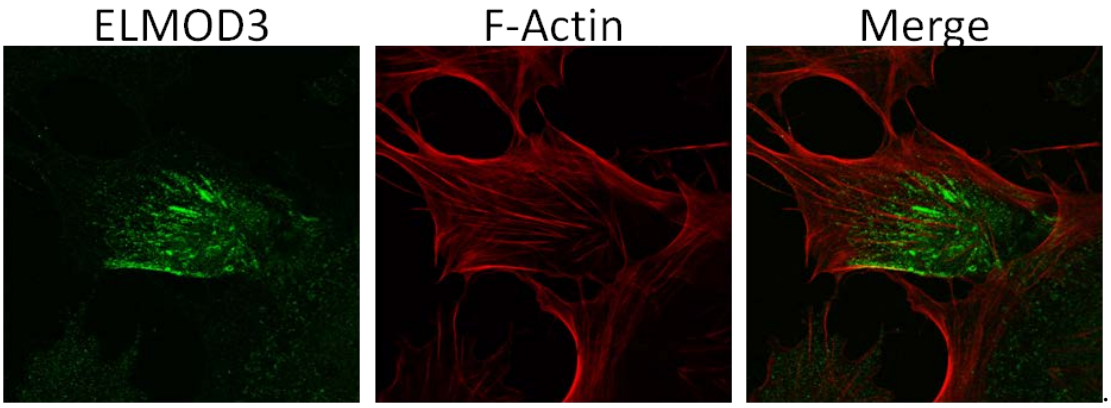

Figure 3: Endogenous ELMOD3 has a punctate staining pattern with organization along actin fibers in non-polarized mouse embryonic fibroblasts (MEFs). MEFs were fixed and permeabilized as described in Materials and Methods before being developed with a rabbit polyclonal antibody to ELMOD3 (left panel) and with rhodamine-phalloidin to stain F-Actin (middle panel).

polymerizing drug cytochalasin D resulted in a loss in the organization of endogenous ELMOD3 puncta (Fig 5: bottom row). Instead, ELMOD3 staining was predominantly in the form of larger foci that co-localized with rhodamine-phalloidin staining of aggregates of short actin filaments. Loss of normal ELMOD3 staining and the co-localization of ELMOD3 with actin aggregates in HeLa cells treated with cytochalasin D suggests that ELMOD3 is physically associated with the actin cytoskeleton. These findings were consistent with previously published work examining GFP-ELMOD3 in a confluent monolayer of MDCK cells [7] where GFP-ELMOD3 primarily localized to the cell cortex and redistributed to puncta upon treatment of cells with Cytochalasin D. Linear arrays were readily observable in MEFs, HeLa, and NIH/3T3 cells but were less prominent in other cell lines including MDCK and Sf295 cells. In MEFs, NIH/3T3 and HeLa cells, not all cells had the linear organization of puncta and only a portion of puncta in each cell with linear arrays aligned along them. It is unclear why some cells display this higher organization of ELMOD3 puncta along stress fibers while others do not, but localization of endogenous ELMOD3 is clearly linked to the actin cytoskeleton.

ELMOD3 protein has a long half-life in cells. We used cycloheximide to new protein synthesis to approximate the half-life of ELMOD3 protein in cells by immunoblot of ELMOD3 (Fig 4). There was no decrease in signal intensity for ELMOD3 in immunoblots after incubation of HeLa cells with cycloheximide for 16 hours. Cellular levels of another unrelated protein, β-tubulin, showed >50% decrease in signal intensity by immunoblot at the same time. Thus, the half-life of ELMOD3 protein is greater than 16 hours. Longer time courses of protein synthesis inhibition were not possible due to toxicity and cell death. We were also unable to use metabolic labeling and pulse-chase experiments to more accurately determine the half-life of ELMOD3 because we lack an antibody that works for immunoprecipitation of the endogenous protein. Attempts at knocking down ELMOD3 in cultured cells using RNAi have been unsuccessful, despite repeated attempts and protocols with several siRNAs and pools (data not shown). The

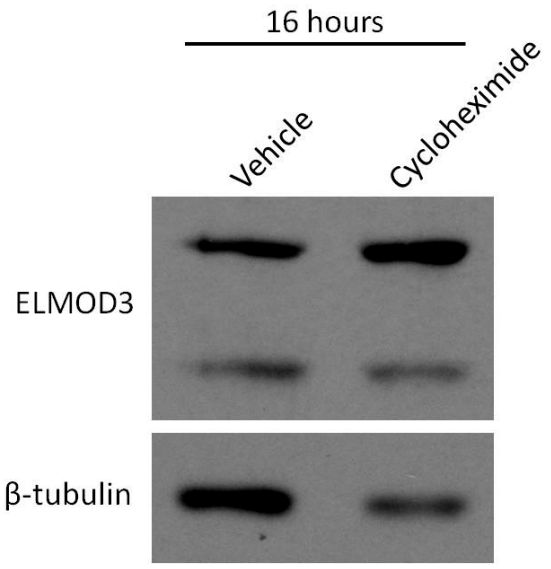

Figure 4: ELMOD3 protein levels are unchanged after inhibiting protein synthesis for 16 hours. HeLa cells were treated cycloheximide (50 µg/mL) or vehicle control for 16 hours at 37°C. Total cell lysates (top panel, 20 µg; bottom panel, 5 µg) were analyzed by immunoblot using antibodies directed against ELMOD3 or β-tubulin.

long-half life of ELMOD3 likely contributed to our failure to knock down ELMOD3 by transient transfection.

Expression of epitope tagged ELMOD3 causes blebbing of the plasma membrane

When expressed by transient transfection in HeLa cells, ELMOD3 tagged at the N-terminus with GFP (GFP-ELMOD3) or at the C-terminus with the HA epitope (ELMOD3-HA) caused extensive blebbing of the plasma membrane (Fig 6) in approximately 25% of transfected cells quantified from static images of fixed cells. Two transfected and two untransfected cells in the same frame were imaged every 10 seconds for 50 seconds using live-cell laser scanning confocal microscopy. Differential interference contrast (DIC) images showed a clear difference in the morphology of GFP-ELMOD3 transfected cells and control cells. Control cells had smooth, static edges during the imaging period in contrast to the dynamic blebbing morphology of the transfected cells. Although morphologically similar to microvesicles, which appear as blebs prior to being released into the media [36], GFP-ELMOD3 blebs are not released and instead are reabsorbed by the cell within 60 seconds. A chevron marks a bleb that initially appears and is fully retracted during the imaging period (Fig 6). GFP fluorescence revealed enrichment of GFP-ELMOD3 at the cell surface and at the periphery of plasma membrane blebs. This staining pattern is indicative of an association of GFP-ELMOD3 with the cell cortex. To further test whether blebs generated by epitope tagged ELMOD3 were being released from cells in the form of microvesicles, we attempted to purify microvesicles from cell culture media of HeLa cells transiently transfected with ELMOD3-HA, as previously described [36]. We failed to detect any microvesicles stimulated by the expression of ELMOD3-HA (data not shown). Thus, plasma membrane blebs are transient and dynamic structures that are re-absorbed by the cell. Over longer live-cell imaging periods, cells expressing GFP-ELMOD3 start and stop blebbing entirely in as short as ten minutes (data not shown). Thus, plasma membrane blebbing is a transient phenotype which may explain why only ~25% of transfected cells display the blebbing

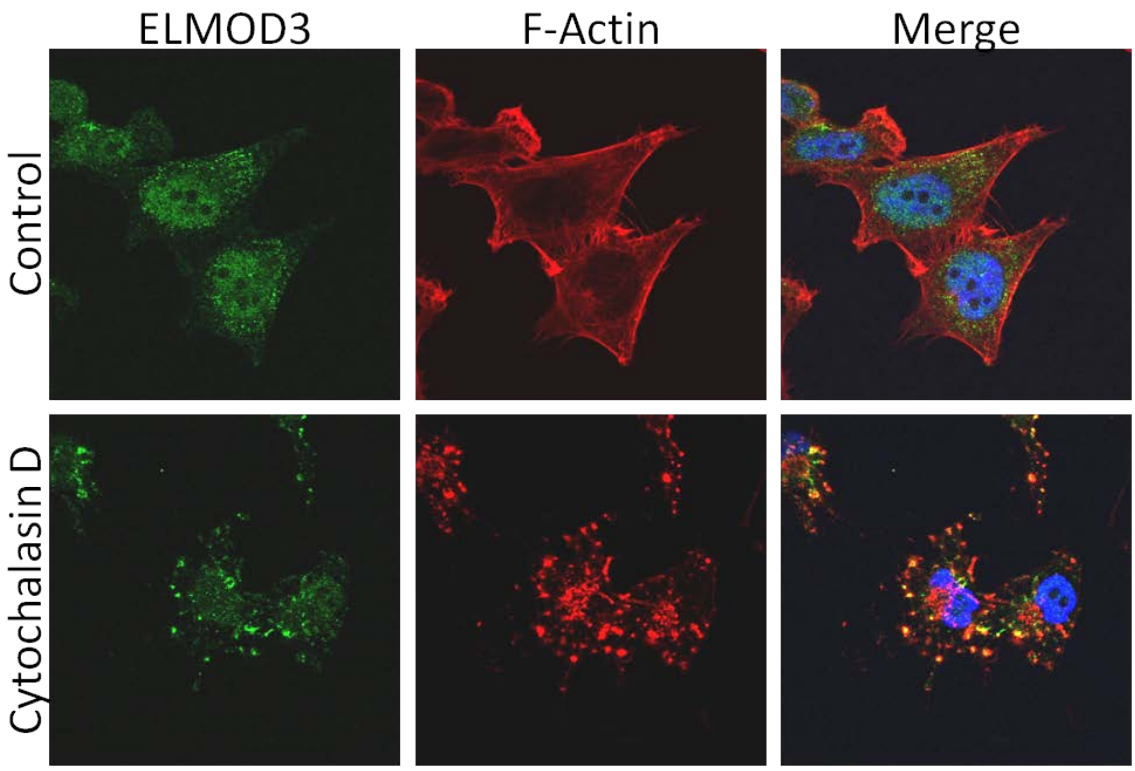

Figure 5: Endogenous ELMOD3 associates with the actin cytoskeleton. HeLa cells were treated with 1 µg/mL cytochalasin D (bottom row) or vector only (top row) for 1 hr then fixed and permeabilized as described in Materials and Methods. Cells were stained with a rabbit polyclonal antibody to ELMOD3 (left panels) and with rhodamine-phalloidin (middle panels) to stain F-actin.

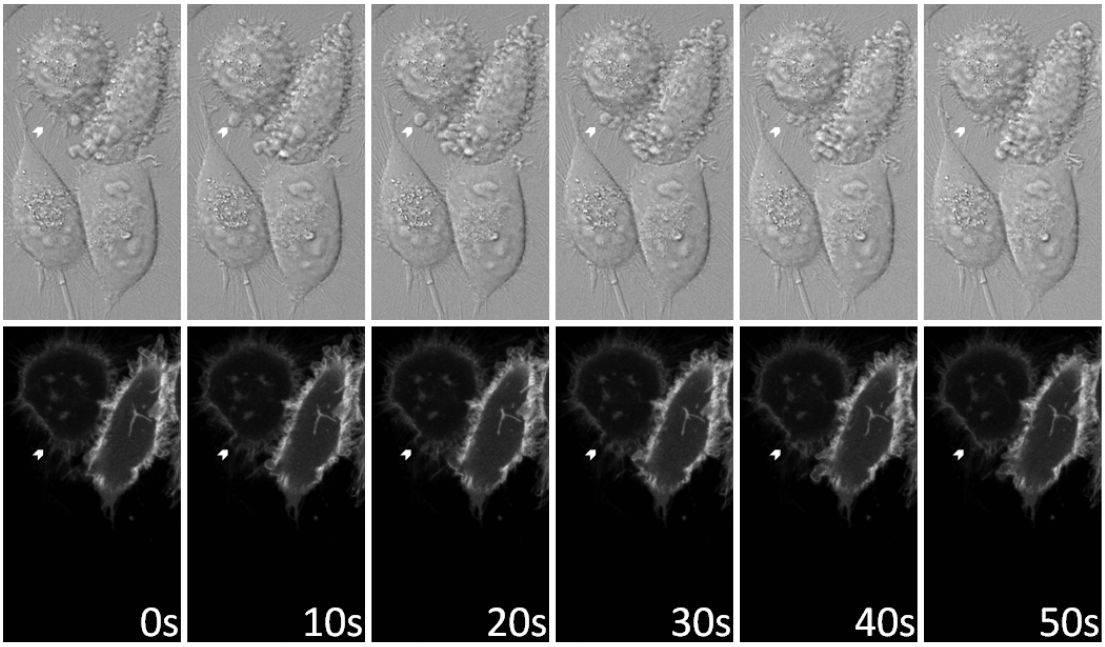

Figure 6: GFP-ELMOD3 causes dynamic plasma membrane blebbing. HeLa cells were transfected with GFP-ELMOD3 as described in Materials and Methods. Approximately 16 hours after transfection, DIC (top row) and GFP (bottom row) images were captured every 10 s for 50 s using a live-cell laser scanning confocal microscope. Chevron marks a plasma membrane bleb that appears and is fully retracted during the imaging period.

phenotype at one time in fixed cells. Longer live-cell imaging experiments will likely reveal a much higher percentage of transfected cells that transiently display the blebbing phenotype.

ELMOD3 induced plasma membrane blebs are downstream of RhoA activation

The association of endogenous ELMOD3 with the actin cytoskeleton and cell morphology changes upon expression of GFP-ELMOD3 led us to question whether expression of epitope tagged ELMOD3 had any effects on the actin cytoskeleton. ELMOD3 tagged at the C-terminus with the HA epitope (ELMOD3-HA) was expressed in HeLa cells by transient transfection and cells were fixed and stained with antibodies to the HA epitope and rhodamine-phalloidin, as described in *Materials and Methods*. Control cells transfected with empty vector (Fig 7A: top row) had normal looking f-actin staining with smooth and distinct cell periphery staining and membrane ruffles. Expression of ELMOD3-HA resulted in distinct changes in f-actin staining at the cell periphery in the form of plasma membrane blebs and in an overall loss in membrane ruffling (Fig 7A: bottom row). ELMOD3-HA expressing cells were also less spread out when compared to control cells, consistent with disruption of the actin cytoskeleton and the loss of the motile phenotype. Merged images of ELMOD3-HA and f-actin staining revealed a high degree of colocalization at the cell periphery and in plasma membrane blebs. These data are consistent with the association between endogenous ELMOD3 and the actin cytoskeleton (Figs 2-4) and suggest a potential role for ELMOD3 as a novel regulator of the actin cytoskeleton. Expression of a point mutant [6], ELMOD3(R211K)-HA, that is catalytically dead for GAP activity resulted in identical phenotypes. This supports the conclusion that effects of ELMOD3 on blebbing are not mediated by its GAP activity toward a GTPase.

Membrane blebbing is a naturally occurring phenomenon typically associated with amoeboid cell motility and apoptosis [33, 37]. Blebbing induced by the expression of epitope tagged ELMOD3 was not attributed to cellular apoptosis because we failed detect release of

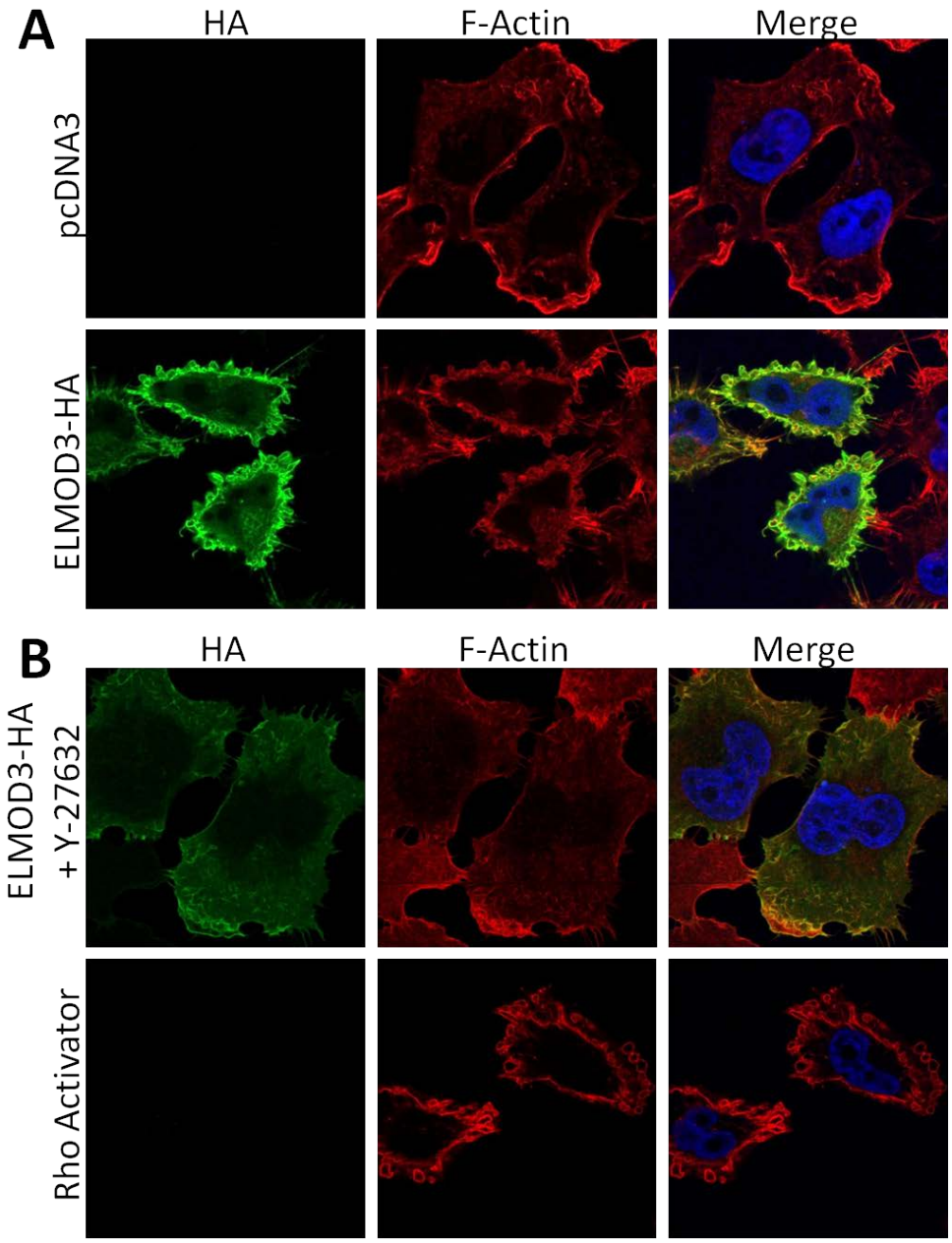

Figure 7: ELMOD3-HA causes changes in the actin cytoskeleton in a Rho-dependent fashion. HeLa cells were transfected with ELMOD3-HA or empty pcDNA3 vector. Approximately 16 hours after transfection cells were fixed and permeabilized, as described in Materials and Methods, before being developed with a mouse monoclonal antibody to the HA epitope (left panels) and with rhodamine-phalloidin to stain f-actin (middle panels). *A.* ELMOD3-HA changes cell shape and rhodamine-phalloidin stains membrane blebs. *B.* (Top panels) HeLa cells transfected with ELMOD3-HA vector were treated with 10 µM Y-27632, a specific ROCK inhibitor, for 3 hours at 37C. Note the smooth plasma membrane appearance and absence of

cytochrome c from mitochondria or any increase in nuclear fragmentation in blebbing cells (data not shown) or the cell population at these or later time points. Thus, the blebbing phenotype is likely representative of the biology of ELMOD3 and is not a secondary effect of apoptosis. Blebbing is initiated when the association between the plasma membrane and the actin cortex is disrupted by either a loss in adhesion or local rupture of the actin cortex [33, 37]. Hydrostatic pressure from the cell body leads to expansion of the bleb followed by re-assembly of the actin cortex within the bleb and finally retraction of the bleb to restore normal membrane/cortex morphology. This entire process occurs within 60 seconds which is consistent with blebs resulting from GFP-ELMOD3 expression observed in live cell imaging experiments (Fig 6). One of the prevailing models for the initiation of plasma membrane blebs is through the activation of the RhoA/ROCK/MLC signaling pathway [38, 39]. Activation of myosin in this pathway leads to localized contraction and shortening of the actin cortex puckering the plasma membrane out from the cell body and initiating bleb formation. Treatment of HeLa cells with a prolonged activator of RhoA signaling resulted in membrane blebbing and similar changes to cell morphology as observed with ELMOD3-HA expression (Fig6B: top row). Staining of f-actin revealed distinct membrane blebs in approximately 25% of cells (Fig 9), smaller cells, and an overall loss in membrane ruffling. To test whether ELMOD3 induced blebs were the product of activation of RhoA/ROCK/MLC, HeLa cells expressing ELMOD3-HA were treated with a potent inhibitor ROCK, Y-27632 (Fig 7B: bottom row). Pharmacological inhibition of ROCK nearly ablated the membrane blebbing phenotype (Fig 9) and reversed the changes in cell size and morphology. Treated cells favored a more spread out morphology with clearly visible membrane ruffles, as seen in controls that do not express ELMOD3-HA. Thus, ELMOD3 induced blebs are likely a product of excessive activation of the RhoA/ROCK/MLC signaling pathway. These data are also consistent with ELMOD3 functioning upstream of ROCK in this pathway. ELMOD3-HA staining also retained extensive co-localization with f-actin in Y-27632 treated cells, further supporting an association between ELMOD3 and the actin cytoskeleton (Fig 7B: bottom row).

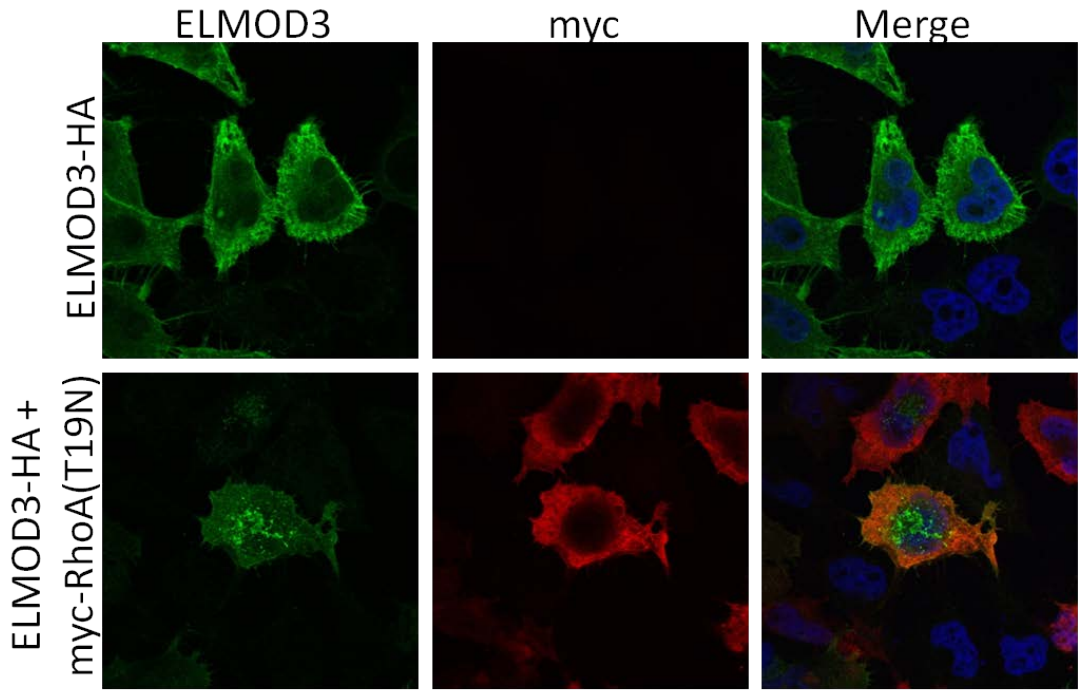

Figure 8: Expression of dominant negative RhoA (T19N) inhibits blebbing and changes ELMOD3-HA localization. HeLa cells were transfected with ELMOD3-HA and either empty vector or one directing expression of myc-RhoA(T19N). Approximately 16 hours after transfection cells were fixed and permeabilized, as described in Materials and Methods, before being developed with a rabbit polyclonal antibody to ELMOD3 (left panels) and with rhodamine-phalloidin to stain F-Actin (middle panels).

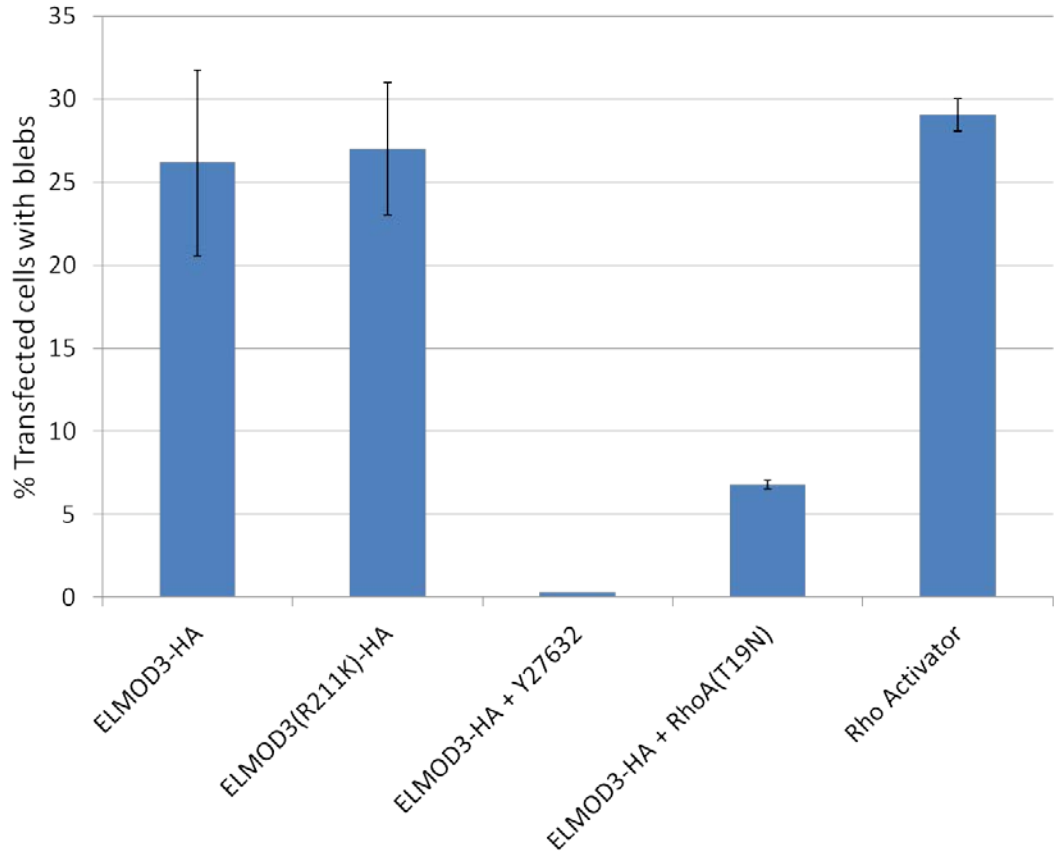

Figure 9: ELMOD3-HA induced plasma membrane blebbing is dependent on the RhoA signaling pathway. The number of blebbing cells was quantified in each condition using stains for ELMOD3-HA and f-actin. Values reported are the percent of transfected cells with membrane blebs. Each bar indicates quantification from 3 experiments in which 350 cells were counted. Error bars represent standard error of the mean.

To further test whether ELMOD3 is a novel regulator of the RhoA/ROCK/MLC signaling pathway, we asked whether a dominant negative mutant of RhoA (myc-RhoA(T19N)) was sufficient to block the membrane blebbing phenotype (Fig 8). The number of blebbing cells was substantially reduced in HeLa cells expressing both ELMOD3-HA and myc-RhoA(T19N) (Fig 9). These data further support our conclusion that membrane blebbing is a result of activation of RhoA/ROCK/MLC by ELMOD3-HA and place ELMOD3 upstream of RhoA in the signaling pathway. Interestingly, co-expression of ELMOD3-HA with myc-RhoA(T19N) also resulted in a striking change in the localization of ELMOD3-HA (Fig 8). For a more direct comparison, images of non-blebbing cells were captured of cells transfected with ELMOD3-HA alone (Fig 8: top row). As expected, HeLa cells expressing ELMOD3-HA alone showed enrichment of ELMOD3-HA at the cell periphery. Cells transfected with both ELMOD3-HA and myc-RhoA(T19N) showed enrichment of ELMOD3-HA staining in puncta and foci in the interior of the cell with a perinuclear distribution (Fig 8: bottom row).

Discussion

In this study, we performed initial characterization of the subcellular localizations and function of the Arf family GAP, ELMOD3. Localization of endogenous ELMOD3 was highly dynamic depending on the polarization state of the cell and was linked to the actin cytoskeleton. Endogenous ELMOD3 localized to puncta in non-polarized cells and to the cell periphery at the trailing edge of polarized, migrating cells. Expression of ELMOD3-HA revealed a role for ELMOD3 at the cell cortex, as evidenced by the induction of plasma membrane blebbing and actin rearrangement at the cortex. Inhibition of the RhoA/ROCK/MLC signaling pathway using two different approaches blocked the blebbing phenotype, suggesting that membrane blebbing is a RhoA-dependent process. We lack direct evidence of RhoA activation by ELMOD3 but these

data suggest that ELMOD3 is a novel activator of the RhoA/ROCK/MLC pathway that acts upstream of RhoA. These findings offer initial insights into the cellular role and mechanism of ELMOD3.

Studies of the subcellular localization of endogenous ELMOD3 revealed a very dynamic localization depending on the polarization state of cells. Localization of endogenous ELMOD3 shifted from a punctate staining pattern in non-polarized cells to the cell edge at the trailing edge of the cell upon adoption of the migratory phenotype. Each of these localizations is linked to the actin cytoskeleton as ELMOD3 puncta organized along actin stress fibers and the cell cortex and trailing edge are both actin based structures. Disruption of the actin cytoskeleton in HeLa cells with cytochalasin D further supported an association between ELMOD3 and the actin cytoskeleton. ELMOD3 staining shifted from puncta with higher organization into linear arrays to much larger foci with no apparent organization upon treatment of cells with cytochalasin D. Intriguingly, ELMOD3 foci colocalized with rhodamine-phalloidin positive structures consisting of short actin filaments and other proteins closely associated with the actin cytoskeleton including the endosomal proteins Rab5 and transferrin receptor [40, 41]. These findings suggest that ELMOD3 physically interacts with the actin cytoskeleton and that ELMOD3 localization is dynamic and actin driven. ELMOD3 puncta may represent endocytic vesicles translocating ELMOD3 from the cell periphery in non-polarized cells consistent with the trailing edge versus punctate staining patterns for ELMOD3 in polarized and non-polarized MEFs. However, we have failed to detect substantial overlap between ELMOD3 puncta and endosomal markers including EEA1 and transferrin receptor in immunofluorescence experiments (data not shown). A tight correlation between localizations of ELMOD3 and actin is also evident in various over-expression experiments throughout this study as epitope tagged ELMOD3 repeatedly co-localized with the actin cytoskeleton under various experimental conditions and caused changes in actin organization in the form of plasma membrane blebbing.

Plasma membrane blebbing has been attributed primarily to cellular apoptosis, RhoA-driven amoeboid-like motility in tumor cells, and in the shedding of microvesicles from the cell surface. We ruled out cellular apoptosis as the cause for plasma membrane blebbing because expression of ELMOD3-HA is not toxic to cells, and did not induce nuclear fragmentation or the release of cytochrome c from mitochondria (data not shown). Although very similar in appearance to microvesicles described by the Cerione group in MDA-MB-231 cells [36, 42], we failed to detect any microvesicles released into cell culture media induced by the expression of ELMOD3-HA. Live-cell imaging also clearly showed membrane blebs being re-absorbed by the cell instead of being released (Fig 6). Thus, the most likely cause of ELMOD3 induced plasma membrane blebbing was through activation of the RhoA signaling pathway. A similar plasma membrane blebbing phenotype was observed when HeLa cells were treated with a potent and prolonged activator of RhoA signaling based on the calpeptin molecule (Fig 7B) and has also been described in the literature upon expression of a fast-cycling mutant of RhoA, although these blebs were attributed to microvesicles. Pharmacological inhibition of RhoA signaling with the inhibitor of ROCK Y-27632 or inhibition of RhoA activation by expression of a dominant-negative mutant of RhoA each substantially reduced the number of blebbing cells induced by the expression of ELMOD3-HA (Fig 9). We interpret these data to indicate that ELMOD3-HA-induced plasma membrane blebbing is the result of activation of the RhoA signaling pathway and that ELMOD3 is a novel regulator of RhoA and ROCK. ELMOD3 is likely acting on or upstream of RhoA as co-expression of dominant negative RhoA blocked the blebbing phenotype (Fig 9). Dominant negative GTPases bind to their respective GEFs with high affinity and prevent activation of the endogenous GTPase. Thus, these results also suggest that the most likely mechanism of RhoA activation by ELMOD3 is via activation of one or more RhoA GEF(s). This mechanism would also closely parallel that of another human ELMO family member ELMO1 which functions as an enhancer of GEF activity of the Rac1 GEF DOCK180. A potential target for ELMOD3 is the RhoA GEF, leukemia-associated Rho-GEF (LARG) because it is essential for

plasma membrane blebbing of MDA-MB-231 cells [30]. Downstream targets of LARG-mediated RhoA activation, including the formins mDia1 and mDia2, have both been linked to plasma membrane blebbing and mDia1 exhibits feedback activation of RhoA through LARG [29, 30]. Future mechanistic studies of ELMOD3 will focus initially on LARG and mDia1 and may be further extended to other Rho GEFs in high throughput RNAi screens using the plasma membrane blebbing phenotype as an output. Preliminary studies using another approach to pulldown activated RhoA GEFs and GAPs developed by the Burridge lab [43] showed no new bands or bands with increased intensity in silver stained gels in response to ELMOD3-HA expression in HeLa or HEK293T cells (data not shown). Mass spectrometry analysis or immunoblot of suspected proteins (e.g. LARG) of these samples may be more informative as only a handful of known RhoA GEFs and GAPs are abundant enough in these pulldowns to be identified by silver stain [43]. Other potential, unknown mechanisms will also be examined with a focus on identification of ELMOD3 binding partners and analysis of other means of RhoA activation including inhibition of RhoA GAPs or GDIs and down-regulation of the activation state of Rac1. Loss of function studies of ELMOD3 will also be rigorously pursued using ELMOD3 knock-out MEFs from the Riazuddin lab and/or targeted knockouts of ELMOD3 in other cell lines using CRISPR technology as attempts at knocking down ELMOD3 in cultured cells using RNAi have been unsuccessful, despite repeated attempts and protocols with several siRNAs and pools (data not shown).

Changes in the localization of ELMOD3-HA when co-expressed with dominant negative myc-RhoA(T19N) (Fig 8) suggest that ELMOD3 localization is governed by RhoA or some RhoA dependent mechanism. The identity of the ELMOD3-HA puncta in these cells is unknown as is the mechanism of ELMOD3-HA enrichment at the cell edge when expressed alone. Thus, these data are difficult to interpret but are consistent with dynamic localization of ELMOD3 and with some association of ELMOD3 with RhoA-induced actin structures.

Immunoblots of endogenous versus epitope tagged exogenous ELMOD3 yielded confusing results (Fig 1). Endogenous ELMOD3 ran as two distinct bands in different cell types with apparent molecular weights approximately 12 and 17 kDa higher than ELMOD3-HA expressed in the same cells. Analyses of the ELMOD3 locus were consistent with both the transcript sequences deposited in GenBank and with ELMOD3 constructs used in this study. The absence of a detectable band at the predicted molecular weight for ELMOD3 (~42 kDa) suggests that this size discrepancy is unlikely to be the result of a dynamic post-translational modification as virtually all of the endogenous protein would need to be modified. This conclusion is further supported by the failure to detect any higher molecular weight bands for ELMOD3 tagged at either the N- or C-terminus expressed in HeLa using antibodies against the epitope tags suggesting that none of the exogenous protein is modified in such a fashion as to support a large shift in electrophoretic mobility. The finding that the exogenous proteins display their expected electrophoretic mobility is evidence that the ELMOD3 protein does not migrate aberrantly in SDS gels as a result of unusual binding of SDS or retention of a (partially) folded state. Thus, it is unclear why endogenous ELMOD3 is running with higher apparent electrophoretic mobility than expected. The two bands representing endogenous ELMOD3 may be the result of the A and B isoforms of the protein which have differing C-termini and lengths of 391 and 381 residues, respectively. However, their predicted molecular weights differ by only 1 kDa with the A isoform being the larger and are inconsistent with the ~5 kDa observed in Figure 1. Alternatively, both bands observed for endogenous ELMOD3 may represent the A isoform only as our expression constructs for ELMOD3 were for the B isoform only. A strong focus will be placed on identifying the reason for the size discrepancy between endogenous and ectopically expressed ELMOD3 in future experiments. Unfortunately, there are very few antibodies available today that bind specifically to ELMOD3 and none have proven capable of immunoprecipitation, that might have allowed ready purification and identification by mass spectrometry.

We conclude that ELMOD3 is a novel regulator of the actin cytoskeleton with presumed roles at the trailing edge of migrating cells and at actin stress fibers. The membrane blebbing phenotype associated with expression of GFP-ELMOD3 or ELMOD3-HA is consistent with activation of myosin motors at the cell cortex. This is indicative of a role for endogenous ELMOD3 as a regulator of actomyosin contraction during migration at the cell tail and at actin stress fibers to govern cell shape, focal adhesion, or some other myosin mediated pathway. Although our evidence is indirect, these data also suggest that ELMOD3 is a novel activator of RhoA. Our initial expectations of ELMOD3 function in cells were as a GAP for Arf family GTPases based on the biochemical GAP activity of ELMOD3 [6] and the proposed role for ELMOD1 as an Arf GAP at the Golgi [1]. This study argues against that role because over-expression of a catalytically (GAP) dead mutant of ELMOD3 phenocopied the wild type protein in promoting blebbing. Instead, ELMOD3 function appears to parallel the role of ELMOs as enhancers of Rho family GTPases providing a functional link between the phylogenetically distinct ELMOs and ELMODs. These findings also contribute to a better understanding of the role of ELMOD3 in deafness and in the actin-based stereocilia of hair cells.

References

1. East, M.P., et al., *ELMO domains, evolutionary and functional characterization of a novel GTPase-activating protein (GAP) domain for Arf protein family GTPases.* J Biol Chem, 2012. **287**(47): p. 39538-53.
2. Grimsley, C.M., et al., *Characterization of a novel interaction between ELMO1 and ERM proteins.* J Biol Chem, 2006. **281**(9): p. 5928-37.
3. Katoh, H. and M. Negishi, *RhoG activates Rac1 by direct interaction with the Dock180-binding protein Elmo.* Nature, 2003. **424**(6947): p. 461-4.

4. Patel, M., et al., *An evolutionarily conserved autoinhibitory molecular switch in ELMO proteins regulates Rac signaling.* Curr Biol, 2010. **20**(22): p. 2021-7.

5. Bowzard, J.B., et al., *ELMOD2 is an Arl2 GTPase-activating protein that also acts on Arfs.* J Biol Chem, 2007. **282**(24): p. 17568-80.

6. Ivanova, A.A., et al., *Characterization of Recombinant ELMOD Proteins as GTPase Activating Proteins (GAPs) for ARF Family GTPases.* J Biol Chem, 2014.

7. Jaworek, T.J., et al., *An alteration in ELMOD3, an Arl2 GTPase-activating protein, is associated with hearing impairment in humans.* PLoS Genet, 2013. **9**(9): p. e1003774.

8. Chung, S., et al., *A common set of engulfment genes mediates removal of both apoptotic and necrotic cell corpses in C. elegans.* Nat Cell Biol, 2000. **2**(12): p. 931-7.

9. Gumienny, T.L., et al., *CED-12/ELMO, a novel member of the CrkII/Dock180/Rac pathway, is required for phagocytosis and cell migration.* Cell, 2001. **107**(1): p. 27-41.

10. Brugnera, E., et al., *Unconventional Rac-GEF activity is mediated through the Dock180-ELMO complex.* Nat Cell Biol, 2002. **4**(8): p. 574-82.

11. Lu, M., et al., *PH domain of ELMO functions in trans to regulate Rac activation via Dock180.* Nat Struct Mol Biol, 2004. **11**(8): p. 756-62.

12. Wu, Y.C., et al., *C. elegans CED-12 acts in the conserved crkII/DOCK180/Rac pathway to control cell migration and cell corpse engulfment.* Dev Cell, 2001. **1**(4): p. 491-502.

13. Zhou, Z., et al., *The C. elegans PH domain protein CED-12 regulates cytoskeletal reorganization via a Rho/Rac GTPase signaling pathway.* Dev Cell, 2001. **1**(4): p. 477-89.

14. Lu, M., et al., *A Steric-inhibition model for regulation of nucleotide exchange via the Dock180 family of GEFs.* Curr Biol, 2005. **15**(4): p. 371-7.

15. deBakker, C.D., et al., *Phagocytosis of apoptotic cells is regulated by a UNC-73/TRIO-MIG-2/RhoG signaling module and armadillo repeats of CED-12/ELMO.* Curr Biol, 2004. **14**(24): p. 2208-16.

16. Grimsley, C.M., et al., *Dock180 and ELMO1 proteins cooperate to promote evolutionarily conserved Rac-dependent cell migration.* J Biol Chem, 2004. **279**(7): p. 6087-97.

17. Santy, L.C., K.S. Ravichandran, and J.E. Casanova, *The DOCK180/Elmo complex couples ARNO-mediated Arf6 activation to the downstream activation of Rac1*. Curr Biol, 2005. **15**(19): p. 1749-54.

18. Santy, L.C. and J.E. Casanova, *Activation of ARF6 by ARNO stimulates epithelial cell migration through downstream activation of both Rac1 and phospholipase D.* J Cell Biol, 2001. **154**(3): p. 599-610.

19. Hiramoto, K., M. Negishi, and H. Katoh, *Dock4 is regulated by RhoG and promotes Rac-dependent cell migration.* Exp Cell Res, 2006. **312**(20): p. 4205-16.

20. Katoh, H., K. Hiramoto, and M. Negishi, *Activation of Rac1 by RhoG regulates cell migration.* J Cell Sci, 2006. **119**(Pt 1): p. 56-65.

21. Myers, K.R. and J.E. Casanova, *Regulation of actin cytoskeleton dynamics by Arf-family GTPases.* Trends Cell Biol, 2008. **18**(4): p. 184-92.

22. Raftopoulou, M. and A. Hall, *Cell migration: Rho GTPases lead the way.* Dev Biol, 2004. **265**(1): p. 23-32.

23. Hall, A., *Rho family GTPases.* Biochem Soc Trans, 2012. **40**(6): p. 1378-82.

24. Sander, E.E., et al., *Rac downregulates Rho activity: reciprocal balance between both GTPases determines cellular morphology and migratory behavior.* J Cell Biol, 1999. **147**(5): p. 1009-22.

25. Ridley, A.J., et al., *Cell migration: integrating signals from front to back.* Science, 2003. **302**(5651): p. 1704-9.

26. Small, J.V., et al., *Assembling an actin cytoskeleton for cell attachment and movement.* Biochim Biophys Acta, 1998. **1404**(3): p. 271-81.

27. Pellegrin, S. and H. Mellor, *Actin stress fibres.* J Cell Sci, 2007. **120**(Pt 20): p. 3491-9.

28. Sahai, E., *Mechanisms of cancer cell invasion.* Curr Opin Genet Dev, 2005. **15**(1): p. 87-96.

29. Wyse, M.M., et al., *Dia-interacting protein (DIP) imposes migratory plasticity in mDia2-dependent tumor cells in three-dimensional matrices.* PLoS One, 2012. **7**(9): p. e45085.

30. Kitzing, T.M., et al., *Positive feedback between Dia1, LARG, and RhoA regulates cell morphology and invasion.* Genes Dev, 2007. **21**(12): p. 1478-83.

31. Sahai, E. and C.J. Marshall, *Differing modes of tumour cell invasion have distinct requirements for Rho/ROCK signalling and extracellular proteolysis.* Nat Cell Biol, 2003. **5**(8): p. 711-9.

32. Wyckoff, J.B., et al., *ROCK- and myosin-dependent matrix deformation enables protease-independent tumor-cell invasion in vivo.* Curr Biol, 2006. **16**(15): p. 1515-23.

33. Fackler, O.T. and R. Grosse, *Cell motility through plasma membrane blebbing.* J Cell Biol, 2008. **181**(6): p. 879-84.

34. Ivanova, A.A., et al., *Characterization of Recombinant ELMOD (Cell Engulfment and Motility Domain) Proteins as GTPase-activating Proteins (GAPs) for ARF Family GTPases.* J Biol Chem, 2014. **289**(16): p. 11111-21.

35. Valnes, K. and P. Brandtzaeg, *Retardation of immunofluorescence fading during microscopy.* J Histochem Cytochem, 1985. **33**(8): p. 755-61.

36. Antonyak, M.A., et al., *Cancer cell-derived microvesicles induce transformation by transferring tissue transglutaminase and fibronectin to recipient cells.* Proc Natl Acad Sci U S A, 2011. **108**(12): p. 4852-7.

37. Charras, G.T., *A short history of blebbing.* J Microsc, 2008. **231**(3): p. 466-78.

38. Charras, G.T., et al., *Non-equilibration of hydrostatic pressure in blebbing cells.* Nature, 2005. **435**(7040): p. 365-9.

39. Paluch, E., et al., *Dynamic modes of the cortical actomyosin gel during cell locomotion and division.* Trends Cell Biol, 2006. **16**(1): p. 5-10.

40. Mortensen, K. and L.I. Larsson, *Effects of cytochalasin D on the actin cytoskeleton: association of neoformed actin aggregates with proteins involved in signaling and endocytosis.* Cell Mol Life Sci, 2003. **60**(5): p. 1007-12.

41. Schliwa, M., *Action of cytochalasin D on cytoskeletal networks.* J Cell Biol, 1982. **92**(1): p. 79-91.

42. Li, B., et al., *RhoA triggers a specific signaling pathway that generates transforming microvesicles in cancer cells.* Oncogene, 2012. **31**(45): p. 4740-9.

43. Garcia-Mata, R., et al., *Analysis of activated GAPs and GEFs in cell lysates.* Methods Enzymol, 2006. **406**: p. 425-37.

Chapter IV

Putative binding partners of ELMODs suggest novel functions and mechanisms

Michael Patrick East

Department of Biochemistry and Program in Biochemistry, Cell, and Developmental Biology, Emory University, Atlanta GA 30322

Introduction

There is currently a wealth of information available for the guanine nucleotide exchange factors (GEFs) and GTPase activating proteins (GAPs) for the Arf and Sar proteins [1-6] but very little is known about the regulators of the Arl proteins. To date, only five GAPs for any of the 22 mammalian Arls have been identified and there are no known GEFs. The five mammalian Arl GAPs include the three ELMOD proteins, cofactor C, and retinitis pigmentosa 2 (RP2) [7-11]. The well characterized Arf GAP Gcs1p in the yeast *S. cerevisiae* was also found to have GAP activity for Arl1 but there is no evidence to support that this activity is conserved in the mammalian ortholog ArfGAP1 [12]. Despite how little is known about the mammalian Arl GAPs, the bulk of the available literature links these proteins to disease. Both ELMOD1 and ELMOD3 have been implicated in deafness [9, 13]. ELMOD2 is linked to idiopathic pulmonary fibrosis (IPF), a debilitating and lethal disease that today is untreatable and poorly understood as to etioloty, and to the antiviral response [14-16]. Several studies have reported mutations in RP2 linked to the most severe form of retinitis pigmentosa and knock out of RP2 in mice or zebrafish results in retinal degeneration [17-20]. Thus, Arl GAPs have substantial clinical significance pointing to some very important roles for these proteins in the cell.

The ELMOD proteins are ancient and have been conserved throughout eukaryotic evolution suggesting some important or essential role for ELMODs in the cell. Our previous work points toward a role for ELMOD1 as an Arf GAP at the Golgi [21]. In the same study we showed that ELMOD1 was predominantly soluble in cell fractionation experiments and was only found to localize to nuclear speckles by indirect immunofluorescence. Upon over-expression, ELMOD1 localized to the Golgi, lipid droplets, and an ER-like reticular structure throughout the cell. Naturally occurring mutations in ELMOD1 in mice have been linked to deafness and to the disruption and loss of actin based mechanosensory stereocilia in inner ear hair cells [13]. We currently lack any functional details for ELMOD1 at any of these locations with the exception of

the Golgi. ELMOD2 localizes predominantly to mitochondria and regulates mitochondrial morphology and motility. Depletion of ELMOD2 in HeLa cells resulted in fragmentation of mitochondria and clustering of mitochondria around the nucleus in a manner that phenocopies depletion of or expression of a dominant negative mutant of Arl2 (Newman *et. al.*, in press). We argue that ELMOD2 is acting as an effector for Arl2 in this phenotype but we lack additional details or components of ELMOD2 and Arl2 pathways in mitochondria. ELMOD2 has also been found at lipid droplets in proteomic studies of purified lipid droplets and by indirect immunofluorescence upon over-expression of epitope tagged ELMOD2 [21-23]. ELMOD3 is linked to the actin cytoskeleton and is a putative activator of the RhoA signaling pathway (Chapter 3). ELMOD3 has been linked to deafness in a human family and localizes to stereocilia in inner ear hair cells [9]. The role of ELMOD3 in stereocilia may be linked to RhoA, but how ELMOD3 activates RhoA remains unknown. Of the three human ELMODs, ELMOD3 has the lowest specific activity as a GAP for each of the GTPases tested [11]. I hypothesize that recombinant preparations of ELMOD3 lack a binding partner and/or cofactor that is important for efficient GAP activity. Thus, each of the three ELMODs displays a diverse array of subcellular localizations and cellular functions, but we desperately lack mechanistic data for most of the functions and means of specific subcellular localizations.

In this study, we use co-immunoprecipitation (co-IP) and quantitative mass spectrometry with stable isotope labeling in cells (SILAC) to identify potential binding partners of the three human ELMODs to provide insight into the functions and mechanisms of the ELMODs. Additional studies are required to confirm interactions between proteins identified in the co-IPs but the SILAC technology provides a high level of confidence in the identified binding partners. Thus, we also interpret the potential functional implications of some of the putative binding partners that we have the highest confidence in and how they relate to the current ELMOD

literature. We also use established Arl2 GAP assays to identify a heat sensitive enhancer of GST-ELMOD3 GAP activity in testis extracts.

Materials and Methods

Antibodies, Cells, and Reagents - All chemicals used were purchased from commercial sources. Mouse monoclonal antibody to HA was purchased from Covance. Rhodamine phalloidin was from Life Technologies. HeLa cells were from the ATCC. Plasmids for the mammalian expression of GFP-PLC-δ1-PH and GFP-BTK-PH were purchased from Addgene [24].

Stable isotope labeling with amino acids assay (SILAC) – HeLa cells and HeLa cells infected with lentivirus encoding Tet-On inducible expression of human ELMOD1-HA or ELMOD2-HA, as previously described [21], were cultured for eleven days in DMEM supplemented with 200 mg/mL proline and 10% FBS without (lite medium) or with ^{13}C and ^{15}N labeled arginine and lysine (heavy medium; Dundee Cell). On the tenth day, ELMOD1-HA and ELMOD2-HA expression was induced with 2 μg/mL doxycycline for 12 hours or 24 hours, respectively. ELMOD3-HA was expressed by transient transfection for 18 hours, where indicated. Cells were harvested and lysed in 25 mM HEPES pH 7.4, 100 mM NaCl, 1% CHAPS, and protease inhibitor cocktail (Sigma). Lysates were cleared by centrifugation at 14,000*xg* for 5 minutes. A total of 1.5 mg of S14 protein was incubated with 1 μL of HA antibody (Covance MMS-101P) for 1 hour at 4°C. Protein G Sepharose 4 Fast Flow beads (GE) were washed twice with lysis buffer and 30 μL of the slurry was incubated with each lysate for 1 hour at 4°C. Beads were collected at 14,000xg for 15 seconds and washed twice with lysis buffer. The final pellets were resuspended in 40 μL Laemmli SDS sample buffer. A sample from cells cultured in heavy medium and induced for ELMOD1-HA expression was combined with an equal volume from a

sample from uninduced cells cultured in lite medium and *vice versa*. Samples were run 0.6 cm into an 11% polyacrylamide SDS gel and the gel was excised for tandem liquid chromatography mass spectrometry/mass spectrometry (LC-MS/MS) analyses at the Emory Mass Spectrometry Core Facility. Mass spectrometry, bioinformatics, and quantitation of peptide fold enrichment were performed as described previously [25, 26].

Preparation of testes extract - Bovine testicles (trimmed) were purchased from Pel-Freez Biologicals (Rogers, AR) and the tunica albuginea was removed before use. Bovine testis was homogenized on ice using a tight-fitting glass/glass Dounce homogenizer (20 passes) in 5 volumes of buffer containing 25 mM HEPES pH 7.4, 100 mM NaCl, 1 mM $CaCl_2$, 5 mM $MgCl_2$, and 1 mM dithiothreitol. Tissue homogenate was cleared by centrifugation at 600×*g* for 10 min at 4°C. Extracts were prepared with the addition of CHAPS to a final concentration of 1% from a 10% stock solution. Extracts were incubated on ice for 30 min then cleared by centrifugation at 14,000×*g* for 30 min at 4°C.

GAP assays and enhancer activity - GST-ELMOD3 was purified from HEK293T/T17 cells as previously described [11]. GST-ELMOD3 enhancer activity was assayed using a variation of the charcoal based Arl2 GAP assay [7]. Purified recombinant Arl2 (1 µM) was pre-loaded with [γ-^{32}P]GTP at 30°C for 15 min in a total volume of 100 µL loading buffer (25 mM HEPES pH 7.4, 100 mM NaCl, 2.5 mM $MgCl_2$, 1 mM EDTA, 25 mM KCl, 0.5 mM ATP). The GAP reaction was performed in a total volume of 50 µL. The buffer consisted of 25 mM HEPES pH 7.4, 2.5 mM $MgCl_2$, 1mM dithiothreitol, 1.6 mM ATP, and 1 mM GTP. The non-radiolabeled nucleotides are present to lower the overall background by decreasing nonspecific and non-GAP-dependent hydrolysis. Reactions were incubated for 4 min at 30°C. Reactions were stopped by adding 750 µL of ice-cold charcoal suspension (5% in 50 mM NaH_2PO_4, pH 7.4) to the tubes with mixing. Charcoal, with bound nucleotides, was pelleted at 4°C by

centrifugation at 3,000×*g* for 5 min. Half (400 µL) of each sample was counted in the liquid scintillation counter to determine the amount of GAP-dependent, $^{32}P_i$ released.

To assay for GAP enhancer activity the following assays were performed in parallel: 1) buffer (25 mM HEPES pH 7.4, 100 mM NaCl), 2) buffer with 4 µg GST-ELMOD3, 3) extract or chromatography fraction, 4) extract or chromatography fraction with 4 µg GST-ELMOD3. Baseline Arl2 GAP activity of GST-ELMOD3 was calculated by subtraction of the activity of 4 µg GST-ELMOD3 (assay 2) from buffer alone (assay 1). Enhancer activity was calculated first by subtracting the background from the extract or chromatography fraction (assay 3) from the same fraction with the addition of 4 µg GST-ELMOD3 (assay 4). Enhancement activity was then defined by any increase in Arl2 GAP activity of GST-ELMOD3 over the baseline activity. CHAPS interferes with the Arl2 GAP assay and background hydrolysis of tissue extract was high so extracts were diluted 10-fold and chromatography extracts were diluted 2-fold in 25 mM HEPES pH 7.4, 100mM NaCl to a final CHAPS concentration of 0.1% or 0.3% respectively, where indicated.

A similar approach was taken to determine whether phosphoinositides enhanced GST-ELMOD3 GAP activity. Three stock solution of mixed phosphoinositides containing 0 µM, 100 µM, or 200 µM each of phosphatidylinositol, phosphatidylinositol 3-phosphate, phosphatidylinositol 4-phosphate, phosphatidylinositol 5-phosphate, phosphatidylinositol 3,4-bisphosphate, phosphatidylinositol 3,5-bisphosphate, phosphatidylinositol 4,5-bisphosphate, and phosphatidylinositol 3,4,5-trisphosphate (Echelon Inc) was prepared by resuspending the phosphoinositides in a solution of 30 mM 1,2-dimyristoyl-sn-glycero-3-phosphocholine (DMPC). The phosphoinositides solution was sonicated for five minutes using a sonicator probe at the lowest setting. Following sonication, cholate was added to a final concentration of 1%. The phosphoinositide solution was diluted 10-fold into the GAP reaction buffer to a final concentration of 3 mM DMPC, 0.1% cholate and 0 µM, 10 µM, or 20 µM of each

phosphoinositides. Alternatively, large unilamellar vesicles (LUVs) with varying phosphoinositides compositions were used in place of the phosphoinositides solutions. LUVs were kindly provided by Paul Randazzo (NIH) and consisted of 40% phosphatidylcholine, 25% phosphatidylethanolamine, 10% cholesterol, 7.5% phosphatidylinositol and 2.5% of PI(4,5)P2, PI(3,4)P2, PI(3,5)P2, or PI(3,4,5)P3 [27]. LUVs lacking additional PIPs had 10% phosphatidylinositol. LUVs were diluted in GAP reaction buffer to a final PIP concentration of 20 μM. The charcoal based GAP assay was then performed as described above.

Protein-lipid overlay assay - GST-ELMOD3 was expressed and purified from HEK-293T/T17 cells as previously described [11]. PIP Strips™ were purchased from Echelon Inc. and the protein-lipid overlay assay was performed as per manufacturer's instructions. PIP Strips™ incubated with blocking buffer (phosphate buffered saline (PBS), 0.1% Tween-20, and 3% BSA) for one hour at room temperature to block. Membranes were then incubated with 10 mL of 0.5 μg/mL GST-ELMOD3 in blocking buffer for one hour at room temperature. Membranes were washed three times for 10 minutes each with washing buffer (PBS with 0.1% Tween-20) before addition of 10 mL of GST antibody (Sigma) in blocking buffer for one hour at room temperature. Membranes were washed three more times with washing buffer then incubated with HRP conjugated anti-rabbit secondary antibody in washing buffer for one hour at room temperature. Membranes were washed three times in washing buffer and once in PBS prior to being developed.

Cell culture and immunofluorescence - HeLa cells were grown in Dulbecco's modified Eagle's medium containing 10% fetal calf serum (Atlanta Biologicals). Cells were transfected with Lipofectamine PLUS according to the manufacturer's directions (Life Technologies) for exogenous expression. For immunofluorescence, cells were fixed using 2% paraformaldehyde at room temperature for 15 minutes, washed four times in PBS, and then permeabilized with 0.05% saponin for 30 min at room temperature in blocking buffer containing 1% BSA in PBS. Cells

were incubated in primary antibody overnight in blocking buffer, washed four times with a solution of 0.05% saponin in PBS (wash buffer) and labeled with Alexa Fluor 594 secondary antibody (Life Technologies) at room temperature for one hour in blocking buffer. Cells were then washed four times with wash buffer then once with PBS before being mounted with Prolong Antifade (Life Technologies) [28].

Results and Discussion

Identification of putative ELMOD1-3 binding partners

To identify potential binding partners of ELMOD1-3, we used a co-immunoprecipitation (co-IP) approach coupled with SILAC in HeLa cells. Each protein was tagged at the C-terminus with the HA epitope and expressed in HeLa cells cultured in normal media or media containing heavy isotope labeled arginine and lysine, as described in Materials and Methods. Co-IPs were performed at least twice for each protein in two different SILAC backgrounds as outlined in Figure 1. In one dimension, unlabeled HeLa were used as control cells with no protein over-expression and epitope tagged proteins were expressed in heavy isotope labeled HeLa cells. Cells were lysed and processed for co-IP with an antibody against the HA epitope separately. After the addition of SDS sample buffer to the final co-IP samples, the two samples were combined and submitted for quantitative LC MS/MS analyses by the Emory Proteomics Core Facility. The reciprocal experiment was also performed where protein expression was induced in unlabeled HeLa cells and heavy isotope labeled cells served as a control. Thus, there are two populations of any given peptide containing arginines or lysines that we can separate by LC MS/MS. We then compared the abundance of the heavily labeled peptide versus the unlabeled peptide to determine the level of enrichment specifically associated with the pulldown of the protein of interest. This method allows for the subtraction of the non-specific proteins and calculation of the fold-

enrichment of proteins that are specifically co-enriched with the protein of interest. Thus, with this method we identified specific binding partners for ELMOD1-3 with a substantially higher level of confidence then standard co-IPs. Proteins identified as putative binding partners in this manner still require confirmation by other methods though such experiments were not performed for the vast majority of the putative binding partners identified.

ELMOD1 - Co-IPs of ELMOD1-HA expressed in HeLa cells using the SILAC protocol described above (Fig 1) were performed twice in two separate experiments. Thus, a total of four Log_2 values are reported for each protein listed in Table 1. Specific binding partners described in Table 1 were co-enriched with ELMOD1-HA in at least three out of four co-IPs. Only those proteins that were enriched by a Log_2 value of >0.5, corresponding to a >1.4 fold enrichment, were included in Table 1.

Based on our functional and localization studies of both endogenous and ectopically expressed ELMOD1, we expected to find predominantly proteins residing at the Golgi (likely associated with vesicular traffic), lipid droplets, nuclear speckles, and the ER. We were surprised to find the list of potential ELMOD1 binding partners consisting mostly of mitochondrial proteins. Several components of the large protein complexes cytochrome c oxidase (complex IV of the electron transport chain) and ATP synthase were reliably and abundantly co-enriched with ELMOD1-HA, providing internal consistency in the dataset and demonstrating enrichment of the protein complexes. Both of these complexes are essential members of the electron transport chain for ATP production in mitochondria suggesting that ELMOD1 may have some role in regulating cellular energy metabolism. Such a role would be consistent with the role of a substrate of ELMOD1, Arl2, which is essential for the maintenance of cellular and mitochondrial ATP levels through an unknown mechanism [29](Newman et. al. submitted manuscript). Despite numerous efforts specifically targeting mitochondria in efforts at follow-up of these data, we have failed to detect endogenous or epitope-tagged ELMOD1 localizing to mitochondria in cell

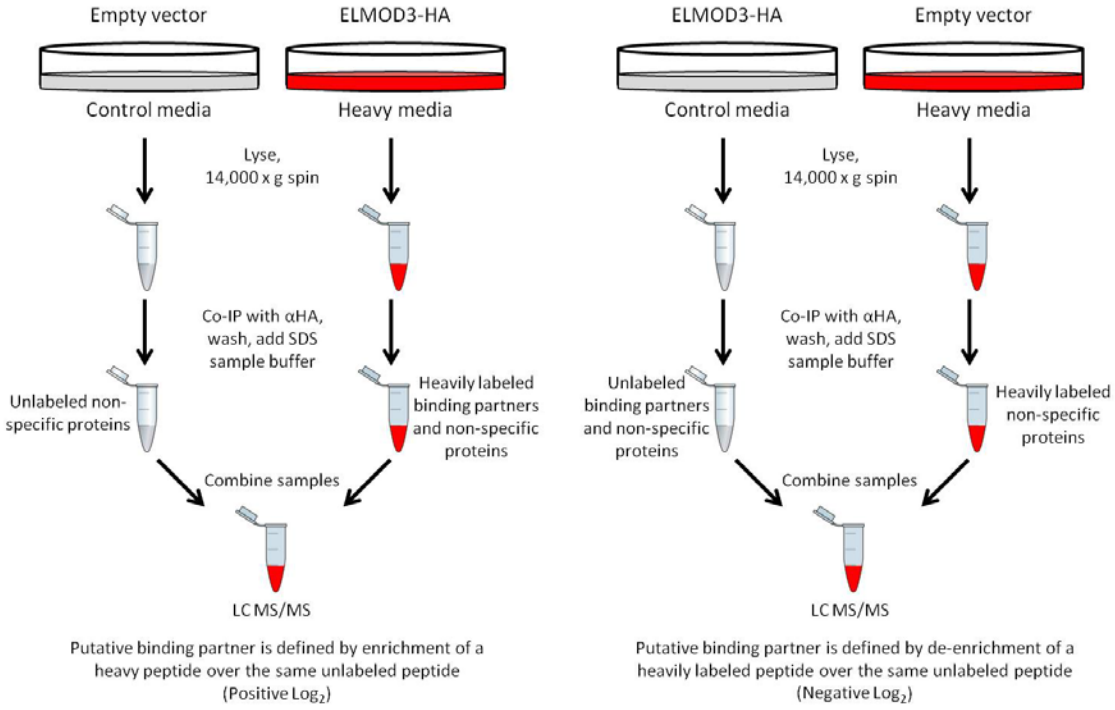

Figure 1: Schematic of the SILAC co-IP methodology. HeLa cells are cultured separately in control medium (grey) or medium containing heavily labeled arginine and lysine (red). Cells are transfected with empty vector or plasmid encoding the protein of interest (ELMOD3-HA). Cells are lysed and cleared by centrifugation. Co-IPs are performed on equal protein amounts from each lysate using the same antibody (αHA). Thus, both co-IPs should have the same non-specific proteins with about the same abundance and as a result are factored out of the dataset of putative interactors. Only the heavy isotope labeled lysate (left panel) has specific binding partners of the protein of interest. The final pellet of beads is resuspended in SDS sample buffer and an equal volume from each co-IP sample is combined in one tube. Proteins that are specifically co-enriched have a much greater abundance of heavily labeled peptides than unlabeled peptides. Fold enrichment is calculated by this ratio as a Log_2 value. The reciprocal experiment is outlined in the right panel where ELMOD3-HA is expressed in unlabeled HeLa cells. In this reciprocal experiment, specific binding partners have a heavy to light peptide ratio that is <1 presented as a negative Log_2 value. A protein with a positive Log_2 value from the left panel and a negative Log_2 value from the right panel is a putative binding partner.

fractionation or indirect immunofluorescence experiments. We have also failed to observe any phenotype of ELMOD1 over-expression on mitochondria. Thus, cytochrome c oxidase and ATP synthase represent compelling candidates for ELMOD1 binding partners with a potentially important role for ELMOD1 in cellular energy metabolism but there is no functional or localization evidence in support of a role for ELMOD1 in mitochondria. Knockdown of ELMOD1 may prove more informative in these experiments but attempts to knock-down ELMOD1 with several targeted siRNAs or pSUPER constructs were unsuccessful.

The most convincing binding partner of ELMOD1 identified in these experiments was the non-opioid receptor, sigma 1 (SigmaR1). SigmaR1 was enriched in ELMOD1-HA pulldowns to near stoichiometric levels with ELMOD1-HA despite estimates of ELMOD1 over-expression of >100 fold in HeLa cells. The interaction between ELMOD1 was later confirmed by co-purification of FLAG-SigmaR1 and GST-ELMOD1 from HEK cells [11]. The same study showed that FLAG-SigmaR1 also co-purified with GST-ELMOD2 and that FLAG-SigmaR1 markedly inhibited Arl2 GAP activity of both GST-ELMOD1 and GST-ELMOD2. Thus, SigmaR1 is a *bona fide* binding partner of both ELMOD1 and ELMOD2 with functional consequences on ELMOD1 and ELMOD2 GAP activities. SigmaR1 is a transmembrane protein residing at the ER and predominantly localizes to the interface between the ER and mitochondria called the mitochondria associated membrane (MAM) [30]. It has been linked to a growing number of neurological and retinal disorders and is a receptor for numerous psychoactive drugs several of which are currently in use [31-41]. Functional studies of SigmaR1 reveal a role as a molecular chaperone for IP3 receptors to modulate calcium signaling at the MAM and for IRE1 to regulate survival pathways in response to ER stress [30, 42]. SigmaR1 binds the mature channel-forming IP3R tetramer to prevent rapid ubiquitination and degradation of IP3R upon activation with IP3 [30]. SigmaR1 also interacts with the cell survival protein IRE1 under conditions of ER stress to prevent its degradation and to regulate the amplitude and duration of

IRE1 signaling [42]. SigmaR1 may have a similar role in the regulation of ELMODs considering the decrease in GAP activity upon binding SigmaR1. SigmaR1 may be acting to attenuate ELMOD GAP activity to prolong GTPase signaling or to facilitate GTPase signaling by allowing ELMODs to function as effectors rather than as GAPs for their substrate GTPase(s). Preliminary studies in our lab (Anna Ivanova) reveal that agonists and antagonists of SigmaR1 added to the purified SigmaR1/ELMOD complexes further modify the inhibitory effects of SigmaR1 on ELMOD GAP activity. Thus, SigmaR1 and SigmaR1 ligands add an intriguing level of complexity for the regulation of ELMODs and provides some potentially very important clinical relevance for the ELMODs as effectors of SigmaR1 and, by extension, psychoactive drugs.

ELMOD2 - Specific binding partners of ELMOD2-HA identified in a reciprocal SILAC experiments (two co-IPs) showing enrichment Log_2 values of at least 0.5 (> 1.4 fold enrichment) are listed in Table 2. Endogenous ELMOD2 localizes predominantly to mitochondria where it functions as a regulator of mitochondria morphology and motility. We were again surprised by the distribution of ELMOD2-HA binding partners identified in this experiment, finding very few mitochondrial proteins and none with established roles in mitochondrial morphology or motility. Instead, ELMOD2 binding partners suggest a role for ELMOD2 in the cytosol as a regulator of glycolysis. Three different glycolysis enzymes were identified in the co-IP; including two isoforms of triosephosphate isomerase (step 5), phosphoglycerate kinase (step 7), and three isoforms of phosphoglycerate mutase (step 8). Identification of several distinct isoforms of phosphoglycerate mutase and triosephosphate isomerase provide internal consistency to the dataset and provide further support that these proteins are *bona fide* ELMOD2 binding partners. Although these data suggest a role for ELMOD2 as a novel regulator of glycolysis, depletion of ELMOD2 showed no discernible effect on cellular ATP levels (Newman et. al., in press). Thus, a role of ELMOD2 in glycolysis is unclear but suggested by this single co-IP approach.

ELMOD3 - Specific binding partners for ELMOD3-HA were also determined from a reciprocal co-IP SILAC experiment and proteins showing enrichment Log_2 values of at least 0.5 are listed in Table 3. Based on the localization and functional studies of ELMOD3 reported in Chapter 3, we expected to find actin or other actin associated proteins specifically co-enriched with ELMOD3-HA. Instead, we identified 13 different tubulin isoforms and several different mitochondrial proteins. The enrichment values for tubulins and most of the mitochondrial proteins showed a <2-fold enrichment over background but the sheer number of different tubulins and related mitochondrial proteins (four members of solute carrier family 25) supports an interaction between ELMOD3 and these proteins. Initial tests revealed no effect of ELMOD3-HA expression on microtubules. We also see no co-localization of endogenous ELMOD3 or ELMOD3-HA with markers of mitochondria. Thus, there are currently no data suggesting a spatial or functional relationship between ELMOD3 and microtubules or mitochondria despite the support for an interaction between tubulin/microtubules and mitochondrial solute carriers from the quantitative co-IP data in Table 3. Failure to detect actin or any known regulators of the actin cytoskeleton certainly does not argue against the role of ELMOD3 in the regulation of actin described in Chapter 3 but offers no mechanistic insight into the specific function of ELMOD3 with respect to actin.

Four members of the solute carrier 25 family (SLC25) of proteins were specifically co-enriched with ELMOD3-HA. The four proteins include members SLC25A3, SLC25A4, SLC25A12, and SLC25A13. These proteins localize to the inner membrane of mitochondria and facilitate the transport of various metabolites between the mitochondrial matrix and the intermembrane space [43]. The strongest evidence for interactions with ELMOD3-HA is for SLC25A13 and SLC25A12. SLC25A13 showed enrichment values approaching that of ELMOD3-HA in both iterations of the SILAC experiment. The enrichment of ELMOD3-HA was approximately 47-fold and 568-fold in heavily labeled control cells and ELMOD3-HA

expressing cells, respectively. SLC25A13 was enriched by approximately 25-fold and 19-fold and SLC25A12 was enriched by 1.6-fold and 32-fold. These values became even more impressive when compared to the protein with the next highest enrichment, zinc finger antiviral protein 2, which was only enriched by 3-fold and 2-fold. SLC25A13 and SLC25A12 are the only two members of the SLC25 family that facilitate the antiport of aspartate from the matrix for glutamate from the intermembrane space. That these proteins were the strongest supported putative binding partners for ELMOD3 in the co-IPs and that they are structurally (71% identity) and functionally similar lends further support to this being a real and functional interaction. SLC25A12 and SLC25A13 are the primary transporters for mitochondrial aspartate to the cytosol where it is used in the biosynthesis of proteins and nucleotides, the urea cycle, and the oxidation of NADH [44]. SLC25A13 and SLC25A12 also have direct links to human diseases. SLC25A13 is the gene responsible for citrullinemia type 2 (CTLN2) with over a dozen mutations in SLC25A13 linked to the disease [45, 46]. CTLN2 is predominantly found in east Asia where it is estimated to affect as many as 1 in 17,000 people in that region [46]. CTLN2 clinical symptoms include hyperammonemia and neuropsychiatric symptoms with a very poor prognosis often leading to death [47]. SLC25A12 has been linked to autism and Asberger syndrome although the role of SLC25A12 in the diseases remains unknown [48, 49]. Thus, SLC25A13 and SLC25A12 represent intriguing targets for further study.

Putative binding partners identified by co-IP in this section require further verification with additional binding assays. However, quantification using SILAC provides confidence levels for each putative binding partner identified and helped trim the list of putative binding partners from several hundred or even thousands down to only a handful listed in Tables 1-3. Each putative binding partner identified in this study was specifically co-enriched with the ELMOD protein of interest in at least two co-IPs lending further support for their legitimacy as binding partners. We have already verified one of the putative binding partners identified in this study for

ELMOD1, SigmaR1, as a *bona fide* binding partner with inhibitory effects on ELMOD1 Arl2 GAP activity [11]. Each of the ELMODs in this study also served as controls for the other proteins as most co-IPs were performed simultaneously using the same reagents. There was very little overlap between putative binding partners for each protein suggesting that the identified proteins, even very abundant proteins like tubulin, were not common contaminants in the co-IPs and were specifically co-enriched with the target ELMOD protein. The non-overlapping binding partner sets for each of the ELMODs also point toward distinct functions for each of the ELMODs within the cell. Such interpretations are largely speculative as they are based on the failure to identify common binding partners but offer insight into various potential roles of each protein in the cell. Interestingly, none of the putative binding partners identified in this study are directly related to any of our models for the cellular functions of the ELMODs. Thus, these experiments do not provide any insight into the mechanisms of the known functions of the ELMODs or much insight into functions at known subcellular localizations. Instead we are presented with new leads suggestive of novel functions and localizations.

Identification of ELMOD3 Arl2 GAP enhancer activity

Of the three human ELMODs ELMOD3 has by far the lowest specific activity as a GAP for any of the GTPases tested [11]. The specific activity of ELMOD3 was found to be between 25 and 15,000-fold lower than ELMOD1 or ELMOD2 for the same GTPases. We hypothesized that the specific activity of purified recombinant ELMOD3 was low due to the absence of an obligate binding partner or cofactor required for efficient GAP activity. To test this hypothesis, GST-ELMOD3 was incubated with detergent extracts of various murine and bovine tissues and GAP activity against Arl2 was assayed using a charcoal-based GAP assay. Bovine testis extract increased GST-ELMOD3 GAP activity by approximately four-fold (Fig 2) after a 10-fold dilution. Dilution of testis extract was necessary to reduce the concentration of CHAPS detergent which interfered with GST-ELMOD3 GAP activity at higher concentrations and to reduce

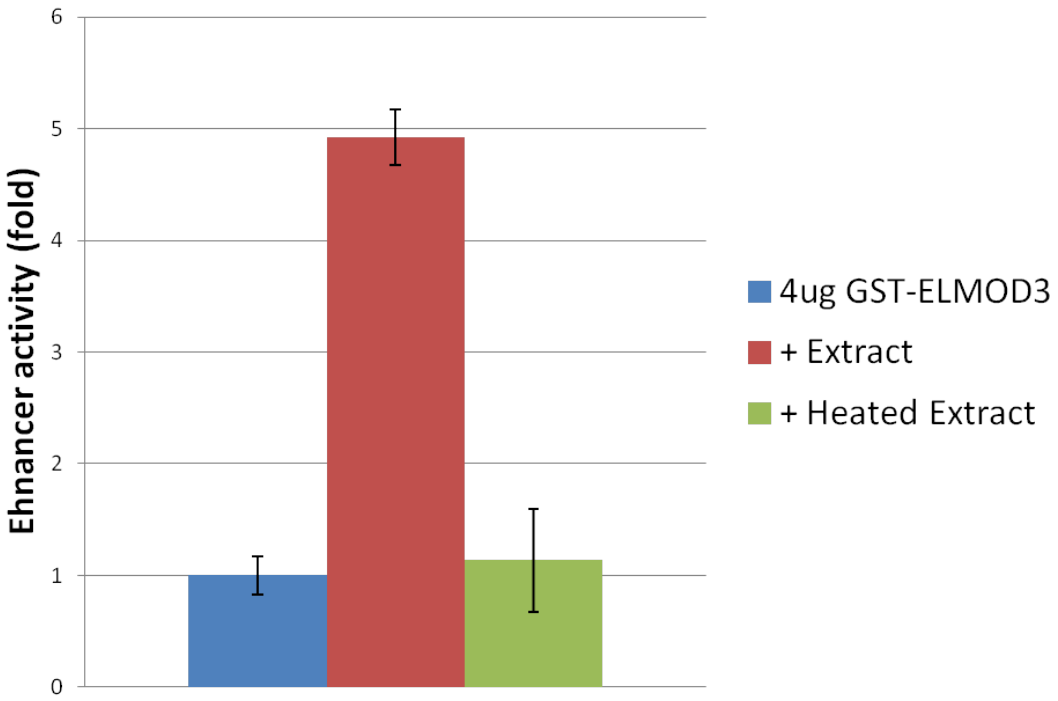

Figure 2: Bovine testis enhances GST-ELMOD3 GAP activity. Purified recombinant GST-ELMOD3 (4 µg) was incubated with buffer (blue bar), bovine testis extract (red bar), or bovine testis extract that had been heated at 95°C for 10 minutes (green bar). The charcoal based Arl2 GAP assay was performed on the mixtures. Background GAP activity (no added GST-ELMOD3) was subtracted and the data were transformed to show activity relative to GST-ELMOD3 in buffer alone. The graph represents data from three different experiments each with 2 technical replicates. Error bars show standard deviation.

background levels of Arl2 GAP activity. The enhancer activity of testis extract was dose-dependent, though only tested over a two-fold range, as a 20-fold dilution of the extract only increased GST-ELMOD3 GAP activity by two-fold (data not shown). To determine whether the enhancing factor in testis extract was a small molecule, protein, RNA, or DNA, extract was treated with DNAse or RNAse or was heated at 95°C for 10 minutes. Treatment with RNAse or DNAse had no effect on enhancer activity (data not shown) suggesting that enhancer activity is not the result of GST-ELMOD3 binding to DNA or RNA. Heating testis extract was sufficient to ablate enhancer activity of the extract (Fig 2). Thus, enhancer activity is heat sensitive and is likely a protein although additional experiments will need to be performed to confirm this. These data suggest that there is a protein binding partner or other cofactor required for efficient GAP activity of ELMOD3. Identification of this protein through a classical biochemical purification of the activity is expected to provide valuable insight in the function(s) and mechanisms of ELMOD3 in the cell.

Enrichment of GFP-ELMOD3 and ELMOD3-HA at the cell edge and the effects on cortical actin (Chapter 3) led us to question whether ELMOD3 interacts with specific phospholipids at the plasma membrane. Phospholipids allosterically regulate several GEFs and GAPs and are regulators of actin dynamics at the cell surface [50-55]. Thus, phospholipids are potential candidates for enhancers of ELMOD3 GAP activity. To survey for an interaction between ELMOD3 and various membrane lipids, we used a protein-lipid overlay assay. GST-ELMOD3 or GST alone was purified from HEK293T/T17 cells as described previously [11] and was incubated with a nitrocellulose strip spotted with lipids (PIP Strip^{TM}) (Fig 3). GST-ELMOD3 interacted with a diverse array of phosphoinositides, but not other lipids abundant at the plasma membrane including phosphatidylethanolamine and phosphatidylserine (Fig 3; middle). Purified recombinant GST showed no binding to any lipid. The PH domain from phospholipase C-δ1 (GST-PLC-δ1-PH) (Echelon Inc.) served as a positive control, yielding the

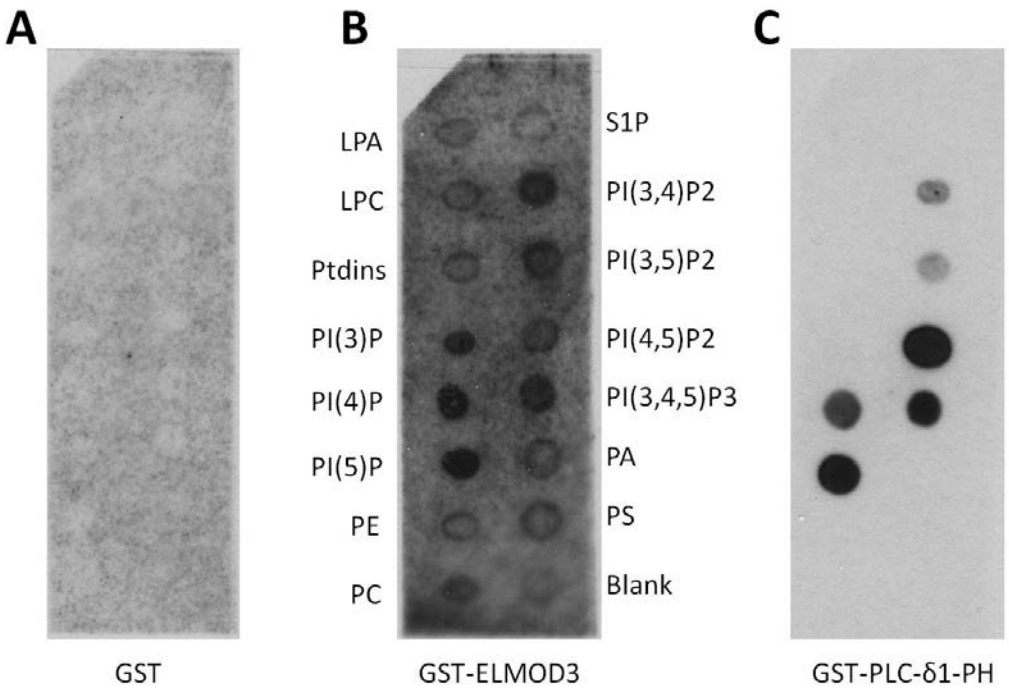

Figure 3: GST-ELMOD3 binds phosphoinositides. Purified recombinant GST (A), GST-ELMOD3 (B), and GST-PLC-δ1-PH(C) (0.5 μg/ml each) was incubated with a nitrocellulose strip spotted with lipids in a protein-lipid overlay assay. Spotted lipids are labeled in panel B (LPA, lysophosphatidic acid; LPC, lysophosphatidylcholine; Ptdins, phosphatidylinositol; PI(3)P, phosphatidylinositol 3-phosphate; PI(4)P, phosphatidylinositol 4-phosphate; PI(5)P, phosphatidylinositol 5-phosphate; PE, phosphatidylethanolamine; PC, phosphatidylcholine; S1P, sphingosine 1-phosphate; PI(3,4)P2, phosphatidylinositol 3,5-bisphosphate; PI(3,5)P2, phosphatidylinositol 3,5-bisphosphate; PI(4,5)P2, phosphatidylinositol 4,5-bisphosphate; PI(3,4,5)P3, phosphatidylinositol 3,4,5-trisphosphate; PA, phosphatidic acid; PS, phosphatidylserine). Bound proteins were detected by immunoblot with a rabbit polyclonal antibody directed against GST. *A.* GST served as a negative control and did not bind any lipids. *B.* GST-ELMOD3 bound an assortment of lipids with strongest binding to various phosphoinositides. *C.* GST-PLC-δ1-PH served as a positive control for lipid binding interacting most strongly with PI(4,5)P2, as expected.

strongest signal to phosphatidylinositol 4,5-bisphosphate ($PI(4,5)P_2$), consistent with its previously documented specificities. Tests of GST-ELMOD1 and GST-ELMOD2 revealed no binding to phosphoinositides (data not shown). We interpret these data to indicate a direct interaction between GST-ELMOD3 and phosphoinositides. Our confidence in these data is limited as attempts to replicate these results in a total of three experiments showed GST-ELMOD3 binding to a different assortment of lipids each time. Two of the three experiments showed a preference for phosphoinositides but the third showed strongest binding to phosphatidylserine. While the PIP Strip™ lipid arrays are commonly used to survey lipid binding, they should not be used as definitive evidence for specific protein-lipid interactions due to their solid-phase presentation on filters instead of their natural environment in a bilayer or vesicle. Thus, future experiments should use sedimentation assays of GST-ELMOD3 with sucrose loaded large unilamellar vesicles (LUVs) of varying lipid and phosphoinositides compositions [52]. These assays would offer better tests of a direct interaction and would provide an approximation of the affinity of GST-ELMOD3 for different lipids and thus an indication of specificity.

Apparent binding of GST-ELMOD3 to different phosphoinositides led us to question whether this interaction occurred in cells and whether expression of ELMOD3-HA had any effect on two phosphoinositides best known for their roles in cell signaling at the plasma membrane, $PI(4,5)P_2$ and $PI(3,4,5)P_3$ [56]. $PI(4,5)P_2$ and $PI(3,4,5)P_3$ are key regulators of the actin cytoskeleton and Rho family GTPases at the cell surface and mediate the physical interactions between the actin cortex and the plasma membrane [57-61]. Thus, the changes in the actin cytoskeleton observed with ELMOD3-HA expression (chapter 3) may be mediated by changes in phosphoinositides at the plasma membrane. When co-expressed with GFP tagged probes for $PI(4,5)P_2$ and $PI(3,4,5)P_3$ using the PH domains of PLCδ1 and BTK, respectively, ELMOD3-HA had no effect on the cellular distribution of $PI(4,5)P_2$ and $PI(3,4,5)P_3$ (data not shown).

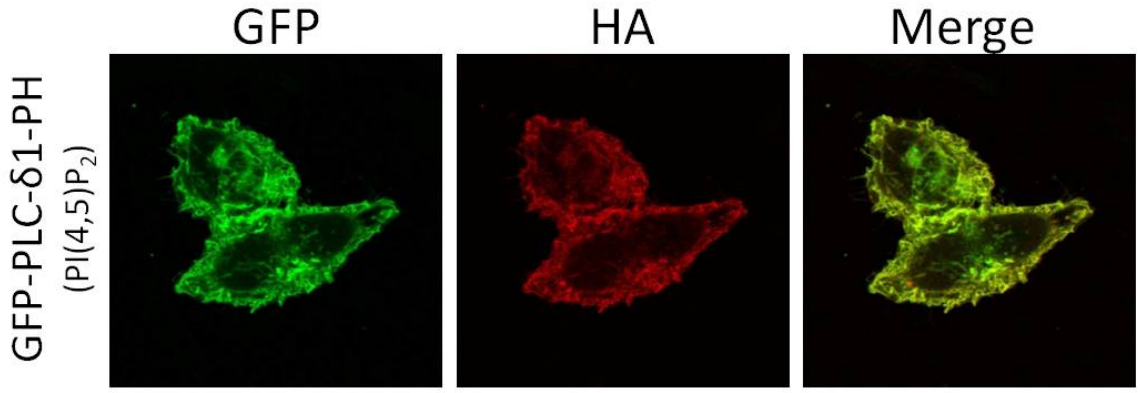

Figure 4: Staining of ELMOD3-HA and of PI(4,5)P2 show extensive overlap at the cell periphery. HeLa cells were transfected with vectors directing the expression of ELMOD3-HA and the PH domain of PLCδ1 tagged at the N-terminus with GFP (GFP-PLC-δ1-PH), a molecular probe for phosphatidylinositol 4,5-bisphosphate ($PI(4,5)P_2$). Approximately 16 hours after transfection cells were fixed and permeabilized, as described in Materials and Methods, before being developed with a mouse monoclonal antibody to the HA epitope (red). The GFP (green) channel shows intrinsic fluorescence of the GFP tag.

ELMOD3-HA and probes for both $PI(4,5)P_2$ and $PI(3,4,5)P_3$ showed extensive overlap in HeLa cells (Fig 4). Note that results showing extensive overlap of ELMOD3-HA with both $PI(4,5)P_2$ and $PI(3,4,5)P_3$ were reproducible in at least three experiments, but collected images were of insufficient quality for $PI(3,4,5)P_3$ and were omitted from figure 4. Probes for both $PI(4,5)P_2$ and $PI(3,4,5)P_3$ appeared to stain the entire plasma membrane. Thus, these data are consistent with enrichment of ELMOD3-HA at the plasma membrane reported in Chapter 3 but are not sufficient to indicate a direct interaction between ELMOD3-HA and the phosphoinositides in cells.

With evidence of direct binding between GST-ELMOD3 and phosphoinositides in the PIP Strip™ lipid arrays, we next tested whether phosphoinositides enhanced the Arl2 GAP activity of GST-ELMOD3 *in vitro.* When added to Arl2 GAP assays for GST-ELMOD3, preparations of LUVs containing individual phosphoinositides or mixtures of phosphoinositides reconstituted in DMPC/cholate micelles had no detectable effect on GST-ELMOD3 GAP activity. Thus, phosphoinositides did not enhance GST-ELMOD3 GAP activity in *in vitro* assays. Phosphoinositides may, instead, govern the localization of ELMOD3 in cells. The dynamic localization of ELMOD3 to the trailing edge and in cytosolic puncta in polarized and non-polarized cells may be regulated by binding to phosphoinositides. This model is consistent with the asymmetrical distribution of $PI(4,5)P_2$ and $PI(3,4,5)P_3$ in migrating cells [57] summarized in figure 5. $PI(4,5)P_2$ and the abundant $PI(3,4,5)P_3$ phosphatase PTEN, which converts $PI(3,4,5)P_3$ to $PI(4,5)P_2$, are enriched at the cell rear and trailing edge. $PI(3,4,5)P_3$ and the $PI(4,5)P_2$ kinase PI3K, which converts $PI(4,5)P_2$ to $PI(3,4,5)P_3$, are enriched at the leading edge of migrating cells. Thus, an interaction with $PI(4,5)P_2$ during cell migration is a potential mechanism for the dynamic localization of endogenous ELMOD3.

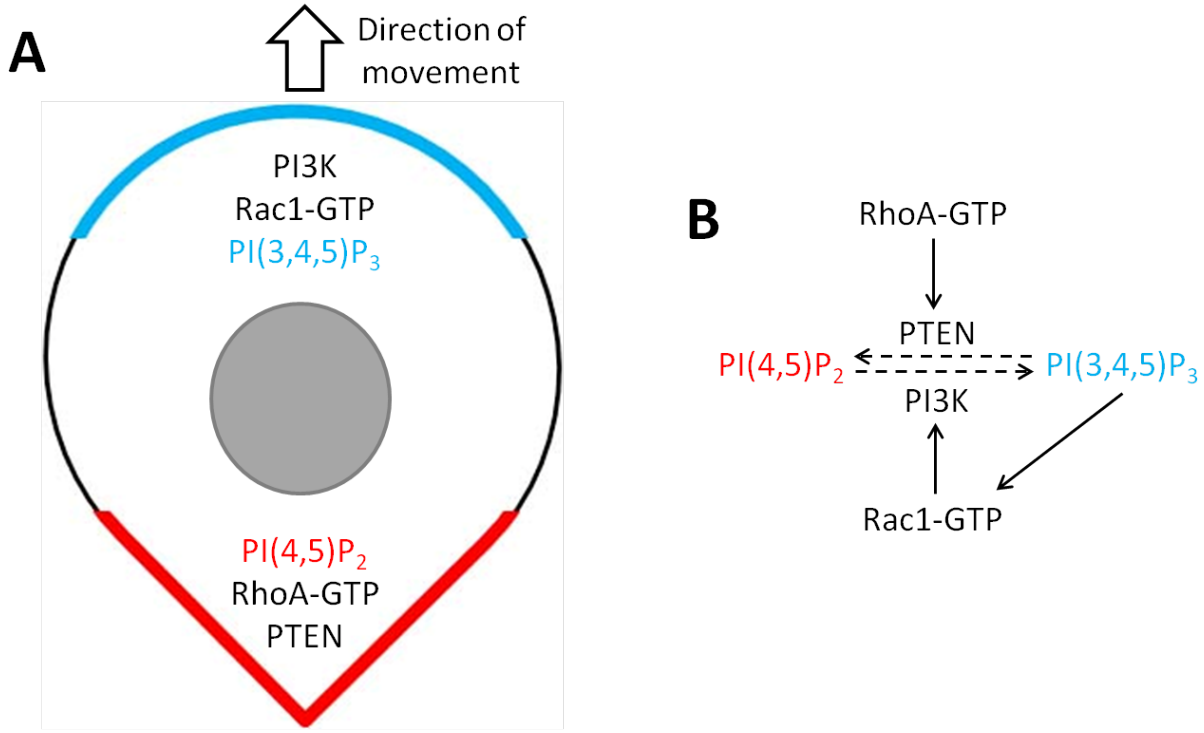

Figure 5: $PI(4,5)P_2$ and $PI(3,4,5)P_3$ have an asymmetrical distribution at the plasma membrane in migrating cells. *A.* $PI(4,5)P_2$ is enriched at the cell rear in migrating cells. Enrichment of $PI(4,5)P_2$ at the cell rear is largely mediated by enrichment of the $PI(3,4,5)P_3$ phosphatase PTEN activated RhoA-GTP at the same location. $PI(3,4,5)P_3$ is enriched at the leading edge. Enrichment of $PI(3,4,5)P_3$ is mediated largely by the PI(4,5)P2 kinase PI3K and activated Rac1-GTP which are also enriched at the leading edge. *B.* PTEN and PI3K interconvert (dashed lines) $PI(4,5)P_2$ and $PI(3,4,5)P_3$ and are activated (solid arrows) by RhoA-GTP and Rac1-GTP. $PI(3,4,5)P_3$ also stimulates Rac1 activation by recruiting and activating guanine nucleotide exchange factors for Rac1 at the leading edge creating an activation loop.

References

1. Casanova, J.E., *Regulation of Arf activation: the Sec7 family of guanine nucleotide exchange factors.* Traffic, 2007. **8**(11): p. 1476-85.
2. Gillingham, A.K. and S. Munro, *The small G proteins of the Arf family and their regulators.* Annu Rev Cell Dev Biol, 2007. **23**: p. 579-611.
3. Kahn, R.A., et al., *Consensus nomenclature for the human ArfGAP domain-containing proteins.* J Cell Biol, 2008. **182**(6): p. 1039-44.
4. Miller, E.A. and C. Barlowe, *Regulation of coat assembly--sorting things out at the ER.* Curr Opin Cell Biol, 2010. **22**(4): p. 447-53.
5. East, M.P. and R.A. Kahn, *Models for the functions of Arf GAPs.* Semin Cell Dev Biol, 2011. **22**(1): p. 3-9.
6. Schlacht, A., et al., *Ancient complexity, opisthokont plasticity, and discovery of the 11th subfamily of Arf GAP proteins.* Traffic, 2013. **14**(6): p. 636-49.
7. Bowzard, J.B., et al., *ELMOD2 is an Arl2 GTPase-activating protein that also acts on Arfs.* J Biol Chem, 2007. **282**(24): p. 17568-80.
8. Veltel, S., et al., *The retinitis pigmentosa 2 gene product is a GTPase-activating protein for Arf-like 3.* Nat Struct Mol Biol, 2008. **15**(4): p. 373-80.
9. Jaworek, T.J., et al., *An alteration in ELMOD3, an Arl2 GTPase-activating protein, is associated with hearing impairment in humans.* PLoS Genet, 2013. **9**(9): p. e1003774.
10. Ivanova, A.A., et al., *Characterization of Recombinant ELMOD Proteins as GTPase Activating Proteins (GAPs) for ARF Family GTPases.* J Biol Chem, 2014.
11. Ivanova, A.A., et al., *Characterization of Recombinant ELMOD (Cell Engulfment and Motility Domain) Proteins as GTPase-activating Proteins (GAPs) for ARF Family GTPases.* J Biol Chem, 2014. **289**(16): p. 11111-21.

12. Liu, Y.W., et al., *Role for Gcs1p in regulation of Arl1p at trans-Golgi compartments.* Mol Biol Cell, 2005. **16**(9): p. 4024-33.

13. Johnson, K.R., C.M. Longo-Guess, and L.H. Gagnon, *Mutations of the mouse ELMO domain containing 1 gene (Elmod1) link small GTPase signaling to actin cytoskeleton dynamics in hair cell stereocilia.* PLoS One, 2012. **7**(4): p. e36074.

14. Pulkkinen, V., et al., *ELMOD2, a candidate gene for idiopathic pulmonary fibrosis, regulates antiviral responses.* Faseb J, 2010. **24**(4): p. 1167-77.

15. Hodgson, U., et al., *ELMOD2 is a candidate gene for familial idiopathic pulmonary fibrosis.* Am J Hum Genet, 2006. **79**(1): p. 149-54.

16. Lawson, W.E., J.E. Loyd, and A.L. Degryse, *Genetics in pulmonary fibrosis--familial cases provide clues to the pathogenesis of idiopathic pulmonary fibrosis.* Am J Med Sci, 2011. **341**(6): p. 439-43.

17. Schwahn, U., et al., *Positional cloning of the gene for X-linked retinitis pigmentosa 2.* Nat Genet, 1998. **19**(4): p. 327-32.

18. Miano, M.G., et al., *Identification of novel RP2 mutations in a subset of X-linked retinitis pigmentosa families and prediction of new domains.* Hum Mutat, 2001. **18**(2): p. 109-19.

19. Li, L., et al., *Ablation of the X-linked retinitis pigmentosa 2 (Rp2) gene in mice results in opsin mislocalization and photoreceptor degeneration.* Invest Ophthalmol Vis Sci, 2013. **54**(7): p. 4503-11.

20. Shu, X., et al., *Knockdown of the zebrafish ortholog of the retinitis pigmentosa 2 (RP2) gene results in retinal degeneration.* Invest Ophthalmol Vis Sci, 2011. **52**(6): p. 2960-6.

21. East, M.P., et al., *ELMO domains, evolutionary and functional characterization of a novel GTPase-activating protein (GAP) domain for Arf protein family GTPases.* J Biol Chem, 2012. **287**(47): p. 39538-53.

22. Hodges, B.D. and C.C. Wu, *Proteomic insights into an expanded cellular role for cytoplasmic lipid droplets.* J Lipid Res, 2010. **51**(2): p. 262-73.

23. Bouchoux, J., et al., *The proteome of cytosolic lipid droplets isolated from differentiated Caco-2/TC7 enterocytes reveals cell-specific characteristics.* Biol Cell, 2011. **103**(11): p. 499-517.

24. Balla, T. and P. Varnai, *Visualization of cellular phosphoinositide pools with GFP-fused protein-domains.* Curr Protoc Cell Biol, 2009. **Chapter 24**: p. Unit 24 4.

25. Dammer, E.B., et al., *Coaggregation of RNA-binding proteins in a model of TDP-43 proteinopathy with selective RGG motif methylation and a role for RRM1 ubiquitination.* PLoS One, 2012. **7**(6): p. e38658.

26. Seyfried, N.T., et al., *Quantitative analysis of the detergent-insoluble brain proteome in frontotemporal lobar degeneration using SILAC internal standards.* J Proteome Res, 2012. **11**(5): p. 2721-38.

27. Che, M.M., Z. Nie, and P.A. Randazzo, *Assays and properties of the Arf GAPs AGAP1, ASAP1, and Arf GAP1.* Methods Enzymol, 2005. **404**: p. 147-63.

28. Valnes, K. and P. Brandtzaeg, *Retardation of immunofluorescence fading during microscopy.* J Histochem Cytochem, 1985. **33**(8): p. 755-61.

29. Nishi, H., et al., *MicroRNA-15b modulates cellular ATP levels and degenerates mitochondria via Arl2 in neonatal rat cardiac myocytes.* J Biol Chem, 2010. **285**(7): p. 4920-30.

30. Hayashi, T. and T.P. Su, *Sigma-1 receptor chaperones at the ER-mitochondrion interface regulate Ca(2+) signaling and cell survival.* Cell, 2007. **131**(3): p. 596-610.

31. Cobos, E.J., et al., *Pharmacology and therapeutic potential of sigma(1) receptor ligands.* Curr Neuropharmacol, 2008. **6**(4): p. 344-66.

32. Hashimoto, K. and K. Ishiwata, *Sigma receptor ligands: possible application as therapeutic drugs and as radiopharmaceuticals.* Curr Pharm Des, 2006. **12**(30): p. 3857-76.

33. Maurice, T. and T.P. Su, *The pharmacology of sigma-1 receptors.* Pharmacol Ther, 2009. **124**(2): p. 195-206.

34. Niitsu, T., M. Iyo, and K. Hashimoto, *Sigma-1 receptor agonists as therapeutic drugs for cognitive impairment in neuropsychiatric diseases.* Curr Pharm Des, 2012. **18**(7): p. 875-83.

35. Skuza, G. and K. Wedzony, *Behavioral pharmacology of sigma-ligands.* Pharmacopsychiatry, 2004. **37 Suppl 3**: p. S183-8.

36. Tsai, S.Y., et al., *Sigma-1 receptor chaperones and diseases.* Cent Nerv Syst Agents Med Chem, 2009. **9**(3): p. 184-9.

37. Tsai, S.Y., et al., *Sigma-1 receptors regulate hippocampal dendritic spine formation via a free radical-sensitive mechanism involving Rac1xGTP pathway.* Proc Natl Acad Sci U S A, 2009. **106**(52): p. 22468-73.

38. Belzil, V.V., et al., *Genetic analysis of SIGMAR1 as a cause of familial ALS with dementia.* Eur J Hum Genet, 2013. **21**(2): p. 237-9.

39. Ha, Y., et al., *Late-onset inner retinal dysfunction in mice lacking sigma receptor 1 (sigmaR1).* Invest Ophthalmol Vis Sci, 2011. **52**(10): p. 7749-60.

40. Feher, A., et al., *Association between a variant of the sigma-1 receptor gene and Alzheimer's disease.* Neurosci Lett, 2012. **517**(2): p. 136-9.

41. Luty, A.A., et al., *Sigma nonopioid intracellular receptor 1 mutations cause frontotemporal lobar degeneration-motor neuron disease.* Ann Neurol, 2010. **68**(5): p. 639-49.

42. Mori, T., et al., *Sigma-1 receptor chaperone at the ER-mitochondrion interface mediates the mitochondrion-ER-nucleus signaling for cellular survival.* PLoS One, 2013. **8**(10): p. e76941.

43. Gutierrez-Aguilar, M. and C.P. Baines, *Physiological and pathological roles of mitochondrial SLC25 carriers.* Biochem J, 2013. **454**(3): p. 371-86.

44. Palmieri, F., *The mitochondrial transporter family SLC25: identification, properties and physiopathology.* Mol Aspects Med, 2013. **34**(2-3): p. 465-84.

45. Kobayashi, K., et al., *The gene mutated in adult-onset type II citrullinaemia encodes a putative mitochondrial carrier protein.* Nat Genet, 1999. **22**(2): p. 159-63.

46. Woo, H.I., H.D. Park, and Y.W. Lee, *Molecular genetics of citrullinemia types I and II.* Clin Chim Acta, 2014. **431C**: p. 1-8.

47. Saheki, T. and K. Kobayashi, *Mitochondrial aspartate glutamate carrier (citrin) deficiency as the cause of adult-onset type II citrullinemia (CTLN2) and idiopathic neonatal hepatitis (NICCD).* J Hum Genet, 2002. **47**(7): p. 333-41.

48. Ramoz, N., et al., *Linkage and association of the mitochondrial aspartate/glutamate carrier SLC25A12 gene with autism.* Am J Psychiatry, 2004. **161**(4): p. 662-9.

49. Durdiakova, J., et al., *Single nucleotide polymorphism rs6716901 in SLC25A12 gene is associated with Asperger syndrome.* Mol Autism, 2014. **5**(1): p. 25.

50. Tu, Y. and T.M. Wilkie, *Allosteric regulation of GAP activity by phospholipids in regulators of G-protein signaling.* Methods Enzymol, 2004. **389**: p. 89-105.

51. Randazzo, P.A., et al., *Molecular aspects of the cellular activities of ADP-ribosylation factors.* Sci STKE, 2000. **2000**(59): p. re1.

52. Campa, F., et al., *A PH domain in the Arf GTPase-activating protein (GAP) ARAP1 binds phosphatidylinositol 3,4,5-trisphosphate and regulates Arf GAP activity independently of recruitment to the plasma membranes.* J Biol Chem, 2009. **284**(41): p. 28069-83.

53. Senoo, H. and M. Iijima, *Rho GTPase: A molecular compass for directional cell migration.* Commun Integr Biol, 2013. **6**(6): p. e27681.

54. Logan, M.R. and C.A. Mandato, *Regulation of the actin cytoskeleton by PIP2 in cytokinesis.* Biol Cell, 2006. **98**(6): p. 377-88.

55. Vitale, N., et al., *GIT proteins, A novel family of phosphatidylinositol 3,4, 5-trisphosphate-stimulated GTPase-activating proteins for ARF6.* J Biol Chem, 2000. **275**(18): p. 13901-6.

56. Czech, M.P., *PIP2 and PIP3: complex roles at the cell surface.* Cell, 2000. **100**(6): p. 603-6.

57. Dawes, A.T. and L. Edelstein-Keshet, *Phosphoinositides and Rho proteins spatially regulate actin polymerization to initiate and maintain directed movement in a one-dimensional model of a motile cell.* Biophys J, 2007. **92**(3): p. 744-68.

58. Murphy, D.A. and S.A. Courtneidge, *The 'ins' and 'outs' of podosomes and invadopodia: characteristics, formation and function.* Nat Rev Mol Cell Biol, 2011. **12**(7): p. 413-26.

59. Saarikangas, J., H. Zhao, and P. Lappalainen, *Regulation of the actin cytoskeleton-plasma membrane interplay by phosphoinositides.* Physiol Rev, 2010. **90**(1): p. 259-89.

60. Moss, S.E., *How actin gets the PIP.* Sci Signal, 2012. **5**(213): p. pe7.

61. Sheetz, M.P., J.E. Sable, and H.G. Dobereiner, *Continuous membrane-cytoskeleton adhesion requires continuous accommodation to lipid and cytoskeleton dynamics.* Annu Rev Biophys Biomol Struct, 2006. **35**: p. 417-34.

Reference Sequence	Description	Log_2	Log_2	Function
NP_061182.3	**ELMO/CED-12 domain containing 1 (ELMOD1)**	**-3.37**	**7.68**	**Golgi Arf GAP**
		-3.41	**5.49**	
NP_671513.1	non-opioid receptor, sigma 1 isoform 2	-3.80	7.38	ER - Protein chaperone
		-2.83	4.64	
NP_001852.1	cytochrome c oxidase subunit IV isoform 1	-3.43	2.10	Mito - Energy metabolism/electron transport chain
		-1.34	2.06	
NP_001853.2	cytochrome c oxidase subunit Vb	-3.40	2.34	Mito - Energy metabolism/electron transport chain
		-1.46	2.17	
NP_536846.1	cytochrome c oxidase subunit II	-3.39	1.97	Mito - Energy metabolism/electron transport chain
		-1.49	2.45	
NP_003357.2	ubiquinol-cytochrome c reductase core protein II	-2.57	1.12	Mito - Energy metabolism/electron transport chain
		-0.67	1.55	
NP_005207.2	dolichyl-diphosphooligosaccharide-protein glycosyltransferase	-2.52	2.32	ER - Glycosylation
		-1.28	2.06	
XP_001133753.1	PREDICTED: hypothetical protein	-2.34	0.83	Mito - Energy metabolism/electron transport chain
		-0.89	3.87	
NP_002941.1	ribophorin I	-2.28	2.39	ER - Glycosylation
		-1.10	2.50	
NP_009204.1	prohibitin 2	-2.27	0.70	Mito - Cell cycle, mitochondrial scaffold
		-0.26	1.21	
NP_002625.1	prohibitin	-2.10	0.88	Mito - Cell cycle, mitochondrial scaffold
		-0.36	1.07	
NP_006818.3	transmembrane emp24 domain-containing protein 10	-2.03	1.57	Golgi/PM - Vesicular traffic
		-0.22	1.29	
NP_002942.2	ribophorin II	-1.92	2.13	ER - Glycosylation
		-1.26	2.04	
NP_057110.3	retinol dehydrogenase 11	-1.78	5.39	ER - Signal transduction/phototransduction
		-0.21	1.33	
NP_005736.3	B-cell receptor-associated protein 31	-1.61	2.67	ER - Vesicular traffic
		-0.45	1.60	
NP_004037.1	ATP synthase, H+ transporting, mitochondrial F1 complex, alpha subunit	-1.51	1.62	Mito - Energy metabolism/electron transport chain
		-0.14	0.90	

NP_001677.2	ATP synthase, H+ transporting, mitochondrial F1 complex, beta subunit	-1.50	1.68	Mito - Energy metabolism/electron transport chain
		0.03	1.11	
NP_004472.1	polypeptide N-acetylgalactosaminyltransferase 2	-1.38	0.39	ER - Glycosylation
		-0.52	1.00	
NP_001001975.1	ATP synthase, H+ transporting, mitochondrial F1 complex, delta subunit	-1.37	1.37	Mito - Energy metabolism/electron transport chain
		0.16	0.72	
NP_005165.1	ATP synthase, H+ transporting, mitochondrial F1 complex, gamma subunit isoform H (heart)	-1.36	1.57	Mito - Energy metabolism/electron transport chain
		0.02	0.74	
NP_001012682.1	solute carrier family 3 (activators of dibasic and neutral amino acid transport), member 2 isoform e	-1.27	1.65	PM - Calcium signaling, amino acid transport
		0.03	0.64	
NP_003477.4	solute carrier family 7 (cationic amino acid transporter, y+ system), member 5	-1.26	1.44	PM - Amino acid transport
		0.47	0.88	
NP_005619.1	solute carrier family 1 (neutral amino acid transporter), member 5	-1.22	2.09	PM - Amino acid transport
		-0.29	0.86	
NP_003850.1	dolichyl-phosphate mannosyltransferase polypeptide 1	-0.87	0.87	ER - Protein processing/GPI anchor
		-0.01	0.54	
NP_001688.1	mitochondrial ATP synthase, O subunit	-0.83	1.45	Mito - Energy metabolism/electron transport chain
		-0.09	0.90	
NP_001121620.1	transferrin receptor	-0.56	1.73	PM - Iron transport
		-0.67	**-0.44**	
NP_002945.1	ubiquitin and ribosomal protein S27a	-0.50	2.42	Cyto - Ubiquitination
		0.20	0.86	
NP_062556.2	kynurenine aminotransferase III isoform 3	-0.50	**-0.25**	
		-3.52	0.69	
NP_689926.1	integral membrane protein 1	-	1.45	ER - Glycosylation
		-1.26	2.04	

Table 1: Putative binding partners of ELMOD1-HA. Proteins listed in this table are from two separate SILAC experiments. Values listed are Log_2 of the ratio of heavily labeled peptides to unlabeled peptides as described in Materials and Methods. Protein functions listed are largely from descriptions of protein function in Entrez Gene and/or GeneCard databases. Cellular localizations are also provided (ER, endoplasmic reticulum; PM, plasma membrane; Mito, mitochondria; cyto, cytoplasm; Golgi, Golgi apparatus; Nuc, nucleus) and are from the same databases.

Reference Sequence	Description	Log_2	Log_2	Function
NP_714913.1	**ELMO/CED-12 domain containing 2 (ELMOD2)**	**-3.47**	**6.17**	**Mitochondrial dynamics**
NP_001145.1	annexin 5	-0.99	0.76	Cyto - Vesicular traffic
NP_005498.1	cofilin 1 (non-muscle)	-0.91	0.73	Cyto - Actin dynamics
NP_002023.2	ferritin, heavy polypeptide 1	-0.88	1.45	Ctyo - Iron storage
NP_066953.1	peptidylprolyl isomerase A	-0.85	0.84	Cent/nuc/cyto - Protein folding
NP_001651.1	ADP-ribosylation factor 4	-0.84	0.69	Cyto/Golgi/Endo - Vesicular traffic
NP_068733.1	cofilin 2	-0.82	0.90	Cyto - Actin dynamics
NP_001279.2	chloride intracellular channel 1	-0.82	1.00	Nuc/PM - Chloride channel
XP_941994.3	PREDICTED: similar to peptidylprolyl isomerase A-like	-0.81	0.93	
XP_001717305.1	PREDICTED: hypothetical protein	-0.79	0.93	
NP_981946.1	stathmin 1	-0.76	0.85	Cyto - Microtubule dynamics
NP_941959.1	RAB15, member RAS onocogene family	-0.69	0.83	Endo - Vesicular traffic
NP_004159.2	succinate dehydrogenase complex, subunit A, flavoprotein	-0.69	0.97	Mito - Energy metabolism/electron transport chain
NP_005909.2	mitochondrial malate dehydrogenase	-0.68	0.89	Mito - Energy metabolism/citric acid cycle
NP_006808.1	endoplasmic reticulum protein 29	-0.66	0.82	ER - Secretory protein processing
NP_003555.1	transgelin 2	-0.66	0.97	
NP_000843.1	glutathione transferase	-0.66	1.2	Cyto - Metabolite detoxification
NP_002620.1	phosphoglycerate mutase 1 (brain)	-0.65	1.25	Cyto - Energy metabolism/glycolysis
NP_001121188.1	electron transfer flavoprotein, alpha polypeptide	-0.64	0.99	Mito - Energy metabolism/fatty acid β-oxidation
NP_001025062.1	phosphoglycerate mutase family 3	-0.64	1.45	Cyto - Energy metabolism/glycolysis
NP_006133.1	stratifin	-0.60	0.98	Cyto - Signal transduction/14-3-3 family
NP_000281.2	phosphoglycerate mutase 2 (muscle)	-0.60	1.25	Cyto - Energy metabolism/glycolysis
NP_000282.1	phosphoglycerate kinase 1	-0.59	0.81	Cyto - Energy metabolism/glycolysis
NP_000356.1	triosephosphate isomerase 1	-0.57	1.13	Cyto - Energy metabolism/glycolysis
XP_001725752.1	PREDICTED: similar to tiosephosphate isomerase 1	-0.55	1.11	Cyto - Energy metabolism/glycolysis
NP_647539.1	tyrosine 3-monooxygenase/tryptophan 5-monooxygenase activation protein, beta polypeptide	-0.54	0.86	Cyto - Signal transduction/14-3-3 family
NP_002071.2	aspartate aminotransferase 2	-0.52	0.81	Mito - Amino acid metabolism

NP_003397.1	tyrosine 3/tryptophan 5 -monooxygenase activation protein, zeta polypeptide	-0.52	0.83	Cyto - Signal transduction/14-3-3 family

Table 2: Putative binding partners of ELMOD2-HA. Proteins listed in this table are from one reciprocal SILAC experiment. Values listed are Log_2 of the ratio of heavily labeled peptides to unlabeled peptides as described in Materials and Methods. Protein functions listed are largely from descriptions of protein function in Entrez Gene and/or GeneCard databases. Cellular localizations are also provided (ER, endoplasmic reticulum; PM, plasma membrane; Mito, mitochondria; cyto, cytoplasm; Golgi, Golgi apparatus; Nuc, nucleus) and are from the same databases.

Reference Sequence	Description	Log_2	Log_2	Function
NP_115589.2	**ELMO/CED-12 domain containing 3 (ELMOD3)**	**-5.56**	**9.15**	**Actin dynamics**
NP_055066.1	solute carrier family 25, member 13 (citrin) (SLC25A13)	-4.63	4.28	Mito - Mitochondrial amino acid transport
NP_078901.3	zinc finger antiviral protein isoform 2	-1.5	1.09	Cyto - Viral immune response
NP_004448.2	acyl-CoA synthetase long-chain family member 3	-1.02	0.53	Mito/ER - Lipid biosynthesis/fatty acid metabolism
NP_005165.1	ATP synthase, H+ transporting, mitochondrial F1 complex, gamma subunit isoform H (heart) precursor	-1.02	0.71	Mito - Energy metabolism/electron transport chain
NP_000173.2	mitochondrial trifunctional protein, alpha subunit	-0.83	1.28	Mito - Energy metabolism/fatty acid β-oxidation
NP_110400.1	beta tubulin 1, class VI	-0.8	1.03	Cyto - Microtubule dynamics
NP_000916.2	pyruvate dehydrogenase (lipoamide) beta	-0.8	1.92	Mito - Energy metabolism/TCA cycle
NP_115914.1	tubulin, beta 6	-0.73	1.05	Cyto - Microtubule dynamics
XP_001713916.1	PREDICTED: similar to tubulin, beta polypeptide 4, member Q	-0.73	1.07	Cyto - Microtubule dynamics
NP_064424.3	tubulin, beta polypeptide 4, member Q	-0.71	1.02	Cyto - Microtubule dynamics
NP_003696.2	solute carrier family 25 (mitochondrial carrier, Aralar), member 12 (SLC25A12)	-0.7	5.01	Mito - Mitochondrial amino acid transport
NP_005992.1	tubulin, alpha 3c	-0.69	0.92	Cyto - Microtubule dynamics
XP_935073.1	PREDICTED: similar to tubulin, beta 5	-0.67	1.07	Cyto - Microtubule dynamics
NP_006000.2	tubulin, alpha 1a	-0.66	0.93	Cyto - Microtubule dynamics
NP_997195.1	tubulin, alpha 3e	-0.65	0.95	Cyto - Microtubule dynamics
NP_006078.2	tubulin, beta 4	-0.65	1.02	Cyto - Microtubule dynamics
NP_079079.1	tubulin, alpha-like 3	-0.64	0.95	Cyto - Microtubule dynamics
NP_006073.2	tubulin, alpha, ubiquitous	-0.63	0.95	Cyto - Microtubule dynamics
NP_006077.2	tubulin, beta, 4	-0.6	1.16	Cyto - Microtubule dynamics
NP_002626.1	solute carrier family 25 member 3 (SLC25A3)	-0.58	1.4	Mito - Mitochondrial phosphate transport
NP_005991.1	tubulin, alpha 4a	-0.57	1.11	Cyto - Microtubule dynamics
NP_061816.1	tubulin, alpha 8	-0.56	0.96	Cyto - Microtubule dynamics
NP_733765.1	ATPase, Ca transporting, cardiac muscle, slow twitch 2	-0.54	3.59	ER - Calcium signaling

NP_001142.2	solute carrier family 25 (mitochondrial carrier; adenine nucleotide translocator), member 4 (SLC25A4)	-0.52	3.85	Mito - Mitochondrial ADP/ATP exchange
NP_001777.1	cell division cycle 2 protein isoform 1	-0.5	0.96	Cyto - Cell cycle

Table 3: Putative binding partners of ELMOD3-HA. Proteins listed in this Table are from one reciprocal SILAC experiment. Values listed are Log_2 of the ratio of heavily labeled peptides to unlabeled peptides as described in Materials and Methods. Protein functions listed are largely from descriptions of protein function in Entrez Gene and/or GeneCard databases. Cellular localizations are also provided (ER, endoplasmic reticulum; PM, plasma membrane; Mito, mitochondria; cyto, cytoplasm; Golgi, Golgi apparatus; Nuc, nucleus) and are from the same databases.

Chapter V

Discussion

Michael Patrick East

Department of Biochemistry and Program in Biochemistry, Cell, and Developmental Biology, Emory University, Atlanta GA 30322

The goal of this dissertation research was to begin the characterization of the ELMODs, a novel group of Arf family GTPase activating proteins (GAPs) first identified in our lab [1]. This goal was driven by both the novelty of the ELMODs as GAPs with uniquely broad substrate specificities within the Arf family [1, 2] and multiple links to human diseases that lack molecular models of dysregulation [3-5]. Prior to this research, there was no functional information available for any of the three human ELMOD proteins aside from their biochemical GAP activity for a diverse array of Arf family GTPases. Building on the biochemical GAP activity of the ELMODs, I identified the GAP domain of the ELMODs and provided initial characterization of this domain by identifying a conserved arginine residue essential for efficient GAP activity in *in vitro* and *in vivo* assays [6]. I have also developed models for the cellular functions of ELMOD1 and ELMOD3 and have identified putative binding partners for each of the three human ELMODs that may point to important and undiscovered functions.

ELMODs as GAPs

The ELMODs were the first GAPs identified among the 22 known mammalian Arl proteins [1, 7]. The ELMODs have uniquely broad specificities for GTPases within the Arf family with activity for both Arls and Arfs [1, 2]. I used phylogenetic analyses, sequence alignments, and both biochemical and cell based assays to identify the GAP domain of the ELMODs (Chapter 2). Within this GAP domain was a very highly conserved arginine that was essential for efficient GAP activity. These data were consistent with a catalytic arginine residue mechanism for GAP activity, as described earlier for both ARF and RAS GAPs [8-11] but further structural studies are required to confirm this model. Identification of the GAP domain of the ELMODs is significant because it represents the first GAP domain identified for any Arl protein and a novel GAP domain for the Arfs. These data also assign a function to the ELMO domain which is the defining characteristic of the ELMO family of proteins. To identify other potential Arl GAPs with the same GAP domain as ELMODs, I used protein BLAST to search for a very

highly conserved motif within the GAP domain of the ELMODs that included the putative catalytic arginine residue (Chapter 2). The highly conserved GAP motif was only found in ELMODs suggesting that the GAP domain is unique to ELMODs. Recently identified Arl GAPs, RP2 and cofactor C, show very little sequence conservation in the GAP domains [12]. The ELMODs are also unique in that the other two Arl GAPs lack any detectable GAP activity for the Arfs. Although the pool of Arl GAPs remains very small, these finding lead me to two major speculations:

1) The promiscuous biochemical GAP activities of the ELMODs will prove to provide cross-talk between both Arfs and Arls and between Arls and other Ras superfamily members, notably members of the Rho family, through distinct mechanisms. We currently have no evidence that any ELMOD regulate more than one GTPase in cells (see below), but our models for the functions of ELMODs include Arfs, Arl2, and RhoA. The field is still very young and very little is known about the cellular roles of the ELMODs. Thus, more functional studies with an emphasis on known Arf and Arl signaling pathways will need to be performed to test this model.

2) The GAPs for Arl proteins will show to be much more structurally diverse than families of GAPs for the Arfs and other Ras superfamily GTPases. GTPase families typically have families of GAPs with well defined and conserved GAP domains. For instance, there are eleven families of Arf GAPs [8] yet every one contains a single, highly conserved arginine finger within a structurally well-defined four-cysteine zinc finger "Arf GAP domain" [7-9, 13].

Lack of a canonical "Arl GAP domain" will likely continue to impede the fields of Arl GAPs and Arl biology as homology searching of genomic and protein databases fails to identify novel members outside of orthologs of the ELMODs (Chapter 2). Structural studies are expected to contribute to a better understanding of the Arl GAP domain. The crystal structure of RP2 has

been solved and residues Gln116, Arg118, Glu138, and Phe177 make up the active site and are important for catalysis [12]. These residues are conserved in cofactor c and two of these residues, Gln116 and Arg118, are also conserved in the ELMODs corresponding to the putative catalytic arginine residue of the ELMODs and to another residue within the highly conserved GAP motif. Thus, while primary structure is not well conserved, tertiary structure may prove to be similar among the known Arl GAPs. Comparing structural data of ELMODs with the known structure of RP2 [12] may provide insight into the "Arl GAP domain" and identify important residues that are far away from the catalytic arginine (e.g. Phe177 of RP2 is 59 residues downstream of the catalytic arginine residue). This information would allow us to screen for other Arl GAPs *in silico*. Structural analyses of the ELMODs would also provide some key insights into the roles of each of the conserved residues in the GAP domain of the ELMODs and is the only way to definitively test the catalytic arginine mechanism suggested in Chapter 2. The structure of ELMOD would also be very interesting on its own merit given the unprecedented dual specificity for Arfs and Arls and its novel Arf GAP domain.

ELMOs and the ELMO domain

The human ELMO family of proteins includes three ELMODs and three ELMOs and is defined by the presence of the ELMO domain [1]. The ELMO domain was formerly a domain of unknown function until I mapped the GAP motif of the ELMODs to this domain (Chapter 2). The domain architecture of the ELMOs has been well characterized and many of the functions and protein binding regions have been mapped to these domains [14-20]. No function or activity of the ELMOs has ever been linked to the ELMO domain and the ELMOs lack any detectable GAP activity [1, 2] leading to the question of the function of the ELMO domain in these proteins. The phylogenetic analysis of the ELMO family of proteins very directly addressed this question as it was performed using only the ELMO domains isolated from each ELMO family homolog (Chapter 2). The most direct and accurate interpretation of the phylogenetic analysis is that the

ELMO domain of the ELMOs is phylogenetically distinct and arose from the ELMO domain of the ELMODs. It was reasonable to extrapolate those data to the full length proteins in Chapter 2 since the ELMO domain is only found in ELMO family members and is the only region of homology between ELMOs and ELMODs. Key differences in the GAP motif region of the ELMOs, described from sequence analysis and biochemical testing of the ELMODs, are consistent with an evolutionary loss in GAP activity as the putative catalytic arginine residue of the ELMODs was not conserved in the ELMOs (Chapter 2). Thus, one of the lingering questions from this study and in the field is the role or function of the ELMO domain in the ELMOs as they lack the evolutionary conserved Arf family GAP activity of the ELMODs.

In my model for the function of the ELMO domain (Fig 1), ELMODs function as both GAPs and effectors of Arf family GTPases while ELMOs serve only as Arf family effectors. Dual roles for ELMODs as effectors and GAPs for Arf family GTPases is well supported by this study (Chapter 2) and by other data from my lab (Newman *et. al. in press*) and from studies of Arf GAPs [21-32]. Over-expression of ELMOD1 led to lower cellular levels of activated Arfs and drastic changes in Golgi morphology, similar to other inhibitors of Arf signaling, including Brefeldin A and over-expression of some Arf GAPs [6, 33-36] (Chapter 2). Expression of a catalytically dead mutant of ELMOD1 had no effect on Golgi morphology or cellular levels of activated Arf. Thus, ELMOD1 appears to function as a GAP for Arfs at the Golgi. ELMOD2 predominantly localizes to mitochondria and knockdown of ELMOD2 by siRNA in HeLa cells caused fragmentation and clustering of mitochondria around the nucleus in a manner that phenocopies knockdown of its substrate, Arl2 (Newman *et. al.* in press). These data support our model that ELMOD2 functions as an effector of Arl2 at mitochondria rather than as a GAP. ELMOD3 also does not appear to function as a GAP for Arf family GTPases as its specific activities are very low for any of the six Arf family members tested [2]. Expression of a catalytically dead mutant of ELMOD3 also precisely phenocopied expression of the WT protein

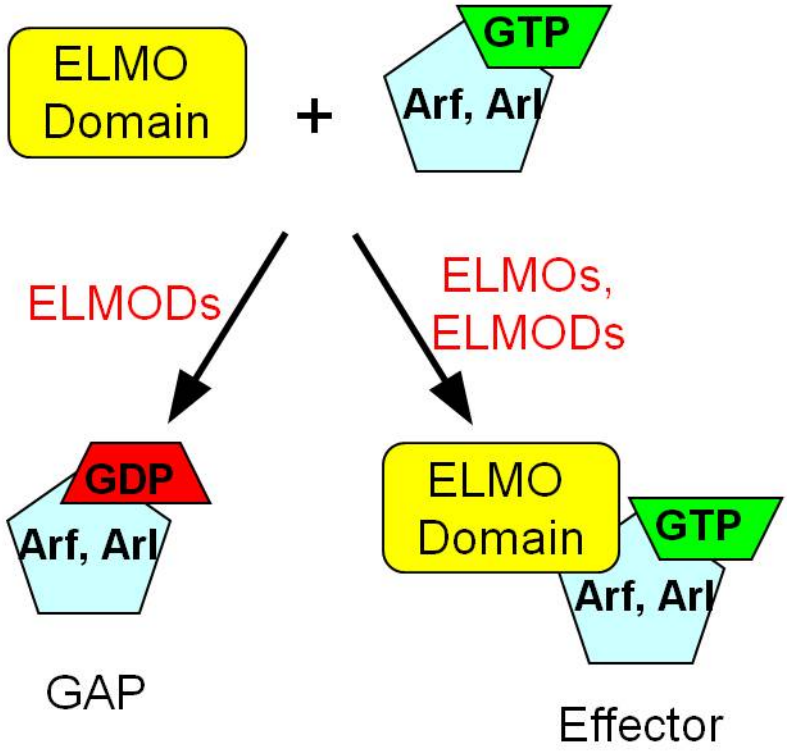

Figure 1: Model for the function of the ELMO domain in ELMOs and ELMODs. ELMODs function as both GAPs and effectors for their substrate GTPases. The ELMOs have not been shown to bind Arf family GTPases but have no detectable GAP activity *in vitro*. This model speculates that the ELMO domain of the ELMODs is a GTPase binding domain to facilitate effector function of Arf family GTPases.

in inducing cell morphology changes and membrane blebbing (Chapter 3), suggesting that GAP activity is not required for those phenotypes. There is no indication that an Arf family GTPase is involved in any of the ELMOD3 phenotypes so calling ELMOD3 an effector is premature, but I expect this will be found to be the case. Taken together, these findings support roles for ELMODs as GAPs and effectors of their substrate GTPases.

I speculate that the ELMOs have evolved to lose GAP activity to more specifically facilitate an effector function for Arf family GTPases (Fig 1). Although GAP activity is lost, this model presumes that ELMOs have retained the ability to bind Arf family GTPases through the ELMO domain and that some aspect of ELMO signaling is regulated by this binding. The ELMOs arose during evolution from the ELMODs, which consist of little more than the ELMO domain itself (Chapter 2), suggesting that the ELMO domain is important or perhaps essential to the proper function of the ELMOs. Disruption of GAP activity by mutagenesis of the GAP domain typically does not prevent GTPase binding and often increases affinity of a GAP for a substrate GTPase [10, 37]. Thus, it is reasonable to speculate that the ELMO domain of the ELMOs retains GTPase binding activity. There is currently no direct evidence that ELMOs interact with Arf family GTPases through the ELMO domain but this model is rooted in a growing body of literature linking the signaling pathways of Rho and Arf family GTPases [38-43]. Numerous studies have established an intimate link between Arf6 and the Rho family GTPase Rac1 [39, 44-47]. The most direct and relevant example of this is that Arf6 and its GEF ARNO are upstream of ELMO1 mediated Rac1 activation and cell motility [38]. Inhibition of other Rac1 GEFs had no effect on Rac1 activation by Arf6 suggesting that ELMO/Dock180s are the primary Rac1 GEFs in this pathway. The mechanism for cross talk between Arf6 and Rac1 via ELMO1 is not yet understood. My model proposes that Arf6 binds directly to ELMO1 through the ELMO domain. Such a model may be more broadly applicable as other studies

report activation of Arf1 is essential for the activation of both Rac1 and RhoA through an unknown mechanism that may also rely on ELMOs and ELMODs [40, 41].

While the focus of this dissertation was on the ELMODs, the function of the ELMO domain in the ELMOs is equally interesting and important, though not addressed directly in my studies. The proposed model (Fig 1) would fill an important gap in the literature and would assign a role for this domain that is consistent with its role in the ELMODs. Initial tests of this model should focus on determining whether Arf family GTPases do, in fact, interact with ELMOs. Recombinant ELMO1 and the ELMO1/DOCK180 complex can be expressed and purified from bacteria or HEK 293T cells, respectively [2, 48]. ELMOs have two autoinhibitory domains where the structure is proposed to fold back on itself [15]. Thus, it may be necessary to truncate the protein and express a smaller fragment lacking the one of the autoinhibitory domains or only the isolated ELMO domain in early tests of this model. Arf family GTPases, including Arf6, are easily expressed and purified from bacteria [49, 50]. Thus, a variety of different protein interaction assays including isothermal titration calorimetry or fluorescence polarization using Arf GTPases pre-loaded with a fluorescent analog of GTP could be used to assay binding and determine affinities. Another approach is to use *in vitro* Rac1 GEF assays to determine whether addition of Arf family GTPases affects GEF activity of the ELMO1/DOCK180 complex directly [51]. ELMODs should also be assayed for GTPase binding using assays independent of GAP activities as they too may function as effectors with poor coupling to GAP activity. Our research has focused primarily on the substrates of the GAP activity and we have not pursued GTPase binding/effector functions. This approach may be particularly informative for ELMOD3 as it has, by a large margin, the lowest specific activity for any of GTPases tested [2]. Expression of a catalytically dead mutant of ELMOD3 resulted in the same plasma membrane blebbing phenotype as the wild type protein further suggesting a role for ELMOD3 as an effector rather than as a GAP (Chapter 3). Thus, ELMOD3 may preferentially serve as an effector and

identifying GTPase binding partners would provide key insights into the functions and mechanisms of ELMOD3 in the cell.

Models for the cellular functions of ELMODs

Functional studies of the ELMODs have revealed a myriad of cellular roles and locations, as summarized in Figure 2. ELMODs are expressed to very low levels in the cultured cell lines and mammalian tissues assayed by immunoblot and few verified reagents exist for each protein. Knockdowns by siRNA have proven unusually difficult, with the exception of ELMOD2, for no obvious reasons. Much of our understanding of their function comes from models of over-expression in cultured cell lines. Thus, our models are still in preliminary stages and yield far more questions than answers. Screens for binding partners of the ELMODs by co-IP have revealed interesting results but offered virtually no insight into the mechanisms of ELMODs for any of our models for their cellular functions. Instead, the putative binding partners suggest novel functions and localizations for each of the ELMODs. Taken together, these data provide a strong foundation and several intriguing and defensible leads for further study of the cellular roles of the ELMODs.

ELMOD1 - My model for the function of ELMOD1 is that it functions as an Arf GAP at the Golgi (Chapter 2). Upon over-expression, ELMOD1 localizes predominantly to the Golgi at early time points and causes fragmentation of the Golgi in a manner consistent with pharmacological inhibition of Arf signaling with Brefeldin A or with the over-expression of the well characterized Golgi Arf GAP ArfGAP1 [33, 36]. Consistent with this model, ELMOD1 has GAP activity for Arf1 *in vitro* and ELMOD1 over-expression lowers the cellular levels of activated Arfs (Chapter 2). Expression of a catalytically dead mutant of ELMOD1 had no effect on Golgi morphology or on the cellular levels of activated Arfs (Chapter 2). These data form the foundation of our model and represent the only known phenotypes of ELMOD1 over-expression

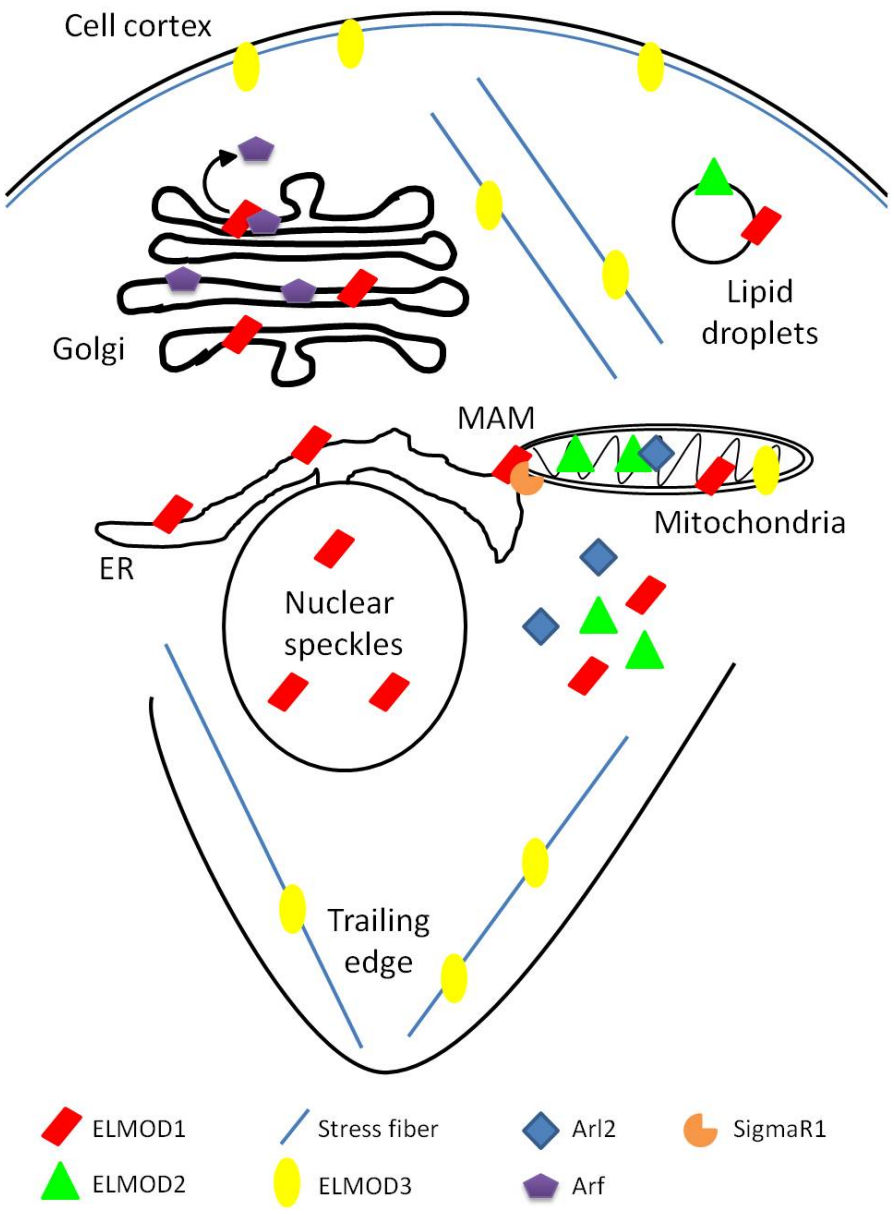

Figure 2: Schematic of confirmed and suspected subcellular localization of the ELMODs throughout the cell. Cellular locations of the ELMODs presented are from cell staining of endogenous and ectopically expressed proteins, sub-cellular fractionation, and inferred from the localization of putative binding partners.

in cells. The weakest aspect of this model is that it is based entirely on over-expression of ELMOD1. I have not found endogenous ELMOD1 at the Golgi in screens of over a dozen different cultured cell lines and the localization of ELMOD1-HA to Golgi was transient after induced expression. Thus, future functional studies of ELMOD1 should focus on the development of new antibodies and on the effects of knockdown and/or knockout of ELMOD1 on the Golgi and on Arf signaling pathways. My efforts to knockdown endogenous ELMOD1 using a handful of different shRNA and siRNA knockdown reagents were unsuccessful. Only protein levels were examined using these assays so it's possible that ELMOD1 is simply a very long-lived protein. Our collaborator, Karen Avraham, has generated an ELMOD1 conditional knockout mouse and MEFs (unpublished data) and these experiments should be possible shortly.

Golgi fragmentation may also have been at least partially mediated by Arl1. ELMOD1 has greater than 100-fold higher specific activity for Arl1 than for Arf1 [2]. Like Arf, Arl1 is essential for the maintenance of Golgi morphology [52-54] and effects on the cellular levels of activated Arfs may have been secondary to the loss of Golgi morphology. Dominant active mutants of Arl1 and Arfs that are insensitive to GAPs exist and could be used to distinguish whether Golgi effects are mediated through Arfs and/or Arl1 [54, 55]. An assay may also be devised to measure the cellular levels of activated Arl1 similar to the GST-GGA3 pulldown assay for activated Arfs (Chapter 2). Similar assays are available for a long list of GTPases [56-59] and several effectors of Arl1 that may work for such an assay are known [54, 60-62]. Determining the substrate of ELMOD1 at the Golgi is particularly important because ELMOD1 represents the best example of an ELMOD protein that functions as a GAP in cells.

Another potentially very important function for ELMOD1 is as a novel regulator or effector of non-opioid receptor sigma-1 (SigmaR1). I identified SigmaR1 as a putative binding partner of ELMOD1 in a quantitative co-IP from HeLa cells (Chapter 4). This interaction was later confirmed *in vitro* and binding of ELMOD1 to SigmaR1 inhibited GAP activity [2].

Preliminary data also suggest that inhibition of GAP activity by SigmaR1 was further modulated by agonists and antagonists of SigmaR1. These data indicate a functional relationship between SigmaR1 and ELMOD1. SigmaR1 is a transmembrane protein residing in the ER [63]. We have not found endogenous ELMOD1 at the ER but ectopically expressed ELMOD1 has a reticular-like staining pattern throughout the cell at later time points of expression that likely represents staining of the ER (Chapter 2). SigmaR1 and ELMOD1 are also heavily enriched in the brain [5, 64]. SigmaR1 regulates calcium signaling at the interface between the ER and mitochondria and cell survival pathways in response to ER stress [63, 65]. SigmaR1 is also a receptor for a large number of psychoactive drugs many of which are currently in use today [66-70]. Thus, ELMOD1 may be involved in SigmaR1 biology at the ER and/or as a downstream effector of the drugs targeting SigmaR1.

Other potential roles for the cellular functions of ELMOD1 include a role at lipid droplets, mitochondria, and nuclear speckles. When over-expressed, ELMOD1 localizes to ring-like structures identified as lipid droplets (Chapter 2). There was no readily observable consequence of ELMOD1 over-expression on lipid droplet size, number, or morphology and I have not found endogenous ELMOD1 at that organelle. Thus, it is unclear whether ELMOD1 localization there is biologically relevant or was simply an artifact of over-expression. Several Arf family GTPases including Arl1, Arf1, and Arfrp1 are essential for proper lipid droplet biogenesis and there is an emerging role for COPI vesicle components and the Arf GEF GBF1 at lipid droplets [71-78]. While we have no direct evidence of a lipid droplet phenotype, ELMOD1 and ELMOD2 are the only Arf GAPs shown to localize to lipid droplets and may be important regulators of Arf family GTPases at that organelle. As our understanding of Arf biology at lipid droplets increases, we are likely to be able to develop specific hypotheses regarding ELMOD1 and ELMOD2 functions there. Livers and hepatocytes should also be examined from the

ELMOD1 and ELMOD2 knockout mice developed by our collaborators (unpublished data) for aberrations in lipid storage or lipid droplet morphology.

Quantitative co-IPs of ELMOD1-HA from HeLa cells using SILAC identified a large number of mitochondrial proteins as putative binding partners of ELMOD1 (Chapter 4). Although this typically would not be convincing enough evidence to justify a function or localization at a particular organelle, the sheer number of putative mitochondrial binding partners offers compelling evidence for further experiments. SILAC helps to prevent false positives by calculating the fold-enrichment of a particular protein/peptide over background and eliminating peptides present in both experimental and controls (see chapter 4). I identified three components of cytochrome c oxidase (complex IV of the electron transport chain) that were co-enriched with ELMOD1-HA in four different co-IPs. The enrichment levels of each component were also consistent within each experiment suggesting pulldown of all or part of the protein complex. The cytochrome c oxidase complex was the most highly enriched putative binding partner after SigmaR1 providing additional confidence that this is a real interaction although protein/peptide abundance in co-IPs is not necessarily suggestive of affinity. An interaction with cytochrome c oxidase would suggest a function of ELMOD1 in the regulation of cellular energy metabolism. A substrate of ELMOD1, Arl2, localizes to mitochondria and is essential for the maintenance of cellular ATP levels through an unknown mechanism (Newman *et. al.*, in press). ELMOD2 also localizes to mitochondria and is proposed to function as an effector of Arl2 (Newman *et. al.*, in press). Thus, there is some precedence for and a potential mechanism as a regulator of Arl2 for ELMOD1 in mitochondria as a novel regulator of the electron transport chain.

The only endogenous localization for ELMOD1 to date is to nuclear speckles, also known as interchromatin granule clusters, but ectopically expressed ELMOD1 is excluded from the nucleus (Chapter 2). Nuclear speckles are understudied organelles but enriched in pre-mRNA splicing factors [79]. I have no defensible hypotheses for ELMOD1 in the nucleus or at nuclear

speckles, though ARL2 is also present in the nucleus and one paper has suggested it plays a role in the regulation of a STAT3 transcriptional response [80].

ELMOD2 - ELMOD2 localizes predominantly to mitochondria (Newman *et. al.*, in press). I have done very little work with ELMOD2 and our model for the function of ELMOD2 in cells is primarily based on experiments done by another member of the lab, Laura Newman. Depletion of ELMOD2 by siRNA results in fragmentation of mitochondria and clustering of mitochondria around the nucleus. This phenotype is very similar to expression of a dominant negative mutant of Arl2 or to depletion of Arl2 by siRNA (Newman *et. al. in press).* Knockdown of Arl2 also caused a substantial drop in cellular ATP levels but knockdown of ELMOD2 had no effect on ATP. Thus, ELMOD2 appears to function as an effector of Arl2 in mitochondria to regulate mitochondrial dynamics and motility.

My attempts to identify binding partners of ELMOD2 using quantitative co-IPs (Chapter 4) did not yield any putative binding partners that might help explain the mitochondrial phenotypes. Instead, most of the proteins that were co-enriched with ELMOD2 were cytosolic including several glycolytic enzymes. When considering the enrichment values, the number of different glycolytic enzymes (three), and that several isoforms of the same enzyme (two triosephosphate isomerase and three phosphoglycerate mutase isoforms) were co-enriched with ELMOD2, the evidence for a role for ELMOD2 in glycolysis is highly suggestive. The role or mechanism for how Arl2 is involved in the maintenance of cellular ATP levels is still unclear (Newman *et. al.*, in press). Thus, Arl2 may be acting to regulate glycolysis through an interaction with ELMOD2. This model is purely speculative since ELMOD2 knockdown does not result in lower ATP levels (Newman *et. al.*, in press) and because binding of ELMOD2 to glycolytic enzymes has not been verified.

The Arf family GTPase Arf4 was also co-enriched with ELMOD2 in quantitative co-IPs. These findings were intriguing because Arf4 is the only GTPase identified in co-IPs of all three of the ELMODs despite their roles as GAPs and effectors of Arf family GTPases. Arf4 is also the least abundant of the five human Arfs [81]. Thus, binding of ELMOD2 to Arf4 is likely biologically relevant and important to the role of ELMOD2. Arf4 is primarily thought to regulate membrane traffic throughout the cell [81, 82] and we have no phenotype for ELMOD2 that might involve Arf4 or that is related to vesicular traffic. Due to technical complications with the expression and purification of Arf4 in bacteria, we have also not determined the specific activity of ELMOD2 for Arf4. Thus, we lack any specific hypothesis for the biological relevance of Arf4 and ELMOD2 binding.

ELMOD3 - My primary model for the cellular function of ELMOD3 is as a novel activator of the Rho family GTPase, RhoA, to regulate the actin cytoskeleton (Chapter 3). ELMOD3 has two distinct localization patterns in non-polarized and migrating cells. In non-polarized cells, ELMOD3 localization is predominantly punctate with a higher organization of the puncta along actin stress fibers in some cells. In migrating cells, ELMOD3 localizes predominantly to the trailing edge of the cell. Thus, ELMOD3 localization is dynamic and suggests a role for ELMOD3 in the regulation of actin, particularly at the trailing edge. Over-expression of ELMOD3 causes changes in the actin cytoskeleton in the form of membrane blebbing. This blebbing phenotype is likely the result of activation of actomyosin contraction at the cell cortex, a process that is downstream of RhoA [83-85]. Inhibition of RhoA signaling using a pharmacological inhibitor of the RhoA effector ROCK or expression of a dominant negative mutant of RhoA was sufficient to block cell blebbing (Chapter 3). Thus, the membrane blebbing phenotype of ELMOD3 is a RhoA-dependent process and ELMOD3 is likely a novel activator of RhoA signaling. This over-expression model is consistent with the endogenous localization of ELMOD3 to the trailing edge (Chapter 3). RhoA is thought to function primarily

at the trailing edge of migrating cells where it activates actomyosin contraction of actin stress fibers to pull the cell rear along in the direction of migration [86-89]. The organization of ELMOD3 puncta along actin stress fibers in non-migratory cells is also consistent with a function for ELMOD3 in regulating RhoA and actomyosin contraction. Stress fibers are another product of RhoA signaling and stress fibers contract to facilitate focal adhesion formation and regulate cell shape [90-93]. Localization of ELMOD3 to stress fibers is also likely to be a regulated process as only a portion of ELMOD3 puncta organize along stress fibers and some cells lack any organization of endogenous ELMOD3 along stress fibers (Chapter 3). Thus, my model suggests that ELMOD3 is recruited to actin stress fibers and the trailing edge of migrating cells to stimulate actomyosin contraction through a RhoA dependent process.

Direct evidence of RhoA activation by ELMOD3 and determining the mechanism of how ELMOD3 activates RhoA is paramount and should be the primary focus of any future studies of ELMOD3 function. The simplest and most likely mechanism is that ELMOD3 activates a RhoA GEF. This model is supported by our observation that a dominant negative mutant of RhoA blocks the blebbing phenotype (Chapter 3). Dominant negative GTPases are thought to bind and sequester GEFs to prevent activation of the endogenous protein [94]. This model for ELMOD3 also very closely parallels the function of the ELMOs in activating Rac1 (Fig 3). Binding of ELMO to the Rac1 GEF DOCK180 is essential for Rac1 activation in cells [51] and there is a precedence in the literature for direct and functional interactions between Arf GAPs and Rho family GEFs [38, 95, 96]. Several other models for how ELMOD3 activates RhoA are also possible. ELMOD3 may deactivate a RhoA GAP to increase cellular levels of activated RhoA. ELMOD3 may also use the antagonistic relationship between RhoA and Rac1 to activate RhoA by de-activating Rac1 although I believe this model to be less likely [97]. Two potentially informative approaches for delineating the mechanism of ELMOD3-mediated Rho activation are to screen RNAi libraries against Rho GEFs and GAPs looking for the loss of the blebbing

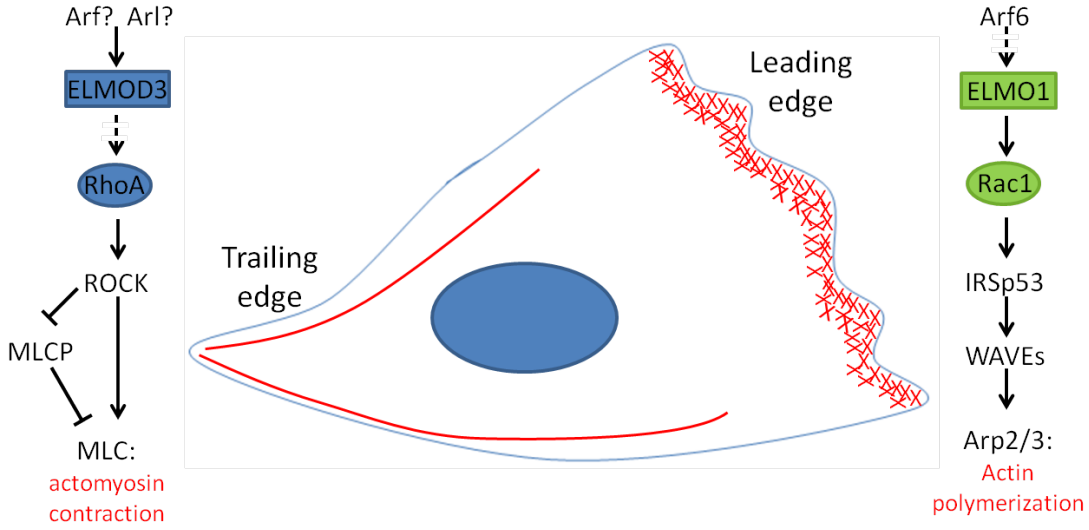

Figure 3: The model for the function of ELMOD3 closely parallels its paralog ELMO1. ELMO1 functions primarily at the leading edge of the cell to initiate actin polymerization through the Arp2/3 complex. ELMO1 binds to an obligate binding partner DOCK180 to form an unconventional Rac1 guanine nucleotide exchange factor (GEF) to activate Rac1 directly. Arf6 is upsteam of ELMO1 in this pathway but the mechanism of activation of ELMO1 by Arf6 is unknown and this step is indicated with a hashed arrow. The model for the function of ELMOD3 is as a regulator of actomyosin contraction at the trailing edge of migrating cells and along actin stress fibers as a novel activator of RhoA signaling. A role for an Arf or an Arl GTPase upstream of ELMOD3 is expected but there is currently no evidence to support this. How ELMOD3 activates RhoA signaling is also unknown so this step is indicated with a hashed arrow. The most likely mechanism is through binding and activation of a RhoA GEF similar to the ELMO1/DOCK180 GEF complex for Rac1.

phenotype and to use an assay to analyze activated RhoA GAPs and GEFs from cell lysates developed by the Burridge lab (University of North Carolina) [98]. The RNAi libraries already exist for Rho GEFs and GAPs [99-101], though how available they may be to the public is uncertain, and the blebbing phenotype should be robust enough for this type of screen. The other approach uses dominant active and negative mutants of RhoA purified from bacteria to pulldown activated RhoA GEFs and GAPs from cell lysates [98]. The samples could then be analyzed by mass spectrometry or western blot looking for a more abundant GEF or less abundant GAP in response to over-expression of ELMOD3.

One of the main weaknesses of my model for the function of ELMOD3 is that it is primarily based on over-expression experiments (Chapter 3). Knockdown or knockout experiments may be particularly informative for ELMOD3 considering the breadth of the literature on cell migration and actin dynamics. My attempts to knock down ELMOD3 by transient transfection of siRNAs were unsuccessful. ELMOD3 has a very long half-life showing no decrease in signal intensity by immunoblot following inhibition of protein synthesis for 16 hours with cycloheximide (Chapter 3). Thus, generating stable cell lines for ELMOD3 knockdown or MEFs from an ELMOD3 knockout mouse may be better for these types of experiments. Because endogenous ELMOD3 localization and over-expression experiments point toward a role for ELMOD3 in regulating actomyosin contraction at the trailing edge, tail retraction and migration assays should be the highest priority. Defects in tail retraction can be readily observed by the emergence of long microtubule and actin rich cell tails that can be quantified by measuring the distance of the nucleus from the leading and trailing edges [102, 103]. Migration assays are fairly standard in many laboratories, with scratch wound assays being one of the most widely used. Should tail retraction be inhibited by ELMOD3 depletion, migration rate should also be inhibited. These experiments may also offer insight into the mechanism of ELMOD3-mediated RhoA activation. Several Rho family GEFs and GAPs have

been implicated in the regulation of tail retraction and would be candidate targets of ELMOD3 [104, 105]. Other experiments testing the requirement of ELMOD3 for RhoA signaling could also be performed following ELMOD3 depletion. Cellular levels of activated RhoA and myosin light chain could be assayed using phospho-specific antibodies in response to activation of RhoA signaling with external ligands (e.g. EGF, LPA, etc.). The number and bundling of actin stress fibers and the number and length of focal adhesions are also products of RhoA signaling and could be quantified in ELMOD3 knockdown/knockout cells [90].

The functions and dynamic localization of ELMOD3 in cells may be regulated by direct binding to phosphoinositides. GST-ELMOD3 bound directly to a number of different phosphoinositides in protein-lipid overlay assays (Chapter 4). In HeLa cells, staining of ELMOD3-HA showed extensive overlap with molecular probes for two important signaling phosphoinositides at the plasma membrane, PI(4,5)P_2 and PI(3,4,5)P_3 (Chapter 4). These results are weakened by variability in the specificity of GST-ELMOD3 for phosphoinositides across experiments and by the apparent staining of the entire cell periphery by both ELMOD3-HA and probes for PI(4,5)P_2 and PI(3,4,5)P_3. Thus, these data are preliminary and require additional experiments to support a functional interaction between ELMOD3 and phosphoinositides. Binding of ELMOD3 to phosphoinositides is suggestive of a mechanism for ELMOD3 recruitment to the trailing edge in migrating cells. PI(4,5)P_2 is asymmetrically distributed at the plasma membrane during migration and is enriched at the cell rear. Thus, PI(4,5)P_2 may recruit ELMOD3 to the trailing edge through direct binding. Apparent binding of GST-ELMOD3 to phosphoinositides led us to question whether phosphoinositides also enhanced GAP activity. Addition of phosphoinositides in large unilamellar vesicles or in DMPC/cholate micelles had no effect on GST-ELMOD3 GAP activity (Chapter 4).

Similar to ELMOD1 and ELMOD2, candidate binding partners identified by quantitative co-IP did not contribute to our understanding of the ELMOD3 phenotypes. Our model suggests

that the primary role of ELMOD3 is in the regulation of the actin cytoskeleton (Chapter 3) but I identified mostly tubulin isoforms and mitochondrial proteins in co-IPs. Tubulin is one of the most abundant proteins in the cell and is a common contaminant of co-IPs but in this case appears to be specifically co-enriched with ELMOD3. Tubulin was not specifically enriched in any of the other co-IPs for ELMOD1 and ELMOD2 which were performed at the same time with the same reagents suggesting that it is not a common contaminant. A total of 14 different tubulin isoforms were also specifically co-enriched in two independent co-IPs. Thus, this is likely a specific interaction with ELMOD3. Microtubules are essential for tail retraction, the actin cytoskeleton is physically tethered to microtubules, and a substrate of ELMOD3, Arl2, has a well defined role in the regulation of microtubule dynamics [102, 106-109]. However, it is unclear how tubulin/microtubules fit into our model for the functions of ELMOD3.

Another putative binding partner of ELMOD3 identified by quantitative co-IP is solute carrier family 25, member 13 (SLC25A13) (Chapter 4). This protein showed a higher level of enrichment than any other protein in the co-IPs with a near 1:1 stoichiometry with ELMOD3. The only other human paralog of SLC25A13, SLC25A12, [110] as well as two other members of solute carrier family 25 (SLC25) were also specifically co-enriched with ELMOD3 adding further support that this is a real interaction. SLC25A13 and the other SLC25 family memers are integral membrane proteins spanning the inner mitochondrial membrane [110]. SLC25A12 and SLC25A13 are the primary transporters for mitochondrial aspartate to the cytosol where it is used in the biosynthesis of proteins and nucleotides, the urea cycle, and the oxidation of NADH [111]. Each of the two transporters has been linked to prevalent human diseases including citrullinemia type 2 (SLC25A13) and autism spectrum disorders (SLC25A12) [112-115]. Thus, SLC25A13 and SLC25A12 are strong candidate binding partners of ELMOD3 and should be verified and followed up on. SLC25A12 and SLC15A13 have no clear role in my model for ELMOD3 function as an activator of RhoA and we have no evidence for ELMOD3 localization to

mitochondria. I note however that localization of a protein to a specific organelle, even in the inner membrane of mitochondria, in no way precludes its localization to other membranes or organelles. One such example is VDAC3, well known as a voltage dependent anion channel in mitochondrial membranes but also recently shown to localize specifically to centrosomes [116]. Thus, this line of investigation may lead to a novel function of ELMOD3 in mitochondria or for these transporters to other sites and may have a substantial impact in our understanding of the diseases linked to SLC25A12 and SLC25A13.

ELMOD3 had detectable GAP activity for a variety of different Arf family GTPases *in vitro,* but the specific activities of ELMOD3 were substantially lower than ELMOD1 or ELMOD2 for the same GTPases [2, 4]. In Chapter 2, I speculated that key differences between ELMOD3 and ELMOD1-2 in the highly conserved GAP motif of the ELMODs were responsible for the loss of ELMOD3 GAP activity. My more recent studies (Chapter 4) suggest that purified, recombinant preparations of GST-ELMOD3 used to determine specific activities of GST-ELMOD3 for GTPases lacked a binding partner or cofactor important for GAP activity. Addition of testis extract to GST-ELMOD3 enhanced Arl2 GAP activity *in vitro*. Testis extract enhanced Arl2 GAP activity of GST-ELMOD3 by approximately four-fold after a 1:10 dilution of the extract to remove detergent that interfered with the assay. Thus, undiluted extract should enhance GST-ELMOD3 GAP activity by up to 40-fold raising the specific activity of GST-ELMOD3 to a level more comparable to GST-ELMOD1 and GST-ELMOD2. Heating the testis extract was sufficient to ablate enhancer activity but treatment with DNAse or RNAse had no effect. These data indicate that the enhancer is heat sensitive and likely is a protein, but additional experiments are required to confirm this. Purification and identification of the enhancer will provide key insights into the functions and mechanisms of ELMOD3 in the cell by identifying a novel, functionally relevant binding partner and will help to better characterize ELMOD3 biochemically as a GAP.

General comments regarding models for the functions of ELMODs

This study offers compelling evidence for roles for ELMODs in a diverse array of cellular processes. My models for each of the ELMODs have experimental support but are still not thoroughly elucidated and/or lack key supporting data. The model for ELMOD1 as an Arf GAP at the Golgi is weakened by our failure to detect endogenous ELMOD1 at that organelle. The model for ELMOD3 as a novel activator of RhoA signaling lacks both a mechanism for RhoA activation and direct evidence that RhoA is activated by ELMOD3. Putative binding partners identified by co-IP require confirmation but are suggestive of additional functions for the ELMODs outside of our current models adding further complexity. Together, these data provide the foundation for understanding the functions of the ELMODs and offer direction for future work on these proteins.

There is virtually no overlap in the phenotypes of the ELMODs in knockdown and over-expression experiments in cultured cells. There is also very little overlap in localization of the three ELMODs with the sole exception of both ELMOD1 and ELMOD2 localization to lipid droplets when over-expressed (Chapter 2). The only other point of convergence in the data comes from the identification of putative binding partners in mitochondria for ELMOD1 and ELMOD3 (Chapter 4) and the localization of ELMOD2 predominantly to mitochondria (Newman *et. al.*, in press). Within these datasets there is still no evidence for functional redundancy as the putative binding partners are involved in entirely different cellular processes. Thus, each of the ELMODs appears to facilitate one or more functions in the cell distinct from those of the other two. This is reminiscent of the diversity of cellular processes regulated by the substrates of the ELMODs, particularly the Arl proteins [117]. While the majority of this work was focused directly on the ELMODs, further tests of Arf and Arls involvement in ELMOD biology may be particularly revealing and I fully expect close functional relatedness of ELMODs with their substrate GTPases.

Clinical aspects of the ELMODs

Both ELMOD1 and ELMOD3 have been linked to deafness in mice and humans. The only observable phenotypes of the ELMOD1 knockout mouse are deafness and secondary balance defects (unpublished data from Karen Avraham). The same phenotypes were also observed in randomly occurring exon deletions or exon duplications within the ELMOD1 gene in laboratory mice [5]. In both cases, there was a progressive degeneration of actin-based, mechanosensory stereocilia in outer hair cells and fusion of stereocilia in inner hair cells. These data suggest that ELMOD1 is essential for the maintenance of stereocilia but there is no indication in the literature about the mechanism or role of ELMOD1 in this process. A point mutation in ELMOD3 (L265S) was also linked to deafness in a human family [4]. The mutation, which lies within the ELMO domain, prevented proper localization of GFP-ELMOD3 to actin structures in cultured cells and inner ear explants and nearly ablated Arl2 GAP activity of GST-ELMOD3 [4]. Mutant ELMOD3(L265S) appears to function in a dominant negative manner as unpublished data from our collaborator, Saima Riazzudin, indicate that targeted knockout of ELMOD3 in mice does not result in deafness. The role of ELMOD3 in hearing and the mechanism of the L265S mutant in causing deafness are unknown but are likely linked to stereocilia as ELMOD3 predominantly localized to stereocilia in inner ear explants [4]. Thus, not only are *ELMOD1* and *ELMOD3* both genes associated with deafness but both are also implicated in maintenance of stereocilia. Our functional studies of ELMOD3 as a novel regulator of actin offer direct insight into the role of ELMOD3 in stereocilia and hearing. Stereocilia are actin based structures and many myosin motors are essential for hearing and for the proper function of stereocilia [118]. Thus, ELMOD3 may be important for the regulation of actin dynamics or of myosin motors in stereocilia. It is less clear how any of my functional models for ELMOD1 are related to hearing or to the biology and/or maintenance of stereocilia since there is no direct link to actin or any actin associated process. The ELMOD1 binding partner SigmaR1

may offer some insight into the role of ELMOD1 in stereocilia and hearing. SigmaR1 regulates intracellular calcium levels and signaling by stabilizing IP3 receptors [63]. Intracellular calcium levels are tightly regulated in stereocilia and are a driving force of mechanotransduction [119, 120]. Thus, the ELMOD1/SigmaR1 complex may regulate intracellular calcium levels in stereocilia. This model is largely speculative based on our limited understanding of ELMOD1 function and the biology of the ELMOD1/SigmaR1 complex.

ELMOD2 is a candidate gene for idiopathic pulmonary fibrosis [3]. There is very little information available for this disease including its cause and the underlying biology at the cellular level. Thus, how ELMOD2 is involved in the disease remains unknown and our models and putative binding partners fail to offer any obvious or tractable leads. Our very limited understanding of the disease and the fact that very few other proteins have ever been linked to the disease makes ELMOD2 an even more important and compelling target for further study of idiopathic pulmonary fibrosis and its cause and treatment.

Concluding remarks

The ELMODs are a unique group of Arf family GAPs. They have a novel GAP domain and unprecedented, promiscuous specificity for Arf family of GTPases. The ELMODs function as both GAPs and effectors of their substrate GTPases and facilitate a diverse array of cellular functions throughout the cell. They are an ancient family of proteins dating back to the last eukaryotic common ancestor suggesting that one or more of these functions are important or essential for eukaryotic life. The ELMODs also have an emerging clinical relevance as they have recently been implicated in deafness, idiopathic pulmonary fibrosis, and in the pharmacology of commonly used psychoactive drugs through their direct binding to Sigma1R. Thus, the ELMODs are intriguing and important molecules worthy of additional study. In this dissertation, I have characterized reagents and provided the foundation for our understanding of the biology of the

ELMODs. This work has contributed some of the only available functional information for these proteins and has provided many compelling leads and directions for further study.

References

1. Bowzard, J.B., et al., *ELMOD2 is an Arl2 GTPase-activating protein that also acts on Arfs.* J Biol Chem, 2007. **282**(24): p. 17568-80.
2. Ivanova, A.A., et al., *Characterization of Recombinant ELMOD (Cell Engulfment and Motility Domain) Proteins as GTPase-activating Proteins (GAPs) for ARF Family GTPases.* J Biol Chem, 2014. **289**(16): p. 11111-21.
3. Hodgson, U., et al., *ELMOD2 is a candidate gene for familial idiopathic pulmonary fibrosis.* Am J Hum Genet, 2006. **79**(1): p. 149-54.
4. Jaworek, T.J., et al., *An alteration in ELMOD3, an Arl2 GTPase-activating protein, is associated with hearing impairment in humans.* PLoS Genet, 2013. **9**(9): p. e1003774.
5. Johnson, K.R., C.M. Longo-Guess, and L.H. Gagnon, *Mutations of the mouse ELMO domain containing 1 gene (Elmod1) link small GTPase signaling to actin cytoskeleton dynamics in hair cell stereocilia.* PLoS One, 2012. **7**(4): p. e36074.
6. East, M.P., et al., *ELMO domains, evolutionary and functional characterization of a novel GTPase-activating protein (GAP) domain for Arf protein family GTPases.* J Biol Chem, 2012. **287**(47): p. 39538-53.
7. Kahn, R.A., et al., *Consensus nomenclature for the human ArfGAP domain-containing proteins.* J Cell Biol, 2008. **182**(6): p. 1039-44.
8. Schlacht, A., et al., *Ancient complexity, opisthokont plasticity, and discovery of the 11th subfamily of Arf GAP proteins.* Traffic, 2013. **14**(6): p. 636-49.
9. Cukierman, E., et al., *The ARF1 GTPase-activating protein: zinc finger motif and Golgi complex localization.* Science, 1995. **270**(5244): p. 1999-2002.

10. Ahmadian, M.R., et al., *Confirmation of the arginine-finger hypothesis for the GAP-stimulated GTP-hydrolysis reaction of Ras.* Nat Struct Biol, 1997. **4**(9): p. 686-9.

11. Scheffzek, K., M.R. Ahmadian, and A. Wittinghofer, *GTPase-activating proteins: helping hands to complement an active site.* Trends Biochem Sci, 1998. **23**(7): p. 257-62.

12. Veltel, S., et al., *The retinitis pigmentosa 2 gene product is a GTPase-activating protein for Arf-like 3.* Nat Struct Mol Biol, 2008. **15**(4): p. 373-80.

13. Ismail, S.A., et al., *The structure of an Arf-ArfGAP complex reveals a Ca2+ regulatory mechanism.* Cell, 2010. **141**(5): p. 812-21.

14. Sevajol, M., et al., *The C-terminal polyproline-containing region of ELMO contributes to an increase in the life-time of the ELMO-DOCK complex.* Biochimie, 2012. **94**(3): p. 823-8.

15. Patel, M., et al., *An evolutionarily conserved autoinhibitory molecular switch in ELMO proteins regulates Rac signaling.* Curr Biol, 2010. **20**(22): p. 2021-7.

16. Komander, D., et al., *An alpha-helical extension of the ELMO1 pleckstrin homology domain mediates direct interaction to DOCK180 and is critical in Rac signaling.* Mol Biol Cell, 2008. **19**(11): p. 4837-51.

17. Park, D., et al., *BAI1 is an engulfment receptor for apoptotic cells upstream of the ELMO/Dock180/Rac module.* Nature, 2007. **450**(7168): p. 430-4.

18. Grimsley, C.M., et al., *Characterization of a novel interaction between ELMO1 and ERM proteins.* J Biol Chem, 2006. **281**(9): p. 5928-37.

19. Lu, M., et al., *PH domain of ELMO functions in trans to regulate Rac activation via Dock180.* Nat Struct Mol Biol, 2004. **11**(8): p. 756-62.

20. Katoh, H. and M. Negishi, *RhoG activates Rac1 by direct interaction with the Dock180-binding protein Elmo.* Nature, 2003. **424**(6947): p. 461-4.

21. East, M.P. and R.A. Kahn, *Models for the functions of Arf GAPs.* Semin Cell Dev Biol, 2011. **22**(1): p. 3-9.

22. Zhang, C.J., M.M. Cavenagh, and R.A. Kahn, *A family of Arf effectors defined as suppressors of the loss of Arf function in the yeast Saccharomyces cerevisiae.* J Biol Chem, 1998. **273**(31): p. 19792-6.

23. Eugster, A., et al., *COP I domains required for coatomer integrity, and novel interactions with ARF and ARF-GAP.* Embo J, 2000. **19**(15): p. 3905-17.

24. Lewis, S.M., et al., *The ArfGAP Glo3 is required for the generation of COPI vesicles.* Mol Biol Cell, 2004. **15**(9): p. 4064-72.

25. Frigerio, G., et al., *Two human ARFGAPs associated with COP-I-coated vesicles.* Traffic, 2007. **8**(11): p. 1644-55.

26. Luo, R., et al., *Arf GAP2 is positively regulated by coatomer and cargo.* Cell Signal, 2009. **21**(7): p. 1169-79.

27. Rein, U., et al., *ARF-GAP-mediated interaction between the ER-Golgi v-SNAREs and the COPI coat.* J Cell Biol, 2002. **157**(3): p. 395-404.

28. Weimer, C., et al., *Differential roles of ArfGAP1, ArfGAP2, and ArfGAP3 in COPI trafficking.* J Cell Biol, 2008. **183**(4): p. 725-35.

29. Lee, S.Y., et al., *ARFGAP1 plays a central role in coupling COPI cargo sorting with vesicle formation.* J Cell Biol, 2005. **168**(2): p. 281-90.

30. Schindler, C., et al., *The GAP domain and the SNARE, coatomer and cargo interaction region of the ArfGAP2/3 Glo3 are sufficient for Glo3 function.* Traffic, 2009. **10**(9): p. 1362-75.

31. Dai, J., et al., *ACAP1 promotes endocytic recycling by recognizing recycling sorting signals.* Dev Cell, 2004. **7**(5): p. 771-6.

32. Li, J., et al., *An ACAP1-containing clathrin coat complex for endocytic recycling.* J Cell Biol, 2007. **178**(3): p. 453-64.

33. Yu, S. and M.G. Roth, *Casein kinase I regulates membrane binding by ARF GAP1.* Mol Biol Cell, 2002. **13**(8): p. 2559-70.

34. Randazzo, P.A. and D.S. Hirsch, *Arf GAPs: multifunctional proteins that regulate membrane traffic and actin remodelling.* Cell Signal, 2004. **16**(4): p. 401-13.

35. Donaldson, J.G., D. Finazzi, and R.D. Klausner, *Brefeldin A inhibits Golgi membrane-catalysed exchange of guanine nucleotide onto ARF protein.* Nature, 1992. **360**(6402): p. 350-2.

36. Klausner, R.D., J.G. Donaldson, and J. Lippincott-Schwartz, *Brefeldin A: insights into the control of membrane traffic and organelle structure.* J Cell Biol, 1992. **116**(5): p. 1071-80.

37. Wittinghofer, A., K. Scheffzek, and M.R. Ahmadian, *The interaction of Ras with GTPase-activating proteins.* FEBS Lett, 1997. **410**(1): p. 63-7.

38. Santy, L.C., K.S. Ravichandran, and J.E. Casanova, *The DOCK180/Elmo complex couples ARNO-mediated Arf6 activation to the downstream activation of Rac1*. Curr Biol, 2005. **15**(19): p. 1749-54.

39. Santy, L.C. and J.E. Casanova, *Activation of ARF6 by ARNO stimulates epithelial cell migration through downstream activation of both Rac1 and phospholipase D.* J Cell Biol, 2001. **154**(3): p. 599-610.

40. Schlienger, S., S. Campbell, and A. Claing, *ARF1 regulates the Rho/MLC pathway to control EGF-dependent breast cancer cell invasion.* Mol Biol Cell, 2014. **25**(1): p. 17-29.

41. Lewis-Saravalli, S., S. Campbell, and A. Claing, *ARF1 controls Rac1 signaling to regulate migration of MDA-MB-231 invasive breast cancer cells.* Cell Signal, 2013. **25**(9): p. 1813-9.

42. Myers, K.R. and J.E. Casanova, *Regulation of actin cytoskeleton dynamics by Arf-family GTPases.* Trends Cell Biol, 2008. **18**(4): p. 184-92.

43. Randazzo, P.A., H. Inoue, and S. Bharti, *Arf GAPs as regulators of the actin cytoskeleton.* Biol Cell, 2007. **99**(10): p. 583-600.

44. Chen, P.W., et al., *ARAP2 signals through Arf6 and Rac1 to control focal adhesion morphology*. J Biol Chem, 2013. **288**(8): p. 5849-60.

45. Koo, T.H., B.A. Eipper, and J.G. Donaldson, *Arf6 recruits the Rac GEF Kalirin to the plasma membrane facilitating Rac activation.* BMC Cell Biol, 2007. **8**: p. 29.

46. Cotton, M., et al., *Endogenous ARF6 interacts with Rac1 upon angiotensin II stimulation to regulate membrane ruffling and cell migration.* Mol Biol Cell, 2007. **18**(2): p. 501-11.

47. Radhakrishna, H., et al., *ARF6 requirement for Rac ruffling suggests a role for membrane trafficking in cortical actin rearrangements.* J Cell Sci, 1999. **112 (Pt 6)**: p. 855-66.

48. Lu, M. and K.S. Ravichandran, *Dock180-ELMO cooperation in Rac activation.* Methods Enzymol, 2006. **406**: p. 388-402.

49. Randazzo, P.A., O. Weiss, and R.A. Kahn, *Preparation of recombinant ADP-ribosylation factor*. Methods Enzymol, 1992. **219**: p. 362-9.

50. Ha, V.L., et al., *Preparation of myristoylated Arf1 and Arf6.* Methods Enzymol, 2005. **404**: p. 164-74.

51. Brugnera, E., et al., *Unconventional Rac-GEF activity is mediated through the Dock180-ELMO complex.* Nat Cell Biol, 2002. **4**(8): p. 574-82.

52. Munro, S., *The Arf-like GTPase Arl1 and its role in membrane traffic.* Biochem Soc Trans, 2005. **33**(Pt 4): p. 601-5.

53. Lowe, S.L., S.H. Wong, and W. Hong, *The mammalian ARF-like protein 1 (Arl1) is associated with the Golgi complex.* J Cell Sci, 1996. **109 (Pt 1)**: p. 209-20.

54. Lu, L., et al., *Regulation of Golgi structure and function by ARF-like protein 1 (Arl1).* J Cell Sci, 2001. **114**(Pt 24): p. 4543-55.

55. Zhang, C.J., et al., *Expression of a dominant allele of human ARF1 inhibits membrane traffic in vivo.* J Cell Biol, 1994. **124**(3): p. 289-300.

56. Ren, X.D. and M.A. Schwartz, *Determination of GTP loading on Rho.* Methods Enzymol, 2000. **325**: p. 264-72.

57. Yoon, H.Y., J.S. Bonifacino, and P.A. Randazzo, *In vitro assays of Arf1 interaction with GGA proteins.* Methods Enzymol, 2005. **404**: p. 316-32.

58. de Rooij, J. and J.L. Bos, *Minimal Ras-binding domain of Raf1 can be used as an activation-specific probe for Ras.* Oncogene, 1997. **14**(5): p. 623-5.

59. Castro, A.F., J.F. Rebhun, and L.A. Quilliam, *Measuring Ras-family GTP levels in vivo--running hot and cold.* Methods, 2005. **37**(2): p. 190-6.

60. Van Valkenburgh, H., et al., *ADP-ribosylation factors (ARFs) and ARF-like 1 (ARL1) have both specific and shared effectors: characterizing ARL1-binding proteins.* J Biol Chem, 2001. **276**(25): p. 22826-37.

61. Panic, B., et al., *Structural basis for Arl1-dependent targeting of homodimeric GRIP domains to the Golgi apparatus.* Mol Cell, 2003. **12**(4): p. 863-74.

62. Wu, M., et al., *Structural basis for recruitment of GRIP domain golgin-245 by small GTPase Arl1.* Nat Struct Mol Biol, 2004. **11**(1): p. 86-94.

63. Hayashi, T. and T.P. Su, *Sigma-1 receptor chaperones at the ER-mitochondrion interface regulate Ca(2+) signaling and cell survival.* Cell, 2007. **131**(3): p. 596-610.

64. Kitaichi, K., et al., *Expression of the purported sigma(1) (sigma(1)) receptor in the mammalian brain and its possible relevance in deficits induced by antagonism of the NMDA receptor complex as revealed using an antisense strategy.* J Chem Neuroanat, 2000. **20**(3-4): p. 375-87.

65. Mori, T., et al., *Sigma-1 receptor chaperone at the ER-mitochondrion interface mediates the mitochondrion-ER-nucleus signaling for cellular survival.* PLoS One, 2013. **8**(10): p. e76941.

66. Cobos, E.J., et al., *Pharmacology and therapeutic potential of sigma(1) receptor ligands.* Curr Neuropharmacol, 2008. **6**(4): p. 344-66.

67. Hashimoto, K. and K. Ishiwata, *Sigma receptor ligands: possible application as therapeutic drugs and as radiopharmaceuticals.* Curr Pharm Des, 2006. **12**(30): p. 3857-76.

68. Maurice, T. and T.P. Su, *The pharmacology of sigma-1 receptors.* Pharmacol Ther, 2009. **124**(2): p. 195-206.

69. Niitsu, T., M. Iyo, and K. Hashimoto, *Sigma-1 receptor agonists as therapeutic drugs for cognitive impairment in neuropsychiatric diseases.* Curr Pharm Des, 2012. **18**(7): p. 875-83.

70. Skuza, G. and K. Wedzony, *Behavioral pharmacology of sigma-ligands.* Pharmacopsychiatry, 2004. **37 Suppl 3**: p. S183-8.

71. Hesse, D., et al., *Trans-Golgi proteins participate in the control of lipid droplet and chylomicron formation.* Biosci Rep, 2013. **33**(1): p. 1-9.

72. Bouvet, S., et al., *Targeting of the Arf-GEF GBF1 to lipid droplets and Golgi membranes.* J Cell Sci, 2013. **126**(Pt 20): p. 4794-805.

73. Hommel, A., et al., *The ARF-like GTPase ARFRP1 is essential for lipid droplet growth and is involved in the regulation of lipolysis.* Mol Cell Biol, 2010. **30**(5): p. 1231-42.

74. Nakamura, N., et al., *ADRP is dissociated from lipid droplets by ARF1-dependent mechanism.* Biochem Biophys Res Commun, 2004. **322**(3): p. 957-65.

75. Nakamura, N., Y. Banno, and K. Tamiya-Koizumi, *Arf1-dependent PLD1 is localized to oleic acid-induced lipid droplets in NIH3T3 cells.* Biochem Biophys Res Commun, 2005. **335**(1): p. 117-23.

76. Thiam, A.R., et al., *COPI buds 60-nm lipid droplets from reconstituted water-phospholipid-triacylglyceride interfaces, suggesting a tension clamp function.* Proc Natl Acad Sci U S A, 2013. **110**(33): p. 13244-9.

77. Guo, Y., et al., *Functional genomic screen reveals genes involved in lipid-droplet formation and utilization.* Nature, 2008. **453**(7195): p. 657-61.

78. Soni, K.G., et al., *Coatomer-dependent protein delivery to lipid droplets.* J Cell Sci, 2009. **122**(Pt 11): p. 1834-41.

79. Spector, D.L. and A.I. Lamond, *Nuclear speckles.* Cold Spring Harb Perspect Biol, 2011. **3**(2).

80. Muromoto, R., et al., *BART is essential for nuclear retention of STAT3.* Int Immunol, 2008. **20**(3): p. 395-403.

81. Cavenagh, M.M., et al., *Intracellular distribution of Arf proteins in mammalian cells. Arf6 is uniquely localized to the plasma membrane.* J Biol Chem, 1996. **271**(36): p. 21767-74.

82. Volpicelli-Daley, L.A., et al., *Isoform-selective effects of the depletion of ADP-ribosylation factors 1-5 on membrane traffic.* Mol Biol Cell, 2005. **16**(10): p. 4495-508.

83. Charras, G.T., et al., *Life and times of a cellular bleb.* Biophys J, 2008. **94**(5): p. 1836-53.

84. Charras, G.T., *A short history of blebbing.* J Microsc, 2008. **231**(3): p. 466-78.

85. Fackler, O.T. and R. Grosse, *Cell motility through plasma membrane blebbing.* J Cell Biol, 2008. **181**(6): p. 879-84.

86. Amano, M., et al., *Phosphorylation and activation of myosin by Rho-associated kinase (Rho-kinase).* J Biol Chem, 1996. **271**(34): p. 20246-9.

87. Dawes, A.T. and L. Edelstein-Keshet, *Phosphoinositides and Rho proteins spatially regulate actin polymerization to initiate and maintain directed movement in a one-dimensional model of a motile cell.* Biophys J, 2007. **92**(3): p. 744-68.

88. Kimura, K., et al., *Regulation of myosin phosphatase by Rho and Rho-associated kinase (Rho-kinase).* Science, 1996. **273**(5272): p. 245-8.

89. Matsumura, F., et al., *Role of myosin light chain phosphorylation in the regulation of cytokinesis.* Cell Struct Funct, 2001. **26**(6): p. 639-44.

90. Pellegrin, S. and H. Mellor, *Actin stress fibres.* J Cell Sci, 2007. **120**(Pt 20): p. 3491-9.

91. Katoh, K., et al., *Rho-kinase--mediated contraction of isolated stress fibers.* J Cell Biol, 2001. **153**(3): p. 569-84.

92. Katoh, K., et al., *Stress fiber organization regulated by MLCK and Rho-kinase in cultured human fibroblasts.* Am J Physiol Cell Physiol, 2001. **280**(6): p. C1669-79.

93. Chrzanowska-Wodnicka, M. and K. Burridge, *Rho-stimulated contractility drives the formation of stress fibers and focal adhesions.* J Cell Biol, 1996. **133**(6): p. 1403-15.

94. Powers, S., K. O'Neill, and M. Wigler, *Dominant yeast and mammalian RAS mutants that interfere with the CDC25-dependent activation of wild-type RAS in Saccharomyces cerevisiae.* Mol Cell Biol, 1989. **9**(2): p. 390-5.

95. Frank, S.R. and S.H. Hansen, *The PIX-GIT complex: a G protein signaling cassette in control of cell shape.* Semin Cell Dev Biol, 2008. **19**(3): p. 234-44.

96. Shiba, Y. and P.A. Randazzo, *GEFH1 binds ASAP1 and regulates podosome formation.* Biochem Biophys Res Commun, 2011. **406**(4): p. 574-9.

97. Sander, E.E., et al., *Rac downregulates Rho activity: reciprocal balance between both GTPases determines cellular morphology and migratory behavior.* J Cell Biol, 1999. **147**(5): p. 1009-22.

98. Garcia-Mata, R., et al., *Analysis of activated GAPs and GEFs in cell lysates.* Methods Enzymol, 2006. **406**: p. 425-37.

99. Tsuji, T., et al., *Involvement of p114-RhoGEF and Lfc in Wnt-3a- and dishevelled-induced RhoA activation and neurite retraction in N1E-115 mouse neuroblastoma cells.* Mol Biol Cell, 2010. **21**(20): p. 3590-600.

100. Sanz-Moreno, V., et al., *Rac activation and inactivation control plasticity of tumor cell movement.* Cell, 2008. **135**(3): p. 510-23.

101. Kim, J.Y., et al., *The RhoG/ELMO1/Dock180 signaling module is required for spine morphogenesis in hippocampal neurons.* J Biol Chem, 2011. **286**(43): p. 37615-24.

102. Ganguly, A., et al., *Microtubule dynamics control tail retraction in migrating vascular endothelial cells.* Mol Cancer Ther, 2013. **12**(12): p. 2837-46.

103. Worthylake, R.A., et al., *RhoA is required for monocyte tail retraction during transendothelial migration.* J Cell Biol, 2001. **154**(1): p. 147-60.

104. Sastry, S.K., et al., *PTP-PEST couples membrane protrusion and tail retraction via VAV2 and p190RhoGAP.* J Biol Chem, 2006. **281**(17): p. 11627-36.

105. Iwanicki, M.P., et al., *FAK, PDZ-RhoGEF and ROCKII cooperate to regulate adhesion movement and trailing-edge retraction in fibroblasts.* J Cell Sci, 2008. **121**(Pt 6): p. 895-905.

106. Margaron, Y., N. Fradet, and J.F. Cote, *ELMO recruits actin cross-linking family 7 (ACF7) at the cell membrane for microtubule capture and stabilization of cellular protrusions.* J Biol Chem, 2013. **288**(2): p. 1184-99.

107. Etienne-Manneville, S., *Microtubules in cell migration.* Annu Rev Cell Dev Biol, 2013. **29**: p. 471-99.

108. Beghin, A., et al., *ADP ribosylation factor like 2 (Arl2) protein influences microtubule dynamics in breast cancer cells.* Exp Cell Res, 2007. **313**(3): p. 473-85.

109. Zhou, C., et al., *Arl2 and Arl3 regulate different microtubule-dependent processes.* Mol Biol Cell, 2006. **17**(5): p. 2476-87.

110. Gutierrez-Aguilar, M. and C.P. Baines, *Physiological and pathological roles of mitochondrial SLC25 carriers.* Biochem J, 2013. **454**(3): p. 371-86.

111. Palmieri, F., *The mitochondrial transporter family SLC25: identification, properties and physiopathology.* Mol Aspects Med, 2013. **34**(2-3): p. 465-84.

112. Sinasac, D.S., et al., *Genomic structure of the adult-onset type II citrullinemia gene, SLC25A13, and cloning and expression of its mouse homologue.* Genomics, 1999. **62**(2): p. 289-92.

113. Woo, H.I., H.D. Park, and Y.W. Lee, *Molecular genetics of citrullinemia types I and II.* Clin Chim Acta, 2014. **431**: p. 1-8.

114. Ramoz, N., et al., *Linkage and association of the mitochondrial aspartate/glutamate carrier SLC25A12 gene with autism.* Am J Psychiatry, 2004. **161**(4): p. 662-9.

115. Durdiakova, J., et al., *Single nucleotide polymorphism rs6716901 in SLC25A12 gene is associated with Asperger syndrome.* Mol Autism, 2014. **5**(1): p. 25.

116. Majumder, S., et al., *VDAC3 regulates centriole assembly by targeting Mps1 to centrosomes.* Cell Cycle, 2012. **11**(19): p. 3666-78.

117. Gillingham, A.K. and S. Munro, *The small G proteins of the Arf family and their regulators.* Annu Rev Cell Dev Biol, 2007. **23**: p. 579-611.

118. Ciuman, R.R., *Auditory and vestibular hair cell stereocilia: relationship between functionality and inner ear disease.* J Laryngol Otol, 2011. **125**(10): p. 991-1003.

119. Mammano, F., *Ca2+ homeostasis defects and hereditary hearing loss.* Biofactors, 2011. **37**(3): p. 182-8.

120. Mammano, F., et al., *Ca2+ signaling in the inner ear.* Physiology (Bethesda), 2007. **22**: p. 131-44.